




2022

## Regulation of Skeletal Muscle Plasticity by the Gut Microbiome

Taylor R. Valentino

University of Kentucky, [taylorvalentino@gmail.com](mailto:taylorvalentino@gmail.com)

Author ORCID Identifier:

 <https://orcid.org/0000-0002-7191-1827>

Digital Object Identifier: <https://doi.org/10.13023/etd.2022.032>

[Right click to open a feedback form in a new tab to let us know how this document benefits you.](#)

### Recommended Citation

Valentino, Taylor R., "Regulation of Skeletal Muscle Plasticity by the Gut Microbiome" (2022). *Theses and Dissertations--Physiology*. 57.

[https://uknowledge.uky.edu/physiology\\_etds/57](https://uknowledge.uky.edu/physiology_etds/57)

This Doctoral Dissertation is brought to you for free and open access by the Physiology at UKnowledge. It has been accepted for inclusion in Theses and Dissertations--Physiology by an authorized administrator of UKnowledge. For more information, please contact [UKnowledge@lsv.uky.edu](mailto:UKnowledge@lsv.uky.edu).

## **STUDENT AGREEMENT:**

I represent that my thesis or dissertation and abstract are my original work. Proper attribution has been given to all outside sources. I understand that I am solely responsible for obtaining any needed copyright permissions. I have obtained needed written permission statement(s) from the owner(s) of each third-party copyrighted matter to be included in my work, allowing electronic distribution (if such use is not permitted by the fair use doctrine) which will be submitted to UKnowledge as Additional File.

I hereby grant to The University of Kentucky and its agents the irrevocable, non-exclusive, and royalty-free license to archive and make accessible my work in whole or in part in all forms of media, now or hereafter known. I agree that the document mentioned above may be made available immediately for worldwide access unless an embargo applies.

I retain all other ownership rights to the copyright of my work. I also retain the right to use in future works (such as articles or books) all or part of my work. I understand that I am free to register the copyright to my work.

## **REVIEW, APPROVAL AND ACCEPTANCE**

The document mentioned above has been reviewed and accepted by the student's advisor, on behalf of the advisory committee, and by the Director of Graduate Studies (DGS), on behalf of the program; we verify that this is the final, approved version of the student's thesis including all changes required by the advisory committee. The undersigned agree to abide by the statements above.

Taylor R. Valentino, Student

Dr. John J. McCarthy, Major Professor

Dr. Kenneth Campbell, Director of Graduate Studies

REGULATION OF SKELETAL MUSCLE PLASTICITY BY THE GUT  
MICROBIOME

---

DISSERTATION

---

A dissertation submitted in partial fulfillment of the  
requirements for the degree of Doctor of Philosophy in the  
College of Medicine  
at the University of Kentucky

By  
Taylor Rees Valentino  
Lexington, Kentucky  
Director: Dr. John J. McCarthy, Professor of Physiology  
Lexington, Kentucky  
2022

Copyright © Taylor Rees Valentino 2022  
[<https://orcid.org/0000-0002-7191-1827>]

## ABSTRACT OF DISSERTATION

### REGULATION OF SKELETAL MUSCLE PLASTICITY BY THE GUT MICROBIOME

Recent evidence suggests that the gut microbiome could play a role in skeletal muscle plasticity, providing novel treatments for muscle wasting diseases and/or performance enhancements. I first sought to determine if the gut microbiome is necessary for skeletal muscle adaptation to exercise. Forty-two, four-month old, female C57Bl/6J underwent nine weeks of weighted wheel running or remained in cage with a locked wheel, without or without the administration of antibiotics (treated). In response to wheel running, I found that antibiotic depletion of the microbiome led to a blunted hypertrophic response in the soleus muscle as measured by normalized muscle wet weight and mean and fiber-type specific cross-sectional area (CSA). The plantaris muscle of mice who ran with antibiotic-induced dysbiosis showed a blunted glycolytic to oxidative fiber-type shift, decreased myonuclear accretion and satellite cell abundance compared to non-treated runners. These results are the first to demonstrate that an intact microbiome is necessary for skeletal muscle adaptation to exercise.

I next tested if the gut microbiome mitigates skeletal muscle atrophy induced by hind limb immobilization. Eighteen, four-month old, female C57Bl/6J mice were divided into two groups (n=9/group), that received cecal microbial transfers from either exercise-trained or sedentary donors. After four weeks of cecal transplants, the recipient mice underwent 10-days of single leg hind-limb immobilization. Immunohistochemistry analysis revealed that the recipients of the exercise-trained donors experienced significantly less skeletal muscle atrophy of the soleus muscle, as measured by mean fiber and fiber-type specific CSA. The transfer of microbiome from exercise-trained donors also led to a preservation of Type-2A fibers in the immobilized soleus muscle. These results demonstrated that the transfer of a microbiome from an exercise-trained host into recipients mitigated skeletal muscle atrophy, in addition to the persevering Type-2A fibers abundance during atrophy.

To better understand how the gut microbiome acts to modulate skeletal muscle mass and fiber-type composition, metagenomic sequencing was performed on donor and recipient of exercise-trained and sedentary cecal content. Sequencing data revealed significant differences in the microbiome between the two recipient groups. Further microbial functional comparisons were made and distinguished significant associations in fucose degradation and histidine metabolism in the recipients who received microbiome from exercised-trained

donors. To further interrogate the metagenomic sequencing, microbial sequence features were analyzed with MelonnPan to determine predictive metabolites associated with each recipient group. Lipids and bile acids metabolites were significantly associated with the recipients of the exercise-trained donors. There was a trend for imidazole propionate to be associated with the recipients of the exercise-trained donors. The metagenomic analysis indicated the microbiome from an exercise-trained host was associated with metabolic pathways that generate short chain fatty acids (fucose degradation) and the histidine-derived metabolite imidazole propionate.

The results from this dissertation provide evidence of crosstalk between skeletal muscle and the gut microbiome, providing for the first-time data that demonstrates the gut microbiome influences both anabolic and catabolic signaling in skeletal muscle. Although a direct mechanism for the skeletal muscle-gut microbiome interaction was not found, the metabolites propionate and imidazole propionate were identified as possible candidate for future studies. A general conclusion from the two studies described in this dissertation provides new evidence for the regulation of skeletal muscle mass and fiber-type composition.

Future work will need to focus on the identification of the gut microbial-derived metabolites promote anabolic pathways in skeletal muscle. Additional studies should also determine if the attenuation in atrophy induced by hind limb immobilization is conserved in other models of atrophy as observed with skeletal muscle wasting diseases and space exploration.

**KEYWORDS:** Skeletal Muscle, Hypertrophy, Atrophy, Gut Microbiome, Metabolism

---

Taylor Rees Valentino

---

01/20/2022

---

REGULATION OF SKELETAL MUSCLE PLASTICITY BY THE GUT  
MICROBIOME

Taylor Rees Valentino

John J. McCarthy PhD

---

Director of Dissertation

Kenneth S. Campbell PhD

---

Director of Graduate Studies

01/20/2022

---

Date

## DEDICATION

To Chris Valentino, my dad. “Trim that!” To my courageous, strong supportive and beautiful wife Rebecca. To think... it all started in Dr. Williams’ anatomy lab. Last, to my Aunt Julie, you left way to early and I miss you every day. You never stopped encouraging me to pursue my dreams-thank you for believing in me.

## ACKNOWLEDGMENTS

The following dissertation, while an individual work, benefited from the insights and direction of several people. First, my Dissertation Chair, John McCarthy, his unbridled optimism, obsessive excitement for skeletal muscle hypertrophy and relentless dedication to his work was a constant source of inspiration. Our morning conversation will be imprinted in my memories and was always the best way to start the day. Next, I wish to thank the complete Dissertation Committee, and outside reader, respectively: Steve Estus PhD, Michael Flythe PhD, Lance Johnson PhD, Mariana Nikolova-Karakashian PhD and Eric Blalock PhD. Your guidance throughout my PhD has been paramount not only for my successful graduation but for my future aspirations. Committee meetings were never a moment of panic or fear, rather a cultivating environment where I got take part in scientific logic and rationale. You are all extremely talented, intelligent, and inspiring people, I was lucky to have you on my committee. To Dr. Blalock, thank you for agreeing to be my outside examiner and for taking the time to be part of my final steps in this most excellent journey.

In addition to the technical and instrumental assistance above, I received equally important assistance from family and friends. Current and formers members of the McCarthy lab and Center for Muscle Biology; Jensen Goh MS, Yuan Wen MD PhD, Alexander Alimov PhD, Ivan Vechetti PhD, Brooks Mobley PhD, Laura Brown PhD, Alex Keeble, Nick Thomas MS, Christine Lantham PhD, Camille Brightwell PhD, Chris Fry PhD, Kevin Murach PhD, Cory Dungan PhD, Kate Kosmac PhD and Charlotte Peterson PhD. You have all helped me tremendously in my time as a graduate student at UKY, THANK YOU!!!



My former mentors Marialice Kern PhD, C. Matthew Lee PhD and Maria Veri PhD. My love of science and exercise physiology began when I was a just a measly undergrad in your classes. You saw something in me I never knew I had and helped bring that person out, I am forever grateful. Some of my fondest memories are being with you all.

I received invaluable help from the administrative staff in the Physiology department- Tanya Graf and Andrew Hernandez. Thank you so very much for always being there to help me or simply just talk. Sometimes just coming down to your office for a quick moment was enough to reset. Ken Campbell PhD, you are a fantastic director of graduate studies and provided many hours of great conversation. Going through your quantitative analysis class was a true test and as much as I felt like giving up you taught me one of the most simple and valuable lesson I have learned- I can figure it out. Thank you for always clearing up my mistakes and inspiring me to start rowing more 😊. All of my fellow graduate students and especially Courtney Kloske PhD, Holden Williams PhD, and Charles Seeks, it was so awesome having you three to battle through PGY 502/602.

My supporting family Nana, Babu, Ma Ketto, Grandpa Tree, Keeley, Sarah, Dylan and Silas (Ratboy) and of course all of your families. My love Rebecca and the two most entertaining creative, crazy, curious, and kind souls ever to be put on Earth, Ellie and Calliope- I LOVE you all. Finally, I wish to thank the respondents of my study (who remain anonymous for confidentiality purposes)

# TABLE OF CONTENTS

<b>ACKNOWLEDGMENTS.....</b>	<b>iii</b>
<b>LIST OF TABLES .....</b>	<b>viii</b>
<b>LIST OF FIGURES .....</b>	<b>ix</b>
<b>CHAPTER 1. Skeletal Muscle and The Gut Microbiome .....</b>	<b>1</b>
1.1 <i>Skeletal Muscle</i> .....	1
1.1.1 Myogenesis: The Development of Skeletal Muscle .....	2
1.1.2 Satellite Cells: Skeletal Muscle Resident Stem Cells .....	4
1.1.2 The Structural Basis of Skeletal Muscle.....	5
1.1.3 Mechanisms of Skeletal Muscle Hypertrophy .....	8
1.1.4 Mechanisms of Skeletal Muscle Atrophy .....	12
1.2 <i>The Microbiome</i> .....	15
1.2.1 The Gut Microbiome Skeletal Muscle Axis .....	17
1.2.2 Gut Microbial Metabolites.....	21
1.2.3 Short-Chained Fatty Acids (SFCA).....	22
1.2.4 Bile Acids .....	24
1.2.5 Amino Acids.....	25
1.2.6 Lipids.....	27
1.3 <i>Conclusion</i> .....	28
<b>CHAPTER 2. dysbiosis of the gut microbiome impairs mouse skeletal muscle adaption to exercise ..</b>	<b>29</b>
2.1 <i>Introduction</i> .....	29
2.2 <i>Methods</i> .....	30
2.2.1 Mice.....	30
2.2.2 Antibiotic Treatment .....	31
2.2.3 Progressive Weighted Wheel Running (PoWeR) .....	31
2.2.4 Immunohistochemistry .....	32
2.2.5 Image Capture and Analysis.....	32
2.2.6 Fecal DNA Extraction .....	32
2.2.7 Metagenomic Sequencing.....	33
2.2.8 Cytokine Assay.....	34
2.2.9 Euthanasia .....	34
2.2.10 Statistical Analysis.....	34
2.3 <i>Results</i> .....	35
2.3.1 Dysbiosis of the Gut Microbiome by Antibiotic Treatment .....	35
2.3.2 PoWeR Increased Food and Water Consumption .....	36
2.3.3 Body Weight.....	36
2.3.4 Running Volume .....	36
2.3.5 Soleus .....	36
2.3.5.1 Muscle Wet Weight .....	36
2.3.5.2 Fiber Cross-Sectional area (CSA).....	37
2.3.5.3 Myonuclei Abundance .....	37
2.3.5.4 Fiber-Type Composition.....	38

2.3.6	Plantaris .....	38
2.3.6.1	Muscle Wet Weight .....	38
2.3.6.2	Fiber Cross-Sectional Area (CSA).....	39
2.3.6.3	Myonuclei Abundance .....	39
2.3.6.4	Satellite Cell Abundance.....	39
2.3.6.5	Fiber-Type Composition.....	39
2.3.7	Serum Cytokine Levels .....	40
2.4	Discussion.....	40
2.4.1	Limitations.....	44
2.4.2	Conclusions .....	45
<b>CHAPTER 3. The gut microbiome from an exercise trained host ameliorates skeletal muscle atrophy.</b>		
<b>56</b>		
3.1	Introduction.....	56
3.2	Methods.....	57
3.2.1	Mice.....	57
3.2.2	PEG Bowel Clearing and Cecal Microbial Transfer.....	58
3.2.3	Cecal Microbial Transfer:.....	59
3.2.4	Limb Immobilization .....	59
3.2.5	Immunohistochemistry .....	59
3.2.6	Image Capture and Analysis.....	60
3.2.7	Microbial DNA Extraction and Sequencing .....	60
3.2.8	Metagenomic Sequencing.....	61
3.3	Statistics .....	61
3.4	Results.....	62
3.4.1	No Adverse Effects of CMT or Immobilization on Body Weight and Food Consumption ..	62
3.4.2	The Gut Microbiome from an Exercise Trained Host Blunts Skeletal Muscle Atrophy in the Soleus	62
3.4.3	The Gut Microbiome from an Exercise Trained Host Preserves Type2a fibers in the Soleus	63
3.4.4	Changes in Microbial Composition and Function after CMT .....	63
3.5	Discussion .....	66
3.6	Limitations .....	70
<b>CHAPTER 4. Discussion .....</b>		<b>82</b>
4.1	Major Findings from Dysbiosis of the Gut Microbiome Impairs Mouse Skeletal Muscle Adaption to Exercise. ....	82
4.2	Major Findings from The Gut Microbiome from an Exercise-Trained Host Ameliorates Skeletal Muscle Atrophy.....	83
4.3	The Gut Microbiome and Skeletal Muscle Mass.....	85
4.4	The Gut Microbiome and Skeletal Muscle Fiber-type .....	86
4.5	Future Directions.....	87
4.5.1	Methods to Induce Dysbiosis .....	<b>Error! Bookmark not defined.</b>
4.5.2	Identifying Gut Microbial Derived Metabolites that Regulate Promote Skeletal Muscle Hypertrophy.....	87
4.5.3	Validating and testing imidazole propionate and SCFAs .....	88

4.5.4	Other models of atrophy .....	90
4.5.5	Characterizing <i>Muribaculaceae bacterium DSM 103720</i> .....	90
4.6	<i>Conclusion</i> .....	92
<b>REFERENCES</b> .....		<b>94</b>
<b>Vita</b> .....		<b>116</b>

## LIST OF TABLES

Table 3.1	Top 20 Significantly Different Taxa Between Recipient Groups.....	72
-----------	---	----

## LIST OF FIGURES

Figure 2.1 Study Design. ....	46
Figure 2.2 Gut Microbial Dysbiosis with Antibiotics.....	47
Figure 2.3 PoWeR and Antibiotic Induced Changes to the Gut Microbiome .....	48
Figure 2.4 Food & Water Consumption, and Body Weights.....	49
Figure 2.5 Antibiotic Induced Dysbiosis of the Gut Microbiome Does Not Impair Exercise Activity.....	50
Figure 2.6 Antibiotic Induced Dysbiosis of the Gut Microbiome Results in a Blunted Hypertrophic Response in the Soleus.....	51
Figure 2.7 Antibiotic Induced Dysbiosis of the Gut Microbiome Does Not Impairs Skeletal Muscle Fiber-Type Shift in the Soleus .....	52
Figure 2.8 Antibiotic Induced Dysbiosis of the Gut Microbiome Results in Blunted Hypertrophy, Myonuclei Accretion and Altered Satellite Cell Abundance in the Plantaris.....	53
Figure 2.9 Antibiotic Induced Dysbiosis of the Gut Microbiome Results in a Blunted Fiber-Type Shift in the Plantaris .....	54
Figure 2.10 10 Weeks of Antibiotics Administration and PoWeR Training did Not Augment Inflammation.....	55
Figure 3.1 No Adverse Effects of CMT or Immobilization on Body Weight or Food Consumption.....	73
Figure 3.2 The Gut Microbiome from an Exercised Trained Host Blunts Skeletal Muscle Atrophy in the Soleus.....	74
Figure 3.3 Alpha Diversity Measures in Recipient and Donor Mice .....	75
Figure 3.4 Beta Diversity Measures in Recipient and Donor Mice .....	76
Figure 3.5 Comparison of Donor and Recipient Microbiomes.....	77
Figure 3.6 Genera and Species Comparison Between Donors and Recipients.....	78
Figure 3.7 Species Comparison Between Recipients Groups.....	79
Figure 3.8 Gene Pathway Analysis.....	80
Figure 3.9 Predictive Metabolite Analysis.....	81

## INTRODUCTION: SKELETAL MUSCLE AND THE GUT MICROBIOME

### CHAPTER 1. SKELETAL MUSCLE AND THE GUT MICROBIOME

#### Skeletal Muscle

Skeletal muscle is one of the largest organs of the body, accounting for roughly 35-40% of body weight [1]. It is comprised of long, multinucleated cylindrical fibers, which are stable in G<sub>0</sub> and considered to be post-mitotic [2]. Skeletal muscle is extremely plastic, that is skeletal muscle specifically adapts to changes in the type and level of contractile activity it experiences [3]. Perturbations in muscle can be both beneficial (exercise) and deleterious (disuse/disease). At the onset of injury, skeletal muscle possesses the ability to regenerate due to the presence of a stem cell population, known as satellite cells, and other supporting cells [4]. Skeletal muscle is also considered to be a secretory organ, whereby it secretes factors, termed myokines and extracellular vesicles which can be taken up by various tissues [5-8], providing a mechanism for how skeletal muscle may contribute to systemic health.

Skeletal muscle loss occurs during physical inactivity, systemic disease, immobilization, and aging, thereby contributing to an increased risk for morbidity, disability, poor prognosis/recovery and dramatically decreasing quality of life [9-11]. Loss of muscle can occur within a few days as shown by Koww and colleagues who found that quadriceps and thigh muscle cross sectional area (CSA) decreased 3.4% and 4.2%, respectively, in just 5.6 days after hip surgery [12]. Individuals with the lowest skeletal muscle mass index were reported to have significantly more hospitalizations, which amount to roughly \$1,200 in extra medical cost per person [13]. Financial reports have estimated a total of \$18.5 billion in healthcare costs due to the loss of skeletal muscle [14]. The prevalence of skeletal muscle loss ranges in at-risk patients ranges from 10% in chronic heart failure, 30% in cancer, 35% in chronic obstructive pulmonary disease and 50% in end-stage renal disease [15].

Treatments aimed at preventing the loss of skeletal muscle include exercise, nutrition and pharmacological interventions; however, these treatments may not always be the most appropriate or impactful. Nutritional interventions may only provide modest benefits in combating atrophy [16] and could become problematic due to cost, satiety and poor taste [17]. Furthermore, these interventions may not be the most appropriate and applicable. For example, in extreme cases of cachexia, the patient may be unable to exercise. Side effects of pharmacologic interventions such as testosterone, have also been reported which include liver damage[18] and cardio-vascular related events [19]. Identifying alternative treatment strategies is paramount to combat conditions in which muscle loss is a major outcome as the onset of muscle loss can be rapid [10].

The cellular and molecular mechanisms that govern skeletal muscle plasticity continue to be a progressive field of study [20-22]. Currently the area of small metabolite regulation is receiving great interest within skeletal muscle biology field [23] due to the highly complex, and unknown nature of how metabolites modify regulatory pathways in skeletal muscle, alter the metabolic program and modify histones. These non-canonical signaling pathways represent potentially new strategies to therapeutically intervene to combat conditions where there is a loss of skeletal muscle mass and function. Skeletal muscle is unique in its ability to rapidly alter its metabolism when transitioning from a period of rest to exercise [24, 25]. Metabolic intermediates such as succinate, isoleucine, acetyl-CoA, lactate, methyl group, glutamate, crontyl-CoA, malonyl-CoA and ketone bodies generated from pathways are involved in post-translation modifications of histones and non-histone proteins [26-29]. This presents new insights of how metabolic factors contribute to skeletal muscle biology. The next sections will outline the development of skeletal muscle, structural anatomy and provide mechanisms that mediate skeletal muscle hypertrophy and atrophy.

### 1.1.1 Myogenesis: The Development of Skeletal Muscle

During gastrulation, the primitive streak forms giving rise to three primary germ layers; the endoderm, the mesoderm and the ectoderm. Gastrulation also marks the time when cells will become committed to a specific fate, following a series of molecular and cellular events that control the progression of development [30]. Skeletal muscle arises



from the mesoderm, specifically the paraxial mesoderm (PM) which forms directly lateral to the neural tube [31]. Segmented portions of the PM interact with the presomatic mesoderm (PSM), developing into somites which progress in a rostral to caudal orientation. The somites eventually differentiate into the dermomyotome and then give rise to the vertebral and limb muscles [32-34]. The dermomyotome contains muscle stem cells and can be further segmented into the hypaxial and epaxial domains in which distinct innervation patterns control specific muscle populations. For example, epaxial muscles (muscles of the back) are innervated by the dorsal branch of the spinal nerve, while hypaxial muscles (body wall muscles, appendicular muscles, diaphragm and tongue muscles) are innervated by the ventral spinal nerves [35]. In these specific sites of skeletal muscle formation, terminal differentiation is governed by a group of four basic helix-loop-helix domain myogenic regulatory factors (MRF); Myogenic factor 5 (*Myf5*), myogenic factor 6 (*Myf6*, sometimes referred to *Myf4*), myogenic differentiation 1 (*MyoD*) and myogenin (*MyoG*) [32, 35, 36]. These transcription factors initiate the cascade of events resulting in the formation of post-mitotic, multinucleated mature muscle fibers. *Myf5* appears to be the first expressed MRFs during embryogenesis at embryonic day 8 [37]. In addition, important signaling cues from upstream transcription factors helps to regulate the MRFs during myogenesis allowing for muscle progenitor cells to proliferate and differentiate into mature myotubes [35].

Cells that comprise the newly formed somites have not yet differentiated into a specific tissue lineage. As reviewed by Maracelle and co-workers, wingless integrated (Wnt), bone morphogenic protein (BMP) and sonic hedgehog (Shh) are major signaling factors that initiate fate determination in somites [38]. Somites will begin to differentiate into various tissues with the medial, lateral and central epithelial somites giving rise to *Pax3/Pax7* positive progenitors [39, 40]. The paired box gene 3 (*Pax3*) was shown to be highly expressed during the developing dermomyotome [41, 42]. Once the dermomyotome is formed, cells will down-regulate *Pax3* expression and begin to express *Myf5* and *Myf4* prior to myotome formation [43]. *Pax3* has been shown to activate *Myf5* expression by binding to a regulatory element located upstream of the *Myf5* transcription start site [44]. Additionally, it was shown that the sine oculis homeobox homologue 1 and 4 (*Six 1* and *Six 4*) regulate *Myf5* expression in conjunction with *Pax3* at the same upstream cis-element

[45]. Other factors such as Shh, Gli transcription factors and doublesex and mab-3 related transcription factors have been shown to activate *Myf5* [46, 47]. The elevated levels of *Myf5* leads to the expression of *MyoD* which is also thought to be under the regulation of Pax3 in the epaxial muscles, whereas Six 1 and Six 4 regulate *MyoD* in the hypaxial muscles. The increase in *MyoD* expression promotes myoblast proliferation and subsequent differentiation. This event marks the irreversible exit from the cell cycle and terminal differentiation. At this stage of myogenesis, myotubes will fuse into mature myofibers which will express specific myosin heavy chain isoforms (MyHC) (discussed in section 1.1.2)

### 1.1.2 Satellite Cells: Skeletal Muscle Resident Stem Cells

Skeletal muscle fibers contain multipotent resident stem cells that reside underneath the basal lamina, which also develop from the dermomyotome [48, 49]. At the time of post-natal development in the mouse, muscle stem cells (MuSC also termed satellite cells), will account for roughly 30% of the nuclei within muscle whereas by adulthood, satellite cells will account for <5% of myonuclei [50, 51]. During cell division, satellite cells will replicate in a symmetric or asymmetric fashion where they give rise to two daughter cells with distinct fates; differentiation into mature myoblast or replenish the existing stem cell population [52]. Satellite cells, express *Pax7*, a paralog of *Pax 3*, which forms the pool of adult muscle stem cells residing between the basal lamina and sarcolemma [53]. *Pax7* was shown to be necessary to direct the specification of satellite cells [54]. Satellite cells reside in a quiescent state, and upon activation, proliferate, differentiate, then fuse into the mature muscle fibers and/or communicate with other cell populations that exist within skeletal muscle environment [55-57]. Satellite cells will begin to express *Pax7* and commit to the satellite cell lineage inducing myogenic differentiation. In terms of self-renewal, dividing satellite cells depends on NOTCH2 and DELTA1 signaling to maintain the satellite cell population [58]. The transition of a satellite cells from a quiescent state to a proliferation state, is also accompanied by a shift in their metabolism, primarily from fatty acid oxidation to glycolysis [59]. Thus, different genetic networks and metabolic programs initiate and control fate determination of satellite cells which allows for precise governing of these stem cells during muscle plasticity in post-miotic mature muscle fibers. Elucidating how

different stimuli such as injury, exercise and various pathologies affect the behavior of satellite cells is of great interest and could help to identify other potential factors that contribute to the development and maintenance of skeletal muscle.

One final contributing factor to myogenesis is through epigenetic control of MRFs and other important genes that control muscle development. One form of epigenetic regulation involves specific enzymes that modify particular amino acid residues on histones [60]. During skeletal muscle development, gene expression has been shown to be regulated by certain epigenetic events [61, 62]. Recently Zhu and co-workers found that the histone lysine demethylase (KDM4A), drove the expression of *MyoD* and *MyoG*. New insights into epigenetic regulation have shown that a multitude of different enzymes and substrates participate in the modification of histones and non-histone proteins [29, 63]. Yucel and co-workers demonstrated that satellite cells redirect their metabolism in order to modulate histone acetylation as a driving factor in myogenic fate determination [64]. These results suggest that epigenetic regulation of satellite cells appears to be critical to myogenic function and behavior.

### 1.1.2 The Structural Basis of Skeletal Muscle

The hierarchy of skeletal muscle anatomy provides one of the best examples of structure-function relationships that exist in biology [65]. Visibly, one can discern gross anatomical differences between various muscles based upon the varying architectural properties. Skeletal muscle architecture, or the arrangement of muscle fibers (myofibers) relative to the axis of force generation [66, 67], contributes to overall muscle function, allowing for a diverse range of characteristics when considering the roughly 650 different muscles within the human body. A muscle is composed of bundles of fascicles which themselves are composed of thousands of muscle cells known as myofibers. In horses, Grotmol and co-workers found the average number of fascicles per muscle was roughly 20. These authors also determined the average muscle fiber per fascicle ranged between 140-200 fibers depending if the fascicle was superficial or deep [68]. The myofiber itself is packed with myofibrils which are primarily composed of the thin actin myofilament and the thick, myosin, myofilament. The myofilaments are arranged into the sarcomere which is the smallest functional unit of muscle contraction [69]. In addition to actin and myosin,

the sarcomere is comprised of many other proteins that enable the contraction of muscle (described below). While viewing whole muscle, it can be seen that myofibers are arranged such that they may run parallel to the axis of force generation (longitudinal) or they can run at one fixed (unipennate) or several (multipennate) angles relative to the axis of force generation [67]. These inherent anatomical differences allow for myofibers of roughly the same diameter and composed of the same proteins to perform different functions such as force production or excursion [67].

Skeletal muscle is surrounded by different layers of connective tissue that compartmentalize muscle fibers. These layers are the epimysium which ensheathes the entire muscle, giving rise to the tendons; the perimysium surrounds each fascicle within the muscle, and the endomysium surrounds each individual myofiber [70]. Beneath the endomysium, the muscle cell is surrounded by a basement membrane, known as the basal lamina which constitutes the extracellular matrix (ECM). These layers of connective tissue function to connect muscle to bone, faithfully transmit force and participates in muscle repair after injury [71-73]. This surrounding connective tissue meshwork also consists of various collagens, glycoproteins, proteoglycans and elastins which contributes to the overall structure and signaling cascades within a muscle [70, 74].

Within each myofiber, there are approximately 500-10,000 myofibrils which are composed of millions of functional units called sarcomeres [65]. Sarcomeres are 2-3 $\mu$ m in length and 1 $\mu$ m in diameter [65]. Sarcomeres are defined laterally by Z-discs that anchor the actin containing thin filaments in an anti-parallel fashion, with additional proteins, nebulin,  $\alpha$ -actinin, myozenin, myotilin, myopalladin and titin providing structural and mechanical support [75]. Adjacent to each Z-discs are regions of the sarcomere known as the I-band which contain only actin thin filaments [76]. In the center of each sarcomere is the M-band which anchors the myosin containing thick filaments. The H-zone, located in the center of the M-band, contains only thick filaments and are flanked by regions known as the A-bands, which contain both myosin and actin filaments. The force of muscle contraction is generated by a shortening of the sarcomere when the thin myofilament is pulled through the action of the thick myofilament to the center of the sarcomere. According to the sliding filament mechanism, the globular heads of myosin heavy chain

become activated and bind to exposed myosin binding sites on the actin filaments forming a cross-bridge. Through the hydrolysis of ATP and the subsequent dissociation of the inorganic phosphate, the myosin heads undergo a conformation change which effectively pull the actin myofilaments towards the M-band in what is known as the power stroke [75, 77, 78]. New findings on the molecular basis for skeletal muscle contraction and sarcomere organization are still being discovered, highlighting the complexity of myofilament interactions during muscle contraction [79].

Myofibrillar organization does not only include the contractile machinery mentioned above, but also consists of the cytoskeletal and other membrane-bound organelles typical of all cells [80]. Proteins associated with these structures provide connection points between the sarcomeres and organelles, supports the contractile apparatus, participates in mechanotransduction and signaling cascades which regulate skeletal muscle plasticity [69]. The presence of proteins such as integrins, which span from the sarcolemma to the ECM, allows for bidirectional signaling to take place between the internal and external environments of the muscle fiber [81]. First described in 1983 by Criag and Pardo, costameres localized over the Z-discs, link the sarcolemma to the cytoskeleton [80, 82, 83]. Costameres are protein assemblies, mainly consisting of two major complexes, 1) the dystrophin-glycoprotein complex (DGC) and 2) the integrin-vinculin-talin complex [84]. These protein assemblies help to transmit force from the sarcolemma to the surrounding extracellular matrix and may contribute to the organization of thin and thick filaments [85]. The critical role of these other myofibrillar proteins in muscle function is easily seen when considering pathologies such as muscular dystrophy. For example, a mutation in dystrophin gene can lead to either reductions in the amount of dystrophin protein or in more severe cases, the complete loss of the dystrophin protein [86, 87]. Finally, components of the ECM and the protein titin contribute to the force of passive stiffness observed when a muscle is stretched in the absence of cross-bridge activation [88].

Architectural differences result in whole muscle variations allowing for specific roles for each muscle found within the body. Each muscle is composed of different type of myofibers that contribute to functional characteristics of a muscle. There are three major

types of myofibers, slow-twitch, fast-oxidative and fast-glycolytic, that exhibit distinct phenotypic properties. One of the major differences in fiber-type is due to the expression of specific adult myosin heavy chain proteins. There are three primary myosins in human and four in rodents expressed throughout the muscles of the body with other myosins restricted to development or specialized muscles [89]. The functional characteristics of each fiber-type can also be attributed to differences in fiber size, pattern of neural innervation, metabolism and force production [90]. Slow-twitch muscle fibers (MYH7, Type 1) are characterized by having a slow time to peak tension, high capacity for lipid oxidation, enriched with mitochondria, highly vascularized and are fatigue resistant [75, 91]. Fast oxidative (MYH2, Type 2A) fibers exhibit faster time to peak tension, highly oxidative with a greater propensity for glycolysis compared to slow-twitch fibers and are also fatigue resistant [92]. The fast-glycolytic fibers (MYH1, Type 2X, in humans, MYH 1 and MYH 4, Type 2B in rodents) generate peak tension the fastest of myofibers, exhibit a high reliance on glycolytic metabolism, relatively low mitochondrial content and are highly fatigable [93]. With the advantage of cutting-edge techniques, such as single-cell RNA--sequencing, Rubenstein and co-workers determined specific gene signatures for Type 1 and Type 2A muscle fibers which showed differential expression of sarcomeric, calcium transport and metabolic genes between the two fiber types [94].

### 1.1.3 Mechanisms of Skeletal Muscle Hypertrophy

Skeletal muscle has the extraordinary ability to remodel the size and physiological characteristics in response to mechanical loading, contractile activity, anabolic signaling, nutrient availability and/or metabolic changes [95-98]. Skeletal muscle responds to these stimuli by increasing the size of each muscle fiber (hypertrophy), while the addition of new muscle fibers (hyperplasia) is minimal if at all under normal situations. The cellular and molecular pathways that govern skeletal muscle hypertrophy act to modulate the balance of protein synthesis and breakdown. Increasing the rates of protein synthesis while mitigating protein degradation will lead to skeletal muscle growth [99]. The cell's master regulator of protein synthesis is known as mechanistic target of rapamycin (TORC-1 or TORC-2, described below), a serine/threonine protein kinase [100]. Additional pathways that are thought to TORC-1 be independent also contribute to skeletal muscle hypertrophy

but will not be the focus of this section [101]. In order to increase protein synthesis, the myofiber needs to modulate two primary factors- 1) translational efficiency; the amount of mRNA that is successfully translated into protein and 2) translational capacity; how much translational machinery (ribosomes) are available [97]. These factors are controlled by the cells ability to increase ribosome biogenesis which facilitates an increase in mRNA translation.

TORC-1 has been shown to regulate both transcriptional efficiency and capacity, leading to enhanced protein synthesis and subsequent hypertrophy [20]. TORC-1 promotes to the synthesis of ribosomal RNA (rRNA) by activating the transcription factors Transcription Initiation Factor 1a (TIF1a) and Upstream Binding Factor (UBF) which upregulate the activity of RNA polymerase 1 (Pol I) [102, 103]. The regulation of the 79 ribosomal proteins (RP) is also thought to be under the control of TORC-1 activation of RNA Pol II [104]. All the mammalian mRNAs for RPs contain a 5'-terminal oligopyrimidine tract (5'-TOP), in addition to other non-RP mRNAs[105]. Using an TORC-1 ATP site inhibitor, Hsieh and co-workers determined that 68% of the 144 TORC-1 sensitive genes were 5'-TOP mRNAs [106]. This implies that TORC-1 regulates ribosome biogenesis through interacting with some RPs. Another substrate for TORC-1 is p70S6 kinase (p70S6K) which, when activated by TORC-1, phosphorylates ribosomal protein S6 (rpS6) [107]. Activation of rpS6 facilitates the translation of 5'-TOP mRNAs, leading to enhanced synthesis of proteins required for translation [108] The activation of TORC-1 can also phosphorylate and inhibit Maf1, a repressor of rRNA Pol III[109]. Additionally, TORC1 also associates with RNA Pol III through the interaction with Transcription Factor IIIC which was shown to be crosslinked with tRNA and 5S rRNA genes, both of which are transcribed by RNA Pol III [109]. These studies demonstrate that TORC-1 acts to increase ribosome biogenesis by increasing the translational machinery required to enhance protein synthesis. Another downstream target of TORC-1 is eukaryotic translation initiation factor 4E binding protein (4E-BP1) [110]. By phosphorylating and inactivating 4E-BP1, mRNA translation initiation and elongation is enhanced [111]. The phosphorylation of 4E-BP1 inhibits its repression of Eukaryotic Initiation Factor 4E (eIF4e) which recruits the translational initiation machinery (eIF3, eIF4A, eIF4B and eIF4G) to the 5' cap of mRNA facilitating the binding of ribosomes [112]. These studies highlight the

central role of mTOR in the regulation of cellular growth and its significant role in skeletal muscle hypertrophy.

In 1999 Baar and Esser demonstrated that prolonged muscle contraction, induced by electrical stimulation of the sciatic nerve, resulted in a significant increase in skeletal muscle hypertrophy in rats [113]. These authors found the high force contractions lead to the phosphorylation of the TORC-1 substrate p70S6K, with a concomitant increase in polysome profiles during the first six hours after stimulation, suggesting increases in protein synthesis as a result of force production [113]. The importance of TORC-1 signaling during hypertrophy was further highlighted by Bodine and co-workers. They demonstrated that blocking TORC-1 by the administration of rapamycin rendered the plantaris muscle unable to grow in response to synergist ablation [114]. In addition, these authors showed that the upstream kinase (protein kinase B/Akt), was necessary for TORC-1 activation and subsequent skeletal muscle hypertrophy [114].

mTOR exists in two different protein complexes, TORC-1 and TORC-2, distinct from one another in binding partners and substrates. TORC-1 associates with the rapamycin-sensitive protein RAPTOR, while TORC-2 contains RICTOR, which is rapamycin-insensitive. These proteins provide a scaffold by which TOR substrates can assemble and bind to the kinase domain located at the C-terminal of TORC-1/2 [115, 116]. Additional components of the TORC-1 complex include the mammalian lethal with sec-13 protein 8, mLST8/GβL (TORC-1) and mLST8/Gbl (TORC-2), DEP domain containing TOR-interacting protein (DEPTOR) and Ttil1 and telomere maintenance 2 (Tel2) [115, 117]. Less is known about the TORC-2 complex and its function in skeletal muscle with one study showing that TORC-2 is important for glucose uptake during exercise [118]. TORC-1 on the other hand is the master regulator of protein synthesis [96]. Growth factors binding to their receptors on the sarcolemma (insulin like growth factor, frizzled homolog 7 and β-Adrenergic receptors) initiates the autophosphorylation on tyrosine residues on these receptors. This phosphorylation recruits phosphatidylinositol-3-kinase (PI3K) to the membrane, which binds to the phosphotyrosine residues of the growth factor receptors. The activation of PI3K results in the phosphorylation of the inositol ring of the membrane phospholipid phosphatidylinositol-3,4,5-triphosphate (PI3,4,5-P3/PIP3) by the catalytic



subunit (p110) of PI3K [119]. PIP3 recruits signaling proteins containing a pleckstrin homology (PH) domain such as Akt.

Akt phosphorylates and inhibits the GTPase activating protein (GAP)- tuberous sclerosis complex 2 (TSC2) [120]. The inactivation of TSC2 leads to the accumulation of GTP bound Ras homolog enriched in the brain (Rheb) [121]. Rheb binds to TORC-1 inducing a conformational change which brings the active-site residues into the optimal position for catalysis [122]. Additionally, Rag GTPases are necessary to recruit mTOR to the lysosome. In states of high nutrients, the Rag GTPases take on the nucleotide state whereby Rag A/B is GTP loaded, allowing TORC1 to anchor at the lysosomal membrane [123]. Once active TORC-1 can bind to and phosphorylate its substrates. As stated earlier, two important TORC-1 substrates which enhance protein synthesis are P70S6K1 and 4E-BP1 [96]. The activation of P70S6K1 in turn phosphorylates additional substrates facilitating mRNA translation, ribosome biogenesis and the ubiquitination of programmed cell death 4 (PDCD4) [124]. 4E-BP1 phosphorylation leads to it dissociating from eukaryotic initiation factor 4E (eIF4E) which promotes 5'-cap dependent mRNA translation of growth-related genes [125].

Additional TORC-1 targets have been identified leading to increases in TORC-1 activity and/or translation. Proline-rich Akt-substrate of 40kDa (PRAS40), a component of TORC-1 functions to inhibit TORC-1 kinase activity [126]. Oshiro and co-workers determined that TORC-1 can phosphorylate PRAS40 at serine 183 both in-vitro and in-vivo, leading to the dissociation of PRAS40 from RAPTOR [127]. Therefore, TORC-1 may be able to regulate its own kinase activity by modulating the phosphorylation of PRAS40. TORC-1 was also shown to phosphorylate La-related protein (LARP1) which was found to be a repressor of 5' TOP mRNAs [128]. As discussed earlier, 5'TOP mRNAs encode for ribosomal proteins and other elongation factors needed for growth dependent translation [129]. Another target of TORC-1 is the master regulator of hypoxia, HIF-1 $\alpha$  [130] which regulates the expression of genes related to anaerobic metabolism, intracellular pH, and angiogenesis [131]. HIF-1 $\alpha$ 's role in skeletal muscle hypertrophy is not well understood, studies have shown it may be important for skeletal muscle recovery after eccentric exercise [132].

An exciting new area in the regulation of skeletal muscle growth involves small metabolite activation of anabolic pathways. While not part of my dissertation, I took part in a study that explored how metabolism changes during skeletal muscle hypertrophy. It was found that during mechanical induced overload, the pentose phosphate pathway (PPP) is upregulated through an increase in the gene expression of glucose 6 phosphate dehydrogenase (G6PD) [133]. Although not entirely clear, we speculate that this increase in the PPP increases the production of NADPH which helps to combat oxidative stress that accompanies muscle growth and augment nucleotide synthesis. In agreement with our findings, Hoshino and co-workers demonstrated that high-frequency electrical stimulation of C2C12 myotubes resulted in a significant increase in PPP enzymes in addition to NADPH [134]. It appears that during hypertrophy, striated muscle re-wires metabolism to focus on nucleotide synthesis, a finding not well established in the skeletal muscle field. In support of metabolic reprogramming contributing to skeletal muscle adaptations, Reddy and co-workers found that during exercise, succinate becomes protonated, allowing it to exit the skeletal muscle via the monocarboxylate transporter 1. The succinate was found to bind to succinate receptors on adjacent muscle cells and non-muscle cells, facilitating improvement in endurance exercise, differential expression in extracellular matrix (ECM) proteins and inflammatory proteins [135].

These alternative pathways suggest a highly complex and integrated network of signaling pathways that could operate with or independent from mTORC1 signaling. Ongoing research in the field of skeletal muscle hypertrophy strives to further define these novel mechanisms as they represent potentially new targets for therapeutic interventions.

#### 1.1.4 Mechanisms of Skeletal Muscle Atrophy

Skeletal muscle atrophy is not simply the reverse of anabolic signaling. Muscle has distinct cellular pathways that control protein degradation leading to a reduction in both sarcomeric and non-myofibrillar proteins as well as decreases in protein synthesis in some systemic wasting diseases. Atrophy occurs in a wide range of conditions such as disease, disuse, denervation, aging, starvation and overtraining [136, 137]. A major outcome of the reduction in muscle mass is a concomitant decrease in muscle strength, which if significant enough, can lead to a reduced quality of life and exacerbates poor health outcomes [138,

139]. Using a microarray analysis of mice in various muscle wasting conditions, Leker and co-workers identified 120 common genes, referred to as “atrogenes”, that responded to the different muscle wasting models [140]. Notably, these authors found consistent expression of classic “atrogenes” and unexpectedly observed reductions in collagen synthesis and mitochondrial ATP synthesis [140]. The unloading of skeletal muscle through the use of a cast or hind limb suspension apparatus, provide highly effective methods to induce atrophy [141-144] and have been utilized to mimic space flight conditions. However, it is important to note that comparing immobilized and suspension models to space flight resulted distinct patterns of atrogene expression [145]. This finding demonstrates that aspects of the underlying mechanism of atrophy is specific for the form of atrophy induced by unloading, disuse or the weightlessness of space.

The ubiquitination of proteins by E3 ligases, autophagy mediated autophagosomal and lysosomal recycling of cellular proteins are the major mechanism use to degrade protein during atrophy [146]. In 2001, two groups independently reported that transcript levels encoding the E3 ubiquitin ligases Muscle RING Finger 1 (MuRF1, Trim63) and Muscle Atrophy F-box (MAFbx, atrogin 1) were increased in response to muscle atrophy [147, 148]. These proteins act to ubiquitinate selective substrates and target them for proteasomal degradation [148]. Studies have determined that these E3 ligases have a role in some types of atrophy but are not conserved in all atrophic conditions [149]. For example, MuRF1 null mice were shown to be protected against 14 days of dexamethasone induced atrophy and single leg immobilization but not nutritional deprivation or 21 days of space flight [145, 150]. These findings suggest the possibility that there are other, less well-known ubiquitin ligases, that might have a role in skeletal muscle atrophy. Cohen and co-workers found that the tripartite motif-containing protein 32 (Trim32) another RING finger ubiquitin ligase, is required for the loss of thin myofilaments including, actin, actinin, tropomyosin and desmin during fasting induced muscle atrophy [151]. TNF receptor-associated factor 6 (TRAF6) another E3 ubiquitin ligase, promotes the ubiquitination of MyHC proteins [152]. Paul and co-workers determined that skeletal muscle specific TRAF6 knock mice had significantly less muscle atrophy compared to controls in a denervation model [152]. The reduction in muscle loss was shown to be associated with a decrease in the activity of kinases (JNK, p38 MAPK and AMPK) that are linked to muscle

atrophy and a reduction in NF- $\kappa$ B [152]. The E3 ligase neural precursor cell expressed developmentally down regulated protein 4, (Nedd-4), from the HECT family of ligases, was found to play a role in denervation induced muscle atrophy [153]. Specifically, Nedd4 deletion attenuated Type 2a muscle fiber atrophy in the gastrocnemius. These authors identified possible Nedd4 substrates but could not detect differences in MTMR4, FGFR1 and Notch-1 ICD between the Nedd4 knock out and littermate controls [153].

As described in section 1.1.3, activation of Akt leads to the subsequent activation of TORC-1 and downstream regulation of protein synthesis. An additional role of Akt is to phosphorylate a family of forkhead box O (FOXO 1, 3 and 4) transcription factors, which inhibits their translocation into the nucleus [95]. Sandri and co-workers determined that FOXO3 promoted atrogin-1 transcription by binding to the 5' untranslated region of the TATA box and promoter region of the atrogin-1 gene [154]. FOXO3 was shown to activate the lysosomal and proteasomal pathways, increasing protein degradation in myotubes. This was initiated by FOXO3 regulation of myotube autophagy and increased expression of atrogin-1. MuRF1 and the autophagy related genes Bnip3, Bnip3L, Gabarpl and Ulk1 were also shown to be targets of FOXOs demonstrating a wide range of proteins that are regulated by FOXOs during muscle atrophy [155].

Another regulator of skeletal muscle mass is myostatin, a member of the transforming growth factor beta (TGF- $\beta$ ) super family. In 1997, McPherron and co-workers discovered a novel TGF- $\beta$  family member which they called growth/differentiation factor-8 (GDF-8/myostatin). Homozygous GDF-8 mutant mice were shown to be roughly 30% larger compared to heterozygous and wild type controls. This increase in mass was related to substantial increases in both skeletal muscle hypertrophy and hyperplasia [156]. In skeletal muscle, myostatin is first produced as a precursor called premyostatin which subsequently becomes cleaved to promyostatin before being released in the mature form [157]. Working in an autocrine or paracrine fashion, myostatin binds to muscle cell surface receptors called associated activin type 2A and 2B (ActaR2A/2B) initiating the recruitment of the type 1 receptor tyrosine kinases, activin-like kinase-4 and 5 (ALK4,5), that go on to phosphorylate Smad 2 and 3 [157]. The phosphorylation of Smad2 and Smad3 promotes binding to Smad4, forming a

heterocomplex, which translocates to the nucleus where it binds to various transcription factors, coactivators and repressors to influence gene expression [158]. Injecting mice with myostatin resulted in significant decrease in muscle weight and fiber CSA, demonstrating its role in enhancing muscle wasting [159]. Goodman and co-workers determined that Smad3 positively influenced the transcription of Atrogin-1 and suppressed the activity of PGC-1 $\alpha$  [160]. Over expression of Smad3 in skeletal muscle also resulted in a decrease in muscle fiber CSA and protein synthesis [160]. Pharmacological blocking of the ActR2B receptor with a soluble ActR2B-Fc significantly reversed the loss of lean mass and muscle weight compared to controls in a mouse model of cancer cachexia [161]. Inhibiting the action of myostatin with follistatin in adult mice resulted in significant skeletal muscle hypertrophy [162]. Therefore, these studies demonstrate that myostatin acts a powerful negative regulator of skeletal muscle growth.

Other mechanisms of muscle loss have been reported to be driven by systemic inflammation. Chronic inflammation leads to an increase in pro-inflammatory cytokines, which compromises muscle protein synthesis and elevates the ubiquitin-proteasomal system and autophagy [163]. Systemic inflammation initiated by the administration of lipopolysaccharide (LPS), led to a significant reduction in muscle protein synthesis and RNA content [164] and a significant increase in TNF- $\alpha$ , IL-1, IL- $\beta$ , IL-6, CXCL1, RANTES, G-CSF and NF- $\kappa\beta$  [165]. Chronic low-grade systemic inflammation that can be seen with aging, also interferes with protein synthesis as observed in both rodents and humans [166, 167] and Draganidis et al. (2021) (not yet in endnote). These data suggest that during aging and disease, the resulting increase in pro-inflammatory cytokines increase catabolism resulting in skeletal muscle atrophy.

## The Microbiome

The human microbiota comprises all the bacteria, archaea, viruses, phages, yeast, fungi and protozoa on and within the body, including the skin, mouth, nasal cavities, urogenital tract, and digestive system. [168]. Currently, over 90,000 metagenomes have been assembled [169], showcasing the immense complexity and enormous potential interactions between the microbiota and host. The intestinal environment creates unique

niches for microbes to aid in the digestion of macronutrients, micronutrients and other foreign substance consumed by the host and it is thought the gut microbiome harbors the largest number of microbial genes [170]. Moving forward in this dissertation, the term “microbiome” will refer to the bacteria component, unless otherwise stated. The microbiome was first thought to be acquired at the moment of birth, whether the infant was delivered vaginally or by caesarian section, resulted in unique microbial signatures [171]. When sequencing the meconium (the infant’s first intestinal discharge), Gosbales and co-workers determined it was not sterile and in fact reflected the intrauterine microbiome. This was conducted in a small sample of mothers and infants (n=7), but it does present data suggesting the initial acquirement of the microbiome occurs *in-utero* [172]. The subsequent modality of birth may then influence the infant native microbiome. The infant’s developing microbiome, postpartum, is subject to many influencing factors such as diet, environment, stress, hygiene and antibiotics [173]. The stabilization of the infant microbiome begins to occur between years one to three and many of the early colonizers reflect vertical transmission from mother to infant [174, 175]. Recently, Ferretti and co-workers tracked the microbiomes of infants and their mothers from one day postpartum to four months. The infant’s gut microbiome at one day postpartum had 49.3% unique species that were not identified in the mother. By four months, the unique species in the infant declined to 38.9% [176]. Additionally, the infant’s microbiome at day one postpartum, had very high strain level heterogeneity (roughly 6.1-fold more polymorphisms compared to the mother). The intra-strain level diversity begins to decline by one month, suggesting a high degree of selection takes place during the initial postpartum period [176]. Finally, this study showed that bacterial strains acquired vertically from the mother were not replaced by another conspecific strains, concluding that vertically transmitted strains are better suited for colonization [176].

The early colonization of the microbiome is a dynamic process that is constantly adapting as the infant becomes exposed to their new environment. The adult microbiome is also sensitive to perturbations. Environmental stimuli, such as diet, exercise, xenobiotics, stress and trauma [177-182] modulate the composition of the microbiome, creating a complex balance between microbes that are beneficial for the host and those that may contribute to disease [183]. Microbes have been shown to generate numerous metabolites

(reviewed in sections 1.2.2-1.2.6) with beneficial and/or detrimental roles in cancer, autism, Parkinson's, obesity, heart, lung, and bowel disease [184-191]. As the microbes respond to environmental cues, they alter their function which may aid the host to adapt, or conversely contribute to the development of a disease state. Das and co-workers determined in response to excess dietary iron intake, the gut microbiota produced two metabolites (reuterin and 1,3-diaminopropane (DAP)) which helped to lower host iron levels by suppressing Hif2 $\alpha$  [192]. These results demonstrate that the microbiome can sense perturbations occurring in the host and effectively respond via specific metabolites. It is crucial to understand how alterations in microbial composition reflect changes in its functional output and what consequences this can have on the host.

### 1.1.5 The Gut Microbiome Skeletal Muscle Axis

In 2007 Bäckhed and co-workers determined that the gastrocnemius muscle of germ-free mice, mice without any microorganisms, had significantly higher expression of phosphorylated acetyl-CoA carboxylase, AMP-activate protein kinase and carnitine palmitoyl transferase compared to mice with an intact microbiome [193]. These results implied that skeletal muscle from germ-free mice had a higher propensity to oxidize fatty acids. This finding is the first compelling evidence to show the gut microbiome can influence skeletal muscle metabolism. Following their initial work, Everard and co-workers found that feeding obese mice with a prebiotic diet resulted in a significant increase in lean body mass and normalized muscle wet weight compared to control obese mice [194]. Additionally, Bindles and co-workers determined that supplementing mice with *Lactobacillus reuteri* and *Lactobacillus gasseri* significantly lowered the expression of Atrogin-1, MuRF1, LC3 and Cathspin L in both the gastrocnemius and tibialis anterior muscles in a model of cancer [195]. Supplementing mice with the probiotic *Lactobacilli plantarum* (*L. plantarum*) for six weeks significantly increased grip strength, swimming time to exhaustion, normalized muscle weight and the percentage of Type 1 fibers [196]. Yan and co-workers then provided evidence that the gut microbiome could regulate skeletal muscle fiber-type composition [197], expanding the ways in which skeletal muscle can be influenced by the microbiome. Fielding and co-workers transferred the microbiome from high functioning (HF) and low functioning (LF) older adults into germ-free mice and

found that the recipients of the HF microbiome had significantly increased hand grip strength compared to the LF recipients [198]. The results from these pioneering studies indicated that the gut microbiome could regulate skeletal muscle metabolism, atrophy and fiber-type composition. The underlying mechanism through which the gut microbiome affects skeletal muscle remains to be determined.

In one of the most comprehensive studies which examined the relationship between the microbiome and skeletal muscle, Lahiri and co-workers found skeletal muscle from germ-free mice was atrophic compared to specific pathogen free (SPF, mice without any known pathogens)[199]. Germ-free mice had significantly higher expression of *atrogin-1*, *MuRF-1* and *FoxO3*, and significantly lower expression of *MyoD* and *MyoG* compared to SPF mice. Germ-free mice were also found to have significantly lower expression of genes related to oxidative and glycolytic metabolism and higher amounts of intramuscular glycogen [199]. These same authors showed that the administration of short chained fatty acids (SCFA, bacterial metabolites derived from the fermentation of fiber) rescued the muscle atrophy observed in germ-free mice, providing strong support for the idea that metabolites produced from the gut microbiome could regulate skeletal muscle mass [199]. These results also suggest that the microbiome modulates the development of skeletal muscle as shown by the atrophic phenotype and lower expression of *MyoD* and *MyoG*. Although not the focus of this dissertation, the importance of the microbiome during post-natal development is an important consideration.

Most recently, the SCFA butyrate, was found to mitigate skeletal muscle atrophy in diabetic (db/db) mice [200]. To determine a mechanism, Tang and co-workers found that butyrate activated the extracellular free fatty acid receptor 2 (Ffar2), which led to an increase in the phosphorylation of PI3K-AKT-TORC-1 pathway. This ultimately increased muscle protein synthesis and decreased reactive oxygen species and autophagy [200]. In support of skeletal muscle regulation by butyrate, Ly and co-workers used Mendelian Randomization (MR) to estimate skeletal muscle mass and associated gut microbiomes in menopausal females. Two butyrate producing microbes were found to be positively correlated with skeletal muscle index (a measure of appendicular lean mass/body mass) [201]. Furthermore, a one-way MR analysis revealed a significant association between



appendicular lean mass and butyrate producing microbial pathways [201]. These data highlight that SCFAs, especially butyrate, can regulate skeletal muscle mass and be a potential therapy to treat muscle wasting.

In addition to the regulation of skeletal muscle plasticity, evidence suggests the microbiome may also contribute to exercise performance. Initially, Hsu and co-workers determined that germ-free mice have significantly reduced exercise capacity compared to SPF controls [202]. Supplementation with the probiotic *L. plantarum* significantly improved endurance performance in a group of highly trained triathletes as well as mice [203, 204]. Scheiman and co-workers determined that elite endurance athletes possess a microbe *Veillonella atypica*, which contributed to enhanced endurance performance. Transplanting *V. atypica* into mice led to significantly greater time to exhaustion compared to mice receiving a *Lactobacillus bulgaricus* control [205]. These authors also demonstrated that supplementing mice with the SCFA propionate also increased time to exhaustion [205]. In a case study, Grosicki and co-workers determined that *Veillonella* abundance was increased 143-fold in a world class ultramarathon runner after completing a 100-mile race [206]. Jaago and co-workers looked at how endurance training modifies the gut microbiome composition supplemented with a high-fiber supplement in an 18-year-old male champion rower during an eight-month period of heavy training. This study provided interesting data highlighting how training itself modulates the composition of the microbiome, specifically decreasing the alpha-diversity. The addition of a high-fiber supplement with heavy training resulted in an increase in alpha-diversity [207]. It seems that exercise creates a very specific microbial composition when all other factors are left unchanged. The addition of specific nutrients creates a unique microbial signature, that could be exploited to enhance performance and/or recovery. It is not known if the compositional changes provided in this study resulted in enhanced exercise performance. Future research will need to determine the combinatorial effects of exercise and nutrition on functional changes in the microbiome that could act as ergogenic aids to enhance performance.

Early studies demonstrated a connection between the microbiome and hypothalamic pituitary axis, suggesting a connection between the host stress-response and commensal

microbes [208]. As the result of continued research, the microbiome is now considered an endocrine organ, as it can synthesize and release chemical factors into the systemic circulation [209]. Many metabolites of the gut microbiome have been associated with host metabolism, behavior, autoimmunity, and stress [210-212]. Additionally, the microbiome can influence hormone levels through their own network of genes that metabolize host secreted hormones [213]. Weger and co-workers found that the gut microbiome was necessary for regulating sex-specific diurnal fluctuations in serum testosterone, estradiol and growth hormone which was required for sexual maturation [214]. Furthermore, host hormones may modulate the composition of the microbiome, suggesting a bi-directional crosstalk between the microbiome and host [215]. The cross-talk between the microbiome and endocrine system poses another avenue by which gut microbes could influence skeletal muscle plasticity and performance, either by directly contributing to systemic adaptations or indirectly by influencing maturation.

In groundbreaking work from Markel and co-workers, germ-free male and female mice had significantly lower serum testosterone levels compared to their SPF counterparts [216]. Remarkably, transferring the microbiome from a male mouse into young female recipients significantly increased serum testosterone levels [216]. Growth hormone (GH) and insulin like growth factor-1 (IGF) levels also seem to be sensitive to the microbiome, as it was found that germ-free mice had significantly lower levels compared to conventionally raised mice [214, 217]. Monocolonization with *L. plantarum* of germ-free mice resulted in a significant increase in GH, IGF-1, and IGFBP-3 at 28 and 56 days after birth [217]. Monocolonized mice had a 14% increase in the rate of growth that resulted in germ-free mice weighing 52% more than SPF control mice [217]. Although skeletal muscle was not analyzed, the findings from Yan and co-workers are consistent with previous studies showing that the microbiome increased systemic IGF-1 and IGFBP3 levels, which stimulated bone formation [218]. The microbiome-IGF axis was mediated by SCFAs, providing further evidence that microbial-derived metabolites can regulate host hormone levels [218].

Additional evidence for bidirectional crosstalk between the gut microbiome and endocrine system was shown with castrated cattle that have an altered microbiome

compared to the non-castrated controls. The castrated cattle were found to have lower testosterone and greater adiposity with significant differences in their microbiome compositions [219]. When mice received a fecal transplant from either castrated or sham operated male mice, there was a significant decrease in serum testosterone and significant increase in fat deposition in the mice who received the microbiome of castrated mice [219]. These findings have implications for exercise adaptations and human performance given the ability of anabolic hormones such as testosterone and GH to promote greater skeletal muscle mass. Given the endocrine-microbiome axis, manipulation of microbiome represents a potentially new ergogenic aid to enhance athletic performance.

As mentioned earlier, an area of microbiome research is the determining the effect of microbial-derived metabolites on host physiology. Deng and co-workers showed the gut microbiome produces numerous metabolic products including, amino acids, central carbon metabolites, dinucleotide cofactors, vitamin B5 and GABA [220]. The vast number of metabolites generated from the microbiome offers novel mechanisms of host cellular regulation which could result in new therapeutics or biomarkers for disease. Interestingly, a single gut microbial metabolite can be viewed as beneficial or toxic depending on a variety of contributing factors. The next sections will provide a brief overview of microbial-derived metabolites and their effect on the host physiology.

#### 1.1.6 Gut Microbial Metabolites

Microbial metabolites have been broadly classified as short chained fatty acids (SCFA), secondary bile acids, amino acids, neurotransmitters and lipids [221-223]. Microbial metabolites have been implicated in numerous disease states such as obesity, cancer, autism, Parkinson's, depression, anxiety, inflammatory bowel disease, heart and lung disease [189-191, 193, 224, 225]. Microbial metabolites have also been shown to play a role in normal host metabolism; for example, the gut microbiome contributes to the production of NAD<sup>+</sup> a major cofactor involved in redox metabolism that is essential for the removal of acetyl groups from their substrates [226, 227]. Our understanding of the causal role between microbial metabolites and host physiology remains in its infancy but emerging evidence suggests these metabolites contribute to host health [211]. Microbially derived metabolites may also be represent unique biomarkers for certain pathologies as

Gyu Oh and co-workers determined that 17 different gut microbial derived metabolites could predict non-alcoholic liver fatty acid disease [228]. The following sections will outline the major microbial metabolites and present evidence on how they could regulate skeletal muscle physiology.

#### 1.1.7 Short-Chained Fatty Acids (SCFA)

SCFA differ by the number of carbons that make up the backbone of each molecule; formate (C1), acetate (C2), propionate (C3), butyrate (C4) and valerate (C5). SCFAs are the most well-studied bacterial metabolites in microbiome research [229, 230]. SCFAs are produced through bacterial fermentation of carbohydrates mainly through the five metabolic pathways: 1) Wood-Ljungdahl pathway (Acetate) [231]; 2) Acrylate Pathway (Propionate); 3) Succinate Pathway (Propionate) [232]; 4) Propanediol Pathway (Propionate) [232]; and 5) Butyrate Synthesis Pathways (Butyrate), in which L-glutamate, carbohydrates, and succinate are the precursors [233, 234]. SCFAs are primarily utilized by colonic epithelial cells but can be readily detected in the human blood at concentrations of roughly 70-173, 4-5 and 4-8  $\mu\text{mol/l}$  for acetate, propionate and butyrate, respectively [235, 236]. SCFAs participate in numerous signaling cascades, pathologies and recently have been found to modulate the epigenetic landscape of various tissues [237]. The role of SCFAs on host disease are continually emerging and growing evidence supports that these metabolites modulate a wide range of pathologies such as inflammation, Alzheimer's, Parkinson's, obesity, and some forms of cancer [238-241]. Importantly, SCFAs have been suggested to participate in cross-talk with skeletal muscle and the cardiovascular system, proposing a direct link between the microbiome metabolites and striated muscle [200, 242, 243].

Mechanistically, SCFAs have been shown to act in diverse ways which could potentially enhance the function of skeletal muscle. SCFAs act as ligands for G-coupled protein receptors (GPCR), specifically the GPCRs known as free fatty acid receptors (FFAR 1-4), with FFAR 2 and 3 being the most widely studied [244]. SCFAs have also been suggested to increase muscle grip strength, and muscle size [199], increase the abundance of Type 1 muscle fibers [245], increase the expression of phosphorylated AMP-activated protein kinase (AMPK) in both the gastrocnemius muscle and liver [246, 247] and improve

glucose/insulin metabolism [248]. Recent research highlights that the SCFA butyrate could prevent skeletal muscle atrophy [200] making butyrate a potentially valuable therapeutic for conditions where there is a high-degree of muscle loss. Future research needs to establish the mechanism by which SCFA act in skeletal muscle to modulate the anabolic and catabolic pathways.

Microbially produced SCFAs are potentially a major metabolite that could directly or indirectly regulate skeletal muscle by modulating muscle growth and and/or function and they have been shown to improve exercise performance by serving as an alternative energy source. SCFAs can be used as an energy source with the complete oxidation of acetate, butyrate and propionate yielding 10, 27 and 18 ATP/M, respectively [249]. Okomoto and co-workers found that acetate supplementation significantly improved exercise capacity in mice after antibiotic depletion of the gut microbiome [250]. Scheiman and co-workers performed intrarectal administration of propionate in mice, which resulted in a significant increase in treadmill run time [205]. These studies were unable to mechanistically describe exactly how the SCFAs improved running performance, but Scheiman and co-workers hypothesized the muscle might be utilizing propionate for fuel [205]. Data from human studies supports the findings from animal studies that SCFAs contribute to exercise performance as seen by Yu and co-workers who demonstrated higher enrichment of SCFA producing microbes in individuals with higher exercise capacity [251]. Furthermore, Allen and co-workers determined that exercise caused a significant increase in SCFAs producing bacteria in lean but not obese individuals [180]. Moreover, the exercise-induced increase in SCFA producing microbe abundance returned to baseline levels once training ceased [180], demonstrating that exercise promotes the growth of SCFA producing bacteria.

Exciting evidence is emerging that suggests SCFAs can function as inhibitors of histone deacetylases (HDACs) [252] and provide acetyl groups that directly modify histones [253]. These results support the exciting idea that the microbiome participates in gene regulation through modulating the epigenetic landscape of host DNA. Recently epigenetic regulation of enhancer and MYC- associated areas within ribosomal DNA was found to occur in response to resistance exercise [254], providing evidence that gene

modifications are important in skeletal muscle adaptations to exercise. Although to date no study has directly linked the gut microbiome and skeletal muscle epigenetic modifications, it seems plausible this could be a possible mechanism as it has been shown in other tissues [237].

### 1.1.8 Bile Acids

Bile acids are products of cholesterol metabolism synthesized in hepatocytes and play an important role in the absorption of dietary lipids and lipid soluble vitamins [255]. The two main bile acids are cholic acid (CA) and chenodeoxycholic acid (CDCA). CA and CDCA are rendered bile salts upon conjugation to either glycine or taurine, and then are stored in the gallbladder until cholecystokinin stimulates their release [256]. In addition to their role on lipid metabolism, bile acids serve as ligands for three nuclear receptors 1) Farnesoid X-receptor, 2) vitamin D receptor and 3) the GCPR, TGR5 [257]. Roughly 95% of bile salts are reabsorbed via the apical sodium-dependent transporter (ASBT) with the remaining bile salts susceptible to modification by the gut microbiota [257]. Microbes which possess the bile salt hydrolase enzymes can deconjugate the primary bile salts by removing the glycine or taurine amides. Microbial modifications continue as bacteria with bile acid-inducible operon (bai) genes can dehydroxylate the deconjugated bile acids into secondary bile acids [258]. In addition to modifying bile salts, the microbiome has been shown to alter the expression of genes involved with bile acid synthesis and transport in both the ileum and liver [259]. In this way, the microbiome can adjust the production of secondary bile acids by regulating the synthesis of bile acids [258]. Bile acids themselves have also been shown to influence microbial composition of both gram negative and positive bacteria [260] demonstrating a bidirectional interaction between microbes and bile acids.

Bile acids that have been modified by the gut microbiome such as lithocholic acid (LCA) and deoxycholic acid (DCA) have been shown to be an agonist for the G-protein coupled receptor, TGR5 [258]. Chaudhari and co-workers found that the microbiome dependent LCA drove the expression of cholic-acid-7-sulfate which was identified as another agonist for TRG5 receptors [261]. Thus, microbial modified bile acids can directly or indirectly activate TGR5 which is known to control expression of key genes involved in

metabolism and energy expenditure [262]. TGR5 is expressed in skeletal muscle, raising the possibility that microbial derived bile acids could signal to skeletal muscle via TGR5. Studies which have investigated the role of TGR5 in skeletal muscle reported that its activation promotes skeletal muscle hypertrophy, differentiation and glucose homeostasis [263-265]. Abrigo and co-workers recently found that supplementing C2C12 myotubes with DCA resulted in an atrophic effect by significantly increasing the expression of the E3 ubiquitin ligases, atrogin-1 and MuRF-1 [266]. These contrasting results are not fully understood and need to be further validated. None-the-less, these findings highlight that bile acids do have the ability to directly activate TGR5 and cause changes in skeletal muscle size.

#### 1.1.9 Amino Acids

The ability of amino acid supplementation to augment skeletal muscle hypertrophy has been well-documented over the last 20 years [267]. Studies have demonstrated that the ingestion of amino acids, primarily the branched chain amino acids (BCAA, leucine, isoleucine and valine), enhances protein synthesis resulting in increased skeletal muscle growth [268, 269]. Additionally, the amino acid glutamine was found to support the immune system resulting in significantly lower infection rates after completion of a marathon [270]. While amino acids are produced via host metabolism (non-essential amino acids) or acquired through the diet (essential amino acids), stable isotope resolved metabolomics (SIRM) has revealed that the gut microbiome can synthesize 36 different amino acids [220]. These experiments were carried out in an ex-vivo fashion, hindering the ability to determine if these amino acids are taken up by the host. Choi and co-workers demonstrated that microbial fermentation of BCAA resulted in the production of branched chained fatty acids (BCFAs) [271]. These BCFAs were found to promote hepatic insulin resistance, with no effect on skeletal muscle [271].

When Lui and co-workers exercise trained individuals for 12 weeks, they found that those who improved their glycemic responses had increases in SCFA production and BCAA catabolism. Contrastingly the non-responders had increased levels of phenylalanine, indole, histidine, leucine, and p-Cresol. Administration of microbial derived BCAA exerted a pro-growth effect in *Drosophila* by activation of TORC-1 [272]. There

are many factors to consider when looking at the role of amino acid on the microbiome or microbial produced amino acids effect on the host. More studies need to determine what factors may be linked to disease or improvements in host health. It appears that microbially derived amino acids or metabolic derivatives can activate TORC-1. In the context of muscle growth, transient increases in TORC-1 activation mediated by the microbiome would be beneficial, potentially enhancing any pro-growth stimulus. Continuous activation of TORC-1 over time may result in deterrents to skeletal muscle such as impaired glucose handling, anabolic resistance, or autophagy.

Tryptophan (Trp) is the largest amino acid by molecular weight, with a complex structure containing an indole and a bicyclic ring consisting of a benzene and pyrrole linked to the alpha carbon amino acid through a methylene group [273]. Trp is the least abundant amino acid, with a frequency of roughly 1.4% (leucine by comparison is 9%) [274] but because of its complex structure it serves as an excellent source for host-microbiome interactions [223]. Trp has several different fates in the gastrointestinal tract It can be metabolized by host cells and microbes resulting in the production of serotonin, kynurenine and ligands for aryl hydrocarbon receptors (AhR) [275]. Microbial metabolism of Trp results in the production of indole and indole derivative compounds; tryptamine, indoleacetic acid (IAA), indole propionic acid (IPA), indolelactic acid (ILA) and indoleacrylic acid (IA) [223, 276]. The direct effects of microbial derived indoles on skeletal muscle is not known, however they have been found to attenuate inflammation [277, 278]. If these metabolites play a role in mitigating inflammation, they may modulate skeletal muscle plasticity by influencing immune cells within the muscle, such as macrophages, which are known to have an important role of muscle adaptation to exercise [279].

As mentioned above, Trp can also be shuttled to the kynurenine pathway via the rate limiting enzyme IDO. The kynurenine pathway produces many metabolites known as “kynurenines” with the end product being nicotinamide adenine dinucleotide (NAD) [280]. IDO expression has been previously shown to be dependent on the microbiome, as the transcript is not found in germ-free mice [281, 282]. Thus, the generation of kynurenines could be heavily influenced by the microbial regulation of IDO. Interestingly, elevated



expression of PGC-1 $\alpha$ 1 in exercising muscle was associated with increased expression of kynurenine aminotransferases (KAT) which catalyze the conversion of kynurenine to kynurenic acid [283]. Using carbidopa (used to inactivate a co-factor for KAT activity), Agudelo and co-workers determined KAT inhibition resulted in decreased running performance and ex-vivo muscle strength in mice [284]. The increase in kynurenic acid generates glutamate as a byproduct which is then shuttled from the cytosol into the mitochondria where it participates in the reduction of NAD<sup>+</sup> to NADH through the malate aspartate shuttle [284]. From this work it is apparent that exercised muscle can take a toxic chemical and convert it to a beneficial compound that can enhance performance. It remains to be determined if the gut microbiome contributes to an increased utilization of kynurenine by skeletal muscle by modulating the expression of IDOs. This line of inquiry represents an attractive area of research linking the gut microbiome-skeletal muscle-brain axes.

#### 1.1.10 Lipids

One of the fundamental building blocks of the cell is lipids, which consist of thousands of different species, accounting for a diverse set of structural and signaling molecules [285]. Lipids represent a major fuel source to power prolonged endurance exercise, provide energy during periods of low food intake, contributes to thermogenesis and plays a role in the regulation of glucose handling [286-288]. Lipids are primarily synthesized in the endoplasmic reticulum, Golgi apparatus and to a lesser extent mitochondria and peroxisomes [289, 290]. Recently, Brown and co-workers demonstrated that the gut microbe *Bacteroides thetaiotaomicron* (*B. theta*) contributed to host sphingolipid bioavailability and were negatively correlated with intestinal inflammation [291]. In addition, *Bacteroides* sphingolipids were significantly decreased during active periods of ulcerative colitis and Crohn's disease [291]. This work was followed up by Johnson and co-workers who further demonstrated that sphingolipids produced from *B. theta* could be metabolized by host epithelial cells [222]. These same authors determined that supplementation with *B. theta* could modulate host hepatic ceramide production [222], suggesting that bacterial derived lipids contribute to the bioavailability of host lipids. Most recently, Rienzi and co-workers showed that hepatic sphingolipid levels were modulated by the gut microbiome mass in mice, but not plasma fatty acids [292]. Although specific

microbes were not identified in this study these results suggest that the microbiome regulates lipid production with a high degree of specificity. Ceramide is a precursor to complex sphingolipids and has been shown to contribute to insulin resistance [293], cancer cachexia [294], and associated with elevated risk for adverse cardiovascular events [295], implying a negative role of ceramides in health and disease. Interestingly, ceramide levels in skeletal muscle are elevated after exercise and the ceramide derivative, sphingosine-1-phosphate, was shown to reduce muscle fatigue in isolated mouse extensor digitorum longus muscle [296] and is important for maintaining mitochondrial respiration in cardiomyocytes [297].

## Conclusion

Skeletal muscle is an extremely well-organized and complex tissue, which contributes to many aspects of life. In addition, the gut microbiome provides another intricate system that help to shape the host through development, aging and certain pathologies. Research is now demonstrating how the microbiome regulates skeletal muscle in both health and disease. While the details remain to be defined, the emerging evidence provides strong support for microbial- derived metabolites entering systemic circulation and subsequently directly affecting the cellular activity of skeletal muscle. Providing a complete understanding of how the microbiome could shape muscle both in terms of anabolic and catabolic signaling pathways will allow researchers to design new strategies to combat the loss of muscle, rescue developmental disorders or provide ergogenic aids enhance athletic performance.

## CHAPTER 2. DYSBIOSIS OF THE GUT MICROBIOME IMPAIRS MOUSE SKELETAL MUSCLE ADAPTION TO EXERCISE (PUBLISHED IN JOURNAL OF PHYSIOLOGY, SEPTEMBER 2021)

### Introduction

Skeletal muscle is one of the largest organs of the body representing close to 50% of total body mass. Skeletal muscle functions as a biological motor that allows for the production of work, heat generation, regulation of blood glucose and as a reservoir of amino acids [3, 298-301]. A remarkable quality of skeletal muscle is the ability to alter its physical characteristics in a specific manner in response to regular bouts of exercise. The cellular and molecular mechanisms that underlie this adaptive ability are an area of intense research given the importance of skeletal muscle to overall health.

There is exciting evidence to suggest the gut microbiome may play a role in regulating skeletal muscle mass and function. In a pioneering study, Bäckhed and co-workers reported skeletal muscle of germ free (GF) mice (completely devoid of any commensal bacteria) had significantly higher levels of phosphorylated AMPK and acetyl-CoA carboxylase compared to specific pathogen free (SPF) mice, indicating GF mice rely more heavily on fatty acid oxidation as an energy source and might explain why GF mice are more resistant to obesity [193]. Additionally, skeletal muscle of GF mice is atrophic compared to SPF mice and inoculating GF mice with microbiota was able to restore muscle mass [199]. Exercise has been shown to modulate the composition of the microbiome with specific microbes associated with enhanced exercise capacity [205, 206, 302, 303]. Exercise-induced changes in the gut microbiome were reported to have systemic benefits, indicating the microbiome of an exercise trained host is protective against a range of different pathologies [304-307]. These findings have generated great excitement in the exercise physiology field as well as other fields of research seeking to utilize the microbiome to treat diseases such as cancer, depression, obesity, Parkinson's and autism [188, 189, 191, 193, 308]. A better understanding of the role of the gut microbiome in skeletal muscle plasticity could ultimately provide new interventions to treat conditions such as cachexia and sarcopenia, the age-related loss in skeletal muscle mass and function.

Although there is emerging evidence to support the concept of a gut microbiome-skeletal muscle axis [309-313], there remains a scarcity of studies investigating the potential role of the gut microbiome in skeletal muscle adaptation to exercise. The purpose of this study was to test the hypothesis that the gut microbiome is required for skeletal muscle adaptations to exercise. To test this hypothesis, mice were treated with or without antibiotics throughout an nine-week progressive weighted wheel running (PoWeR) protocol which has been shown to induce hypertrophy and a fiber-type shift to a more oxidative phenotype [314]. Despite the same exercise stimulus, antibiotic-treated mice had a blunted hypertrophic response and fiber-type shift compared to the untreated mice. These findings provide the first evidence showing that disruption of the gut microbiome impairs skeletal muscle adaptation to exercise and suggest the exciting possibility that microbially derived metabolites have an important role in skeletal muscle plasticity.

## Methods

### 2.1.1 Mice

Adult (4 months of age), female C57BL/6J mice were purchased from The Jackson Laboratories (Bar Harbor, ME). Upon arrival, mice were housed 4-5 per cage and acclimated for one month to allow for the gut microbiome to become stabilized to the new housing facility [315]. Mice were then randomly assigned to one of four groups (n=10-11/group): 1) Non-running control untreated (CU), 2) PoWeR untreated (PU), 3) Non-running control treated with antibiotics (CT) and 4) PoWeR treated with antibiotics (PT). All non-running control mice were housed individually in a running wheel cage as the PoWeR mice, except the running wheel remained locked for the duration of the study. One mouse in the CT group died unexpectedly three days before completion of the study thus the CT group had n=9. Animals were kept on a 10:14 light cycle with irradiated chow (Teklad 2918 protein rodent diet) and water ad libitum. Fresh, autoclaved water with or with antibiotics was provided each week. Food and water consumption were measured weekly. Cage and bedding were changed each week with dirty bedding from the previous week pooled for each group and then added to clean bedding in a ratio of 2/3

clean bedding and 1/3 dirty bedding in an effort to reduce microbial drift during the course of the study [316].

### 2.1.2 Antibiotic Treatment

Upon completion of the acclimation period, mice were randomly assigned to a group (CU, CT, PU or PT), then placed singly into a running wheel cage with antibiotic treatment initiated for CT and PT groups. Antibiotic treatment was started one week prior to PoWeR training, designated week 0, to allow for depletion of the microbiome prior to exercise [317]. Antibiotics were continuously administered via the drinking water and prepared fresh twice per week. Each time new antibiotics were administered, drinking volume was collected resulting in fluid consumption measurements taken twice per week. In the untreated groups, mice received the same autoclaved water, which was changed at the same time as the antibiotic treated groups. The antibiotic cocktail was modified from [318, 319] and consisted of 100 µg/ml each of metronidazole (Sigma, M1547), neomycin (J&K, 557926), and ampicillin (Sigma, A0166) and 50 µg/ml each of vancomycin (Sigma, V2002) and streptomycin (Life Technologies, 1513783). This antibiotic cocktail was chosen because it was shown to not cause weight loss and lethargy [319].

### 2.1.3 Progressive Weighted Wheel Running (PoWeR)

Mice underwent eight weeks of the PoWeR protocol as previously described by our group; PoWeR training was shown to induce hypertrophy and a fiber-type shift in muscles of the lower hind limbs [314]. Mice were singly housed in running wheel cages with free access to the running wheel. Individual running data (km/d) and total running volume (km) was recorded using ClockLab software (Actimetrics, Wilmette, IL). During the first week of training, mice ran with an unloaded wheel to allow for acclimation to the running wheel. After the acclimation period (week 1), weight was loaded onto the wheel for a training intensity that consisted of 2g during week 2, 3g during week 3, 4g during week 4, 5g during week 5 and 6 and 6g during weeks 7-9. The weight consisted of 1g magnets (product no. B661, K&J Magnetics, Pipersville, PA), that were attached on one side of the running wheel.

#### 2.1.4 Immunohistochemistry

Immunohistochemistry (IHC) analysis was performed as previously described by us [56, 314] on the soleus and plantaris muscles to determine skeletal muscle fiber cross-sectional area, fiber-type composition, and myonuclei abundance. Excised soleus and plantaris muscles were immediately weighed, with one limb snap-frozen in O.C.T using liquid nitrogen-cooled isopentane and muscles from the other limb snap-frozen in liquid nitrogen and then stored in  $-80^{\circ}\text{C}$  for biochemical and molecular analyses. Muscle samples were mounted and cut into  $7\mu\text{m}$  sections. Muscle sections were air-dried overnight at room temperature. After drying, the sections were incubated in a cocktail of iso-type specific anti-mouse primary antibodies against myosin heavy chain (MyHC) 1, MyHC 2a (Developmental Studies Hybridoma Bank, Iowa City, IA) in addition to an antibody against dystrophin (catalog no. ab15277, Abcam, St. Louis, MO). Type 2b and Type 2x were not stained and counted based on the lack of staining. For muscle fiber-type composition, we combined Type 2b and Type 2x fibers based on their similar phenotype [320]. Primary antibodies were diluted 1:100 in PBS with slides incubated for two hours at room temperature, then washed three times in PBS and incubated for 90 minutes at room temperature with the appropriate secondary antibodies at a dilution of 1:250. During the final 10 minutes of the secondary incubation, DAPI (Vector Laboratories, 1:10,000) was added to counterstain nuclei. Sections were then washed three times in PBS and mounted using PBS:glycerol solution at a 1:1 ratio. IHC for Pax7<sup>+</sup> was performed according to the protocol established by our laboratory [56, 321].

#### 2.1.5 Image Capture and Analysis

IHC sections were captured at 20X magnification using an upright fluorescence microscope (AxioImager M1, Zeiss, Oberochen, Germany). Quantification of skeletal muscle cross-sectional area, fiber-type specific cross-sectional area, fiber-type distribution and myonuclei abundance was quantified using MyoVision automated analysis software [322].

#### 2.1.6 Fecal DNA Extraction

Fecal samples were collected upon transferring co-housed mice to individual wheel cages, prior to antibiotic administration and 48 hours prior to euthanasia at week 10.

Fecal samples were collected by placing a single mouse in a clean, sterile plastic cage and allowing the mouse to defecate at will. Fresh feces were placed in a sterile Eppendorf tube and immediately placed in dry ice. Samples were then stored at  $-80^{\circ}\text{C}$  until further analysis. DNA was isolated using the PureLink™ Microbiome DNA Purification kit (catalog no. A29790, ThermoFisher Scientific) according to the manufacturer's instructions. Briefly, samples were weighed and then subjected to mechanical (bead beating), chemical and heat lysis, followed by washing and then final elution in 25  $\mu\text{l}$  of DNase-free water.

### 2.1.7 Metagenomic Sequencing

A subset of samples ( $n=6$  for CU, PU, CT and PT (pre) and  $n=6$  for CU, PT,  $n=5$  for PU and CT (post) were sent to CosmosID® (CosmosID Inc., Rockville, MD, United States) for metagenomics sequencing as previously described [323]. Fecal DNA concentration was quantified via fluorescent spectroscopy with a Qubit (ThermoFisher Scientific) and DNA libraries were prepared using the ThermoFisher IonXpress Plus Fragment Library Kit according to the manufacturer's protocol. Library quantity was assessed with Qubit and sequenced on a ThermoFisher Ion S5 XL sequencer. Single read sequences, without adapters generated kmers between 150-300 base pairs. The short sequence reads were first inputted into the reference genome curated by CosmosID which generated variable length k-mer fingerprints that were associated with distinct phylogeny of microbes. Next, the short reads were aligned against a known set of variable length k-mers to yield a precise taxonomic classification and relative abundance estimates for microbial next generation sequencing datasets. False positives were excluded by using a filtering threshold that was determined by analyzing large numbers of diverse metagenomes. Sequences were referenced with CosmosID's GenBook® database and analyzed using the CosmosID cloud app (CosmosID Metagenomics Cloud, [app.cosmosid.com](http://app.cosmosid.com), CosmosID Inc., [www.cosmosid.com](http://www.cosmosid.com)). The curated database allows for high resolution of millions of short reads corresponding to discrete microorganisms which are void of contamination from the host. The Genbook® contains over 150,000 bacteria, viruses, fungi and protist genomes, including both coding and non-coding sequences [324].

### 2.1.8 Cytokine Assay

Serum cytokines (TNF- $\alpha$ , INF- $\gamma$ , IL-6, IL-10 and IL-17a) were measured using Meso Scale Discovery (MSD, Gaithersburg, MD), U-PLEX customized multiplex immunoassay according to manufacturer's directions. We have chosen to measure the serum concentration of the cytokines because they are accepted markers of systemic inflammation [325-328]. Following collection, blood was centrifuged at 1500 g for 15 minutes with the resulting serum centrifuged at 3000 g for 15 minutes. The cleared serum was stored at -80°C until analysis. To measure serum cytokine levels, the stored serum was thawed in duplicate, 25  $\mu$ l aliquots added per well to MSD plate coated with capture antibodies for TNF- $\alpha$ , INF- $\gamma$ , IL-6, IL-10 and IL-17a.

### 2.1.9 Euthanasia

Twenty-four hours prior to euthanasia, all running wheels were locked for the PoWeR trained mice. In addition, mice were fasted for 5-6 hours prior to euthanasia. Mice were anesthetized by isoflurane (1-2%) inhalation, and once fully sedated, blood was collected followed by excision of the heart (to ensure death) and then skeletal muscles.

### 2.1.10 Statistical Analysis

Data is presented as mean  $\pm$  standard deviation (SD) with significance set at  $p$ -value < 0.050. A normality check was performed using a Shapiro-Wilk test. In the event the data was not normally distributed, we performed a log transformation and reassessed for normality to obtain a normal distribution. Weekly food and water consumption, body weight and running volume was compared using a repeated measures 2-factor ANOVA (Group X Time). Skeletal muscle fiber cross-sectional area, fiber-type specific cross-sectional area, fiber-type distribution, myonuclei and Pax7<sup>+</sup> abundance, end point body weight, ceca weight, number of reads and number of bacterial species were analyzed by a 2-factor ANOVA (Antibiotic treatment X PoWeR training). In the case of significance, post hoc analysis was performed using a Tukey's-HSD to correct for multiple comparisons. During the IHC analysis, one soleus in the CU group was damaged beyond repair and was not included in any of the soleus comparisons. Outliers were detected first



by subtracting 1.5 x (IQR) from the first quartile and adding 1.5 x (IQR) to the third quartile. We then cross checked using the Grubb's test (Graph Pad).

## Results

The study design is presented in Figure 2.1. During the four-week acclimation period there were no reported complications with the mice. Upon completion of the acclimation period, mice were randomly separated into singly housed running wheel cages with a pre-fecal (Pre) sample immediately collected. Once Pre-samples were collected, mice in the antibiotic assigned groups began antibiotic treatment via drinking water for one week, during which time running wheels remained locked. After the first week of antibiotic treatment, running wheels were unlocked for those mice in the PoWeR groups. Upon completion of PoWeR training, feces were collected 48 hours prior to euthanasia from all mice to obtain a post-fecal (Post) sample. No complications were reported at any time during the duration of this study including when the mice were singly housed in wheel running cages, fecal collections or during the training period. One mouse in the CT group died three days prior to the completion of the study with the cause of death unknown.

### 2.1.11 Dysbiosis of the Gut Microbiome by Antibiotic Treatment

As shown in Figure 2.2A, there was no difference in the number of bacterial species detected in the gut microbiome across all groups prior to antibiotic treatment. Antibiotic treatment significantly (main effect of antibiotic treatment,  $p < 0.0001$ ) reduced the number of bacterial species detected within the gut microbiome (Figure 2.2B); furthermore, PoWeR training did not change the number of detected bacterial species compared to their respective non-running control counterparts (Figure 2.2B) Importantly, the loss of bacterial species with antibiotic treatment was not caused by a change in the depth of reads as there was no difference in the number of reads pre- and post-treatment between all groups (Figure 2.2C-D). For the reads at the post time point, one mouse in the CU group was determined to be an outlier (Figure 2.2D). This mouse also had the highest number of species at the post time point (Figure 2.2B), which could be contributing to the higher number of reads. Antibiotic treatment caused a significantly higher cecum weight (main effect of PoWeR training,  $p = 0.0087$ ; main effect of

antibiotic treatment,  $p < 0.0001$ ; interaction,  $p = 0.0352$ ) (Figure 2.2E-F). An overview of the microbiome at the genus taxonomic level revealed the antibiotic treatment was effective in reducing the composition of the microbiota (Figure 2.3). Two of the five CT samples had undetectable levels of bacteria and could not be included in the post lanes of the heat map (Fig. 3). Together, these findings illustrate that antibiotic treatment effectively induced dysbiosis of the gut microbiome which was not affected by PoWeR training.

#### 2.1.12 PoWeR Increased Food and Water Consumption

Time course analysis revealed higher food consumption, starting at weeks 1 and 2, and water consumption, starting at weeks 3 and 5, and remained significantly higher in the PoWeR groups compared to their respective non-running control counterparts for the duration of the study (Figure 2.4A-B).

#### 2.1.13 Body Weight

There was a significant main effect of time ( $p < 0.0001$ ) and group ( $p = 0.0004$ ) with a significant interaction ( $p < 0.0001$ ) for body weight throughout the study. The body weight of the PT group was significantly higher than PU and CU groups from week 3 thru 10. In addition, the body weight of the CT group was significantly higher than the PU for weeks 9 and 10 (Figure 2.4C). The higher final body weight of the antibiotic treated groups was caused by enlargement of the cecum. When the cecum weight was subtracted from the final body weight, there was no difference in body weight between any groups (Figure 2.4D).

#### 2.1.14 Running Volume

As shown in Fig. 5A-B, there was no difference in the weekly or total running volume between the PoWeR groups despite a progressive increase in the amount of weight (2g to 6g) added to the running wheel over the course of the eight-week PoWeR training period.

#### 2.1.15 Soleus

##### 2.1.15.1 Muscle Wet Weight

In response to PoWeR training, there was a significant main effect of PoWeR training ( $p = 0.0002$ ) and interaction ( $p = 0.0005$ ) with a trend ( $p = 0.0540$ ) for a significant effect of antibiotic treatment for normalized (to body weight) soleus wet weight. Normalized soleus wet weight was significantly larger in the PU group compared to CU ( $p < 0.0001$ ), CT ( $p < 0.0008$ ) and PT ( $p < 0.0007$ ). The PT showed no increase in normalized soleus wet weight. These results were not affected by cecum weight as normalizing soleus muscle wet weight to body weight without the cecum weight included still showed the normalized soleus wet weight was significantly higher in the PU group compared to CU ( $p < 0.0001$ ), CT ( $p = 0.0008$ ) and PT ( $p = 0.0007$ ) groups (Figure 2.6B).

#### 2.1.15.2 Fiber Cross-Sectional area (CSA)

In agreement with normalized soleus muscle weight, there was a significant main effect of PoWeR training ( $p = 0.0001$ ) on soleus mean fiber CSA (Figure 2.6C). Post hoc analysis revealed the mean fiber CSA of the PU soleus was 29% larger than CU ( $p = 0.0012$ ) and 31% larger compared to CT ( $p = 0.0007$ ) while there was no difference in mean fiber CSA between the CU, CT and PT groups. When comparing Type 1 fiber CSA, there was a significant ( $p = 0.0302$ ) main effect of PoWeR training on Type 1 fiber CSA. Type 1 fiber CSA was trending towards significance ( $p = 0.0778$ ) between PU and CU groups and was significantly larger ( $p = 0.0464$ ) between PU and CT groups (Figure 2.6D). Fiber-type specific CSA analysis showed the larger mean fiber CSA of the PU soleus was primarily a result of larger Type 2a fiber CSA (main effect of antibiotic treatment,  $p = 0.0330$ ; main effect of PoWeR training,  $p < 0.0001$ ; interaction,  $p = 0.0779$ ) (Figure 2.6D). The PU group had significantly larger Type 2a fiber CSA in comparison to the fiber CSA of CU ( $p < 0.0001$ ), CT ( $p < 0.0001$ ) and PT ( $p = 0.0238$ ) groups. The PT group had significantly larger Type 2a fiber CSA compared to CT ( $p = 0.0463$ ).

#### 2.1.15.3 Myonuclei Abundance

There was a significant ( $p = 0.0330$ ) main effect of PoWeR training on myonuclei abundance in the soleus muscle; however, post hoc analysis revealed no significant difference between groups in response to PoWeR training.

#### 2.1.15.4 Fiber-Type Composition

One mouse in the CT group was classified as an outlier (see Methods) for fiber-type distribution and subsequently removed from all fiber-type distribution analyses. In response to PoWeR training there was a main effect ( $p < 0.0001$ ) for Type 1 fiber abundance. PU had 17% more Type 1 fibers compared to CU ( $p = 0.0058$ ) and 20% more compared to CT ( $p = 0.0026$ ) while PT had 21% more Type 1 fibers compared to CU ( $p = 0.0008$ ) and 23% more compared to CT ( $p = 0.0004$ ) (Figure 2.7B). Comparing the abundance of Type 2a fibers, there was a significant main effect of PoWeR training ( $p < 0.0001$ ). PU had 20% less Type 2a fibers compared to CU ( $p = 0.0220$ ) and 15% less compared to CT ( $p = 0.0116$ ). PT had 25% less Type 2a fibers compared to CU ( $p = 0.0074$ ) and 26% less compared to CT ( $p = 0.0039$ ) (Figure 2.7B). In addition, there was a significant ( $p < 0.0001$ ) main effect of PoWeR training on Type 2b/x fiber abundance. PU had 88% less Type 2b+x fibers compared to CU ( $p = 0.0003$ ) and 87% less compared to CT ( $p = 0.0009$ ). PT had 55% less Type 2b+x fibers than CU ( $p = 0.0312$ ) and a trend towards lower Type 2b/x fiber abundance compared to CT ( $p = 0.0613$ ). There was no difference in the abundance of fibers that co-expressed myosin heavy chain isoforms Type 1+2a (Figure 2.7B).

#### 2.1.16 Plantaris

##### 2.1.16.1 Muscle Wet Weight

Analysis of normalized (to body weight) plantaris muscle wet weight with the cecum included showed a significant ( $p = 0.0001$ ) main effect of antibiotic treatment. Post hoc analysis revealed that PU was significantly heavier compared to CT ( $p = 0.0108$ ) and PT ( $p = 0.0014$ ) groups. Additionally, the CU group was significantly ( $p = 0.0467$ ) heavier compared to PT. In contrast to the soleus muscle, these differences did not persist when plantaris muscle wet weight was normalized to body weight excluding the cecum (Figure 2.8 A-B).

#### 2.1.16.2 Fiber Cross-Sectional Area (CSA)

In response to PoWeR training, there was a significant ( $p = 0.0012$ ) main effect of training on mean fiber CSA (Fig. 8C). PU mean fiber CSA was 23% larger compared to CT ( $p = 0.0109$ ). There was a trend for significantly larger mean fiber CSA between PU and CU ( $p = 0.0767$ ) and between PT and CT groups ( $p = 0.0831$ ) (Fig. 8C). In regards to fiber-type specific CSA, there was a significant ( $p < 0.0001$ ) main effect of PoWeR training on Type 2a fiber CSA. PU had 42% and 47% larger Type 2a fiber CSA compared to CU ( $p < 0.0001$ ) and CT ( $p < 0.0001$ ), respectively (Figure 2.8D). PT had 27% and 31% larger Type 2a fiber CSA compared to CU ( $p = 0.0137$ ) and CT ( $p = 0.0064$ ), respectively (Figure 2.8D). There was a significant main effect of PoWeR training ( $p = 0.0011$ ) and main effect of antibiotic treatment ( $p = 0.0282$ ) for Type 2b/x fiber CSA (Figure 2.8D). Type 2b/x fibers of PU were 24% larger compared to CU ( $p = 0.0257$ ) and 37% larger compared to CT ( $p = 0.0013$ ). Type 2b/x fiber CSA was not different when comparing PT to CU ( $p = 0.8000$ ) and CT ( $p = 0.1827$ ) groups (Figure 2.8D).

#### 2.1.16.3 Myonuclei Abundance

There was a significant ( $p = 0.0120$ ) main effect of PoWeR training for myonuclei abundance. Myonuclei abundance of PU was 65% higher compared to CU ( $p = 0.0136$ ) and 51% compared to CT ( $p = 0.0494$ ) (Figure 2.8E). There was no difference in myonuclei abundance when comparing PT and CT groups ( $p = 0.9443$ ).

#### 2.1.16.4 Satellite Cell Abundance

Satellite cell abundance was determined using Pax7 immunohistochemistry. There was a significant main effect of PoWeR training ( $p = 0.0467$ ) and interaction ( $p = 0.0401$ ) for the abundance of Pax7<sup>+</sup> nuclei/100 fibers. Post hoc analysis revealed PU had 50% more Pax7<sup>+</sup> nuclei compared to the CU ( $p = 0.0236$ ). There was no difference ( $p = 0.2782$ ) in satellite cell abundance between the CU and CT groups. Finally, there was no difference ( $p = 0.6546$ ) when comparing the PU and PT groups in satellite cell abundance (Figure 2.8G).

#### 2.1.16.5 Fiber-Type Composition

There was a significant ( $p < 0.0001$ ) main effect of PoWeR training on the percentage of Type 2a fibers (Figure 2.9B). PU had 89% more Type 2a fibers compared to CU ( $p < 0.0001$ ), 94% more compared to CT ( $p < 0.0001$ ) and 24% more compared to PT ( $p = 0.0467$ ) (Figure 2.9B). PT had 52% more Type 2a fiber compared to CU ( $p = 0.0031$ ) and 57% compared to the CT ( $p = 0.0025$ ) (Figure 2.9B). We also observed a significant main effect of PoWeR training ( $p < 0.0001$ ) and interaction ( $p = 0.0127$ ) for Type 2b/x fiber abundance (Fig. 9C). PU had 66% fewer Type 2b/x fibers compared to CU ( $p < 0.0001$ ), 60% fewer than CT ( $p < 0.0001$ ) and 24% less than PT ( $p = 0.0186$ ) (Figure 2.9B). In addition, PT had 34% fewer Type 2b/x fibers compared to CU ( $p = 0.0004$ ) and 29% less compared to CT ( $p = 0.0040$ ) (Figure 2.9C). As shown in Figure 2.9B, there was no difference in the abundance of Type 1 and hybrid fibers that co-expressed myosin heavy chain isoforms (Type 2a+Type2b/x) across all groups.

#### 2.1.17 Serum Cytokine Levels

IL-6 concentrations of one mouse from the PU group was found to be an outlier. Additionally, IL-17a from another mouse in the PU group was also determined to be an outlier. We moved these values from the specific cytokine analysis. There was no change in the serum concentration of IL-10, IFN $\gamma$ , TNF $\alpha$ , or IL-17a in response to antibiotic treatment and/or PoWeR training (Figure 2.10). When looking at IL-6, there was a significant ( $p = 0.0236$ ) main effect of PoWeR training. Post hoc analysis revealed a trend for IL-6 levels to be elevated when comparing PU to CU ( $p = 0.0590$ ).

#### Discussion

The major finding of the study is that antibiotic-induced dysbiosis of the gut microbiome impaired the ability of skeletal muscle to adapt to exercise training. Despite a similar training stimulus between untreated and antibiotic-treated groups, dysbiosis resulted in blunted hypertrophy in both the soleus and plantaris muscles following PoWeR training. In the soleus muscle of mice with a disrupted gut microbiome, skeletal muscle hypertrophy of Type 1 fibers was blunted and the trend for larger Type 2a fibers observed in untreated mice did not occur. Similarly, in the plantaris muscle, dysbiosis of the microbiome prevented the greater Type 2b/x fiber CSA following PoWeR training

observed in mice with an intact gut microbiome. In untreated mice, the greater abundance of both satellite cells and myonuclei in the plantaris muscle in response to PoWeR training was absent in dysbiotic mice, which likely contributed to their blunted hypertrophic response. We did not find an increase in myonuclei accretion in the soleus muscle and therefore decided to not quantify satellite cell abundance in the soleus muscle. Lastly, the major fiber-type shifts induced by PoWeR training was unaffected by antibiotic-induced dysbiosis of the gut microbiome in the soleus muscle. However, Type 2a fiber abundance nearly doubled in the plantaris muscle which was significantly less in mice with a suppressed microbiome. These findings agree with previous studies showing the gut microbiome influences skeletal muscle mass and fiber-type composition and provide the first detailed evidence that an intact gut microbiome is necessary for skeletal muscle to fully adapt to exercise training [197, 199]

An important finding from our study was that antibiotic-induced dysbiosis of the microbiome did not affect running activity which was critical to ensure a similar training stimulus between the two PoWeR groups. In fact, it might be argued that the training stimulus was greater in the antibiotic treated mice given their heavier body weight caused by an enlarged cecum. In contrast, previous studies found that both antibiotic treated mice and GF mice have reduced exercise performance suggesting a role for the gut microbiome in exercise activity [202, 250, 317]. The discrepancy in exercise activity between these studies and our own could be explained by the lower dose of antibiotics used in the current study or that the mice in this study were given free access to a running wheel while the other studies used time to exhaustion with untrained mice. The antibiotic treatment itself may have negatively impacted exercise time to exhaustion as has been reported in athletes [329]. Alternatively, it could be plausible that an intact gut microbiome is needed for maximal exercise capacity as compared to sub-maximal wheel running exercise activity.

The use of antibiotics in lieu of GF mice is a common method to assess the role of the gut microbiome in health and disease [330]. GF mice are costly, labor intensive and, as shown previously, display muscle atrophy associated with higher expression of atrogenes [199], which creates an issue when trying to investigate the role of the gut

microbiome in skeletal muscle adaptation to exercise. We decided to use antibiotics to suppress the microbiome in order to allow us to use mice in which skeletal muscles, as well as other systems like the immune system, had undergone normal development and maturation with an intact gut microbiome [331, 332]. The lack of an established antibiotic dosing regimen that effectively depletes the gut microbiome with minimal side effects, however, leaves open the possibility that the antibiotics themselves may be directly interfering with cellular and/or molecular mechanisms involved in skeletal muscle adaptation to exercise.

Dysbiosis of the gut microbiome by antibiotics is known to alter immune cell activation which causes a thinning of the mucosal layer with a concomitant increase in intestinal epithelial cell permeability [333-335]. The increase in intestinal permeability with dysbiosis is known to induce low-level systemic inflammation which might induce a state of anabolic resistance leading to the impaired hypertrophic growth observed in antibiotic-treated PoWeR-trained mice. While this possible scenario awaits further investigation, we found no difference in the serum levels of inflammatory cytokines across all groups indicating the absence of low-level systemic inflammation induced by antibiotic treatment. However, these measurements were taken upon completion of PoWeR training allowing for the possibility that systemic inflammation was different at some earlier time point of the study. This concern is offset by the finding that non-running control muscle weights and running activity were not different between antibiotic treated mice nor mice with an intact gut microbiome; thus, indicating antibiotic treatment had minimal effect on skeletal muscle maintenance and function.

What evidence is there to suggest antibiotics might interfere with skeletal muscle adaptation to exercise? A study reported high doses of the antibiotic metronidazole can cause skeletal muscle atrophy; however, this study used a dose 10-fold greater than the dose administered in the current study [336]. Other studies have shown that high doses of aminoglycosides such as gentamycin, neomycin and streptomycin, can affect calcium signaling but these studies used a dose 100-fold greater than the dose used in the current study. Hayo and colleagues utilized eccentric exercise to induce muscle damage in rats who were administered streptomycin, which can reduce intracellular calcium



concentration by blocking stretch activated channels. Although these authors found that streptomycin reduced muscle membrane permeability, it did not affect the amount of myofiber swelling using a dose 80-fold greater than the dose used in the current study [337]. Most recently, Qiu and colleagues reported antibiotic-induced dysbiosis caused muscle atrophy which was shown to be mediated by a suppression of bile acid signaling to FGF15; however, as with the aforementioned studies, these authors used antibiotic doses 100 times greater than those used in the current study [338]. Finally, intraperitoneal injection of the antibiotic imipenem for five consecutive days did not affect muscle specific force [339]. Collectively, these studies demonstrate that antibiotic doses 10-100 times greater than the dose we used can negatively affect muscle size but not muscle function. Given that we observed no difference in muscle phenotype (weight and fiber size and composition) between non-running control groups as well as wheel running activity, we think the relatively low dose of antibiotics administered was able to effectively induce dysbiosis while minimizing any side effects that might have interfered with skeletal muscle adaptation to exercise.

The blunted hypertrophic growth response observed in both slow- and fast-twitch myofibers could be due to a common gut-derived microbial metabolite(s) which is necessary for maximal muscle growth. In support of such a mechanism, Chen and colleagues discovered that *B. theta* C34 bacteria produce L-phenylalanine, an agonist of G-coupled protein receptor 56 (GPCR-56) which was previously shown to be sufficient for skeletal muscle hypertrophic growth as well as required for mechanical overload-induced hypertrophy [340, 341]. Similarly, in a series of studies led by Sato and Sasaki, activation of the G-coupled protein bile acid receptor TRG5 was shown to promote skeletal muscle hypertrophy and improve glucose metabolism [263, 265]. In particular, these authors reported administration of the gut microbial-derived bile acid metabolite, tauro lithocholic acid, induced expression of pro-hypertrophy genes *Nr4a1* and *Pgc-1 $\alpha$*  in transgenic mice that overexpressed TGR5 [263]. Future studies will need to mechanistically determine if gut microbial-derived metabolites play a role in skeletal muscle adaptation to exercise.

Antibiotic dysbiosis of the gut microbiome did not impair the exercise-induced fiber-type shifts in the soleus muscle but did in the plantaris muscle. In the soleus, the loss of Type 2a fibers was similar between the PoWeR-trained groups whereas in the plantaris, the higher abundance of Type 2a fibers was significantly less in mice with a suppressed microbiome. This finding suggests there is some microbial-derived factor(s) that may be necessary to promote the transition to a more oxidative phenotype. In support of this idea, Yan and colleagues demonstrated that the microbiome from two different types of pigs (the obese Rongchang and the lean Yorkshire) could give rise to their distinct muscle fiber-type composition when transferred to GF mice [197]. Based on succinate dehydrogenase staining and gene expression, GF mice were found to have a loss of oxidative capacity across different hind limb muscles that was partially restored following microbial transfer [199]. Collectively, these findings along with the results from the current study support the idea that the gut microbiome facilitate the transition to a more oxidative phenotype in skeletal muscle.

Satellite cell and myonuclei abundance of the plantaris muscle were higher in response to PoWeR training in mice with an intact gut microbiome. The effect of dysbiosis on satellite cells was more ambiguous because some mice in both groups, sedentary and runners, showed higher abundance of satellite cells while other mice appeared to be unaffected by dysbiosis. This variability led to there being no difference in satellite cell abundance between the two PoWeR trained groups. This variable response to dysbiosis may reflect the inherent molecular heterogeneity of satellite cells as revealed by single-cell RNA-sequencing to changes in microbial-derived metabolites, though confirmation of such a mechanism awaits further study [342].

#### 2.1.18 Limitations

The current study has some important limitations that need to be acknowledged. For this initial study, we chose to use C57BL/6J female mice because they are known to be better runners than their male counterparts [343] and we were concerned the disruption of the gut microbiome might negatively impact exercise activity as previously reported [202, 317]. Since the running activity was the same between the antibiotic-treated and untreated groups, thus having an equivalent training stimulus, we were able to draw

stronger conclusions about the influence of the gut microbiome on skeletal muscle adaptation to exercise. Given the reported sexes differences in host-gut microbiome interactions, it will be important for a future study to determine if dysbiosis in males also blunts muscle adaptation to exercise training as observed in females [344, 345]. Beyond wheel running activity, we did not perform any muscle function analyses to determine if the observed phenotypic differences between the PoWeR-trained groups was associated with any change in functional characteristics of the muscle. Thus, future work will need to determine if the changes in fiber size and composition induced by dysbiosis have an impact on maximum and specific force and fatiguability of the muscle. Finally, there is a wide variety of rodent diets used in pre-clinical research which have been reported to significantly alter the composition of the gut microbiome and the production of short-chained fatty acids [346]. Importantly, all mice in the current study consumed exactly the same high protein diet for the duration of the study to ensure adequate protein intake to support skeletal muscle growth in response to PoWeR training.

#### 2.1.19 Conclusions

The findings of this study demonstrate that an intact gut microbiome is required for skeletal muscle to fully adapt to exercise training. Additionally, the findings from this study add to the growing body of evidence supporting a gut microbiome-skeletal muscle axis [195, 198, 199, 219]. Future studies will seek to identify the bacterial species and associated metabolites that play a critical role in facilitating skeletal muscle hypertrophy and the fiber-type shift that occur in response to exercise with the expectation they will be unique for each of these processes.

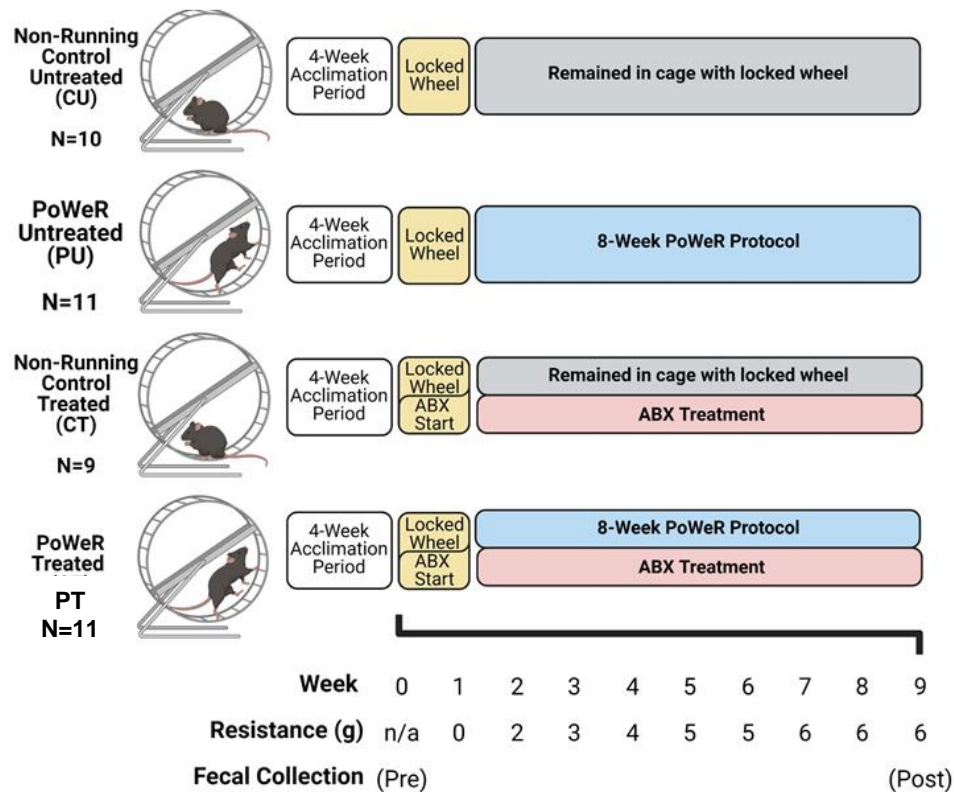


Figure 2.1 Study Design.

Animals were cohoused in groups of four-five for four weeks in order to allow for acclimation to the animal facility at the University of Kentucky. Upon the completion of the acclimation period, mice were randomly split into four different groups and singly housed in running wheel cages. Immediately after randomization into study groups, the first fecal samples were collected (pre), prior to antibiotic administration. During the first week of being singly housed, all wheels were locked, and the antibiotic treatment began. One week after, the wheels were unlocked for those mice in the PoWeR groups, initiating the acclimation week. After the first week of acclimation with an unload wheel, 2g was placed on one side of the running wheel to add resistance. Each week thereafter, an additional 1g was added to the wheel until the load reached a total of 6g for the final three weeks of training. A final fecal sample was collected roughly 48 hours prior to euthanasia. After completion of eight weeks of PoWeR training, mice were euthanized, and tissues were collected for analysis. Image created with BioRender.

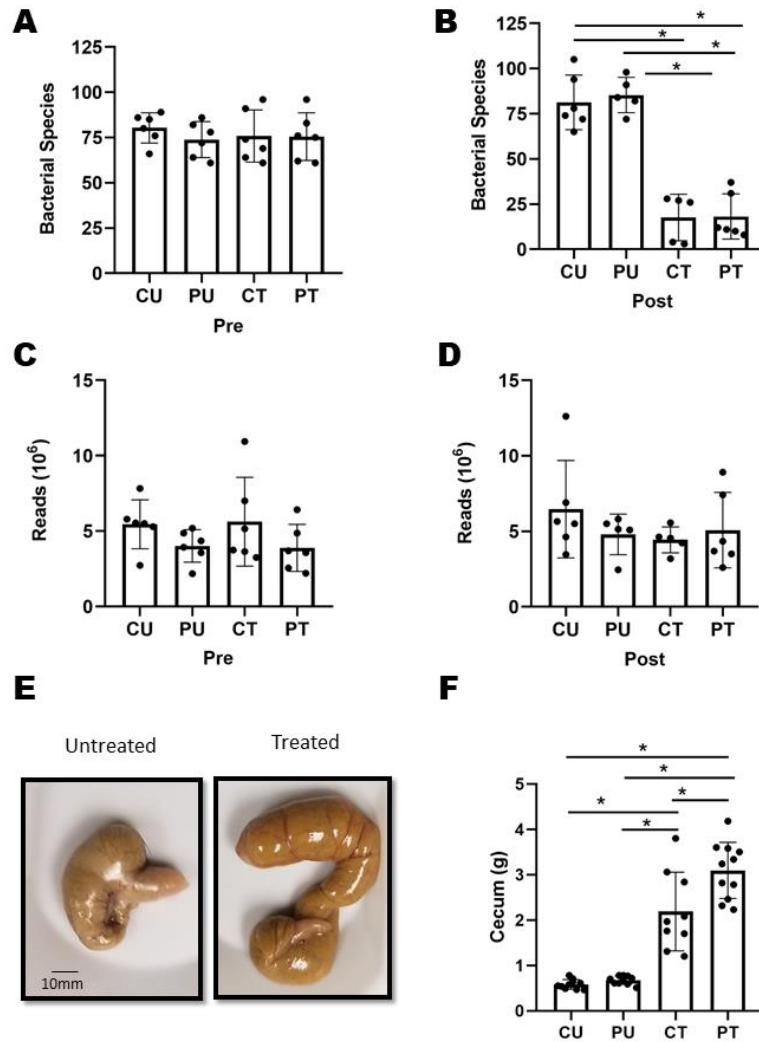


Figure 2.2 Gut Microbial Dysbiosis with Antibiotics

Gut Microbial Dysbiosis with Antibiotics: Antibiotic induced dysbiosis of the gut microbiome. (A) Number of individual bacterial species before (pre) and (B) after (post) antibiotic treatment and PoWeR training n=5-6 per group. (C) Number of reads during sequencing corresponding to the pre and (D) post time points, n=5-6 per group. (E) Representative image of a cecum harvested from an untreated and treated mouse (F) Differences in ceca weight between the groups, n= 9 -11 per group. Bars are mean values, dots represent individual values. Errors bars = standard deviation. \* = p < 0.05

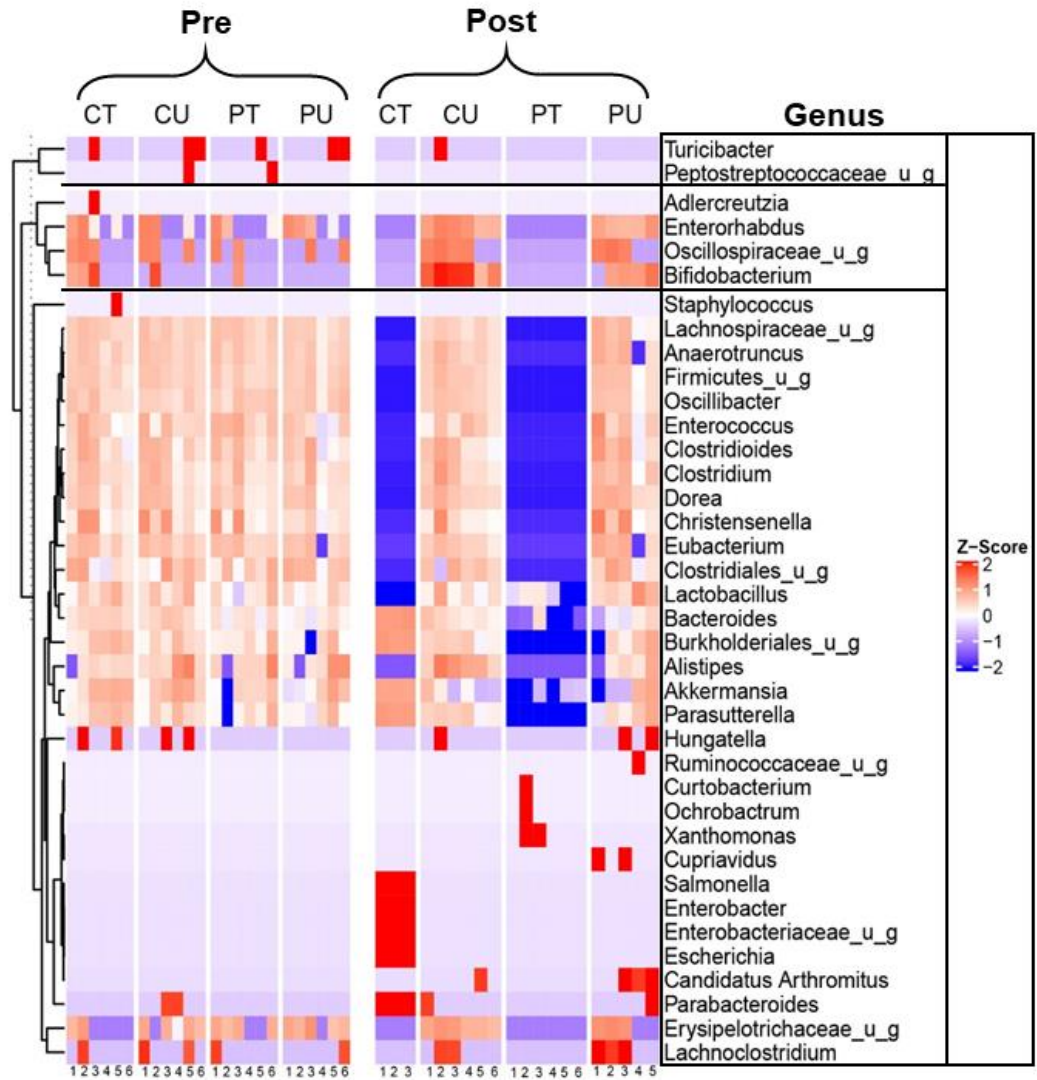


Figure 2.3 PoWeR and Antibiotic Induced Changes to the Gut Microbiome  
Heat map indicating the microbial composition at the genus levels between groups at the pre and post time points. n= 3-6 per group.

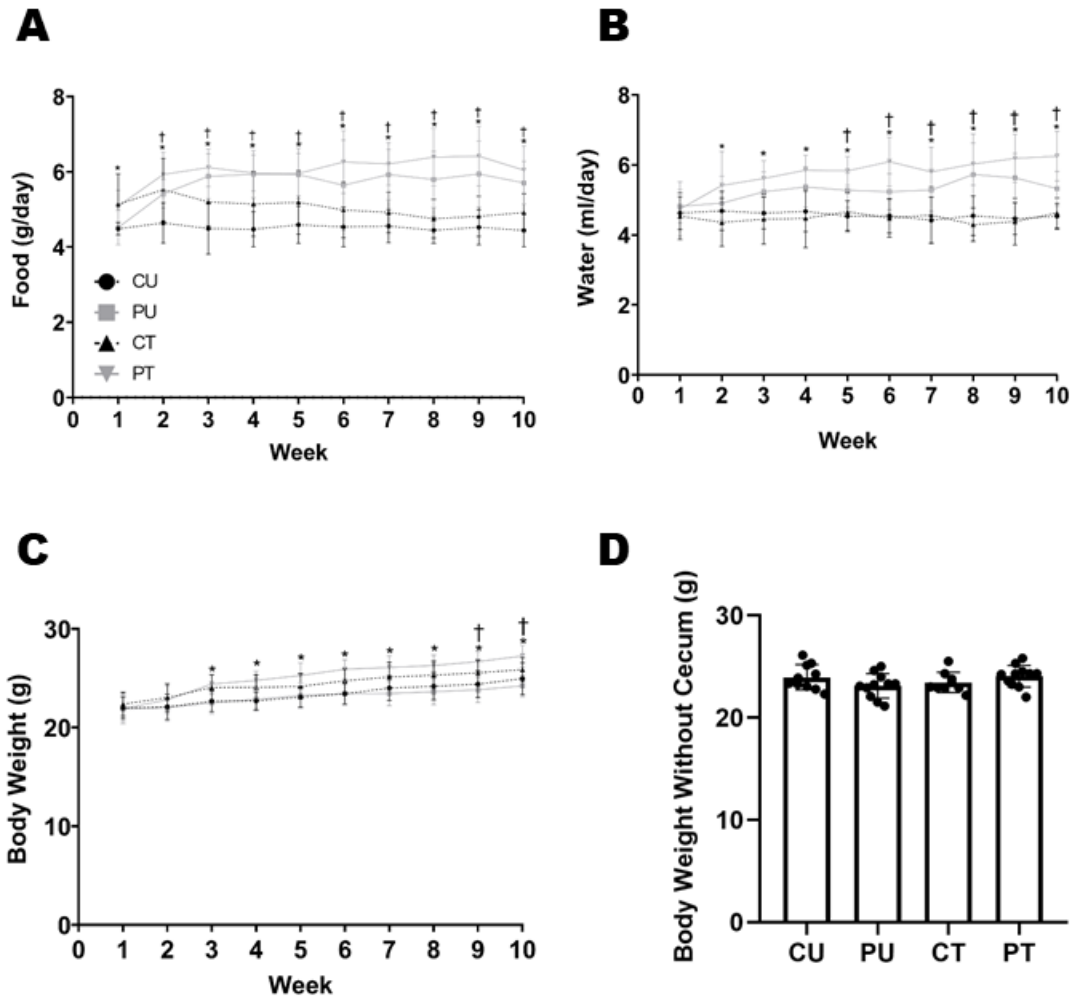


Figure 2.4 Food & Water Consumption, and Body Weights

Food consumption, water intake and body weight changes during PoWeR training. (A) Weekly food consumption during training, (B) Weekly water intake during study, (C) Weekly body weight during study, (D) Body weight at the point of sacrifice with the cecum removed. Bars are means and dots represent individual values. Points on A, B and C represent group averages for that week, Errors bars = standard deviation. n=9 -11 per group. \* significantly different ( $p < 0.05$ ) PT vs CT for food and water intake data. † Significantly ( $p < 0.05$ ) different PU vs CU for food and water intake. \* Significantly ( $p < 0.01$ ) different PT vs CU & PU. † = Significantly ( $p < 0.05$ ) different CT vs PU for body weights.

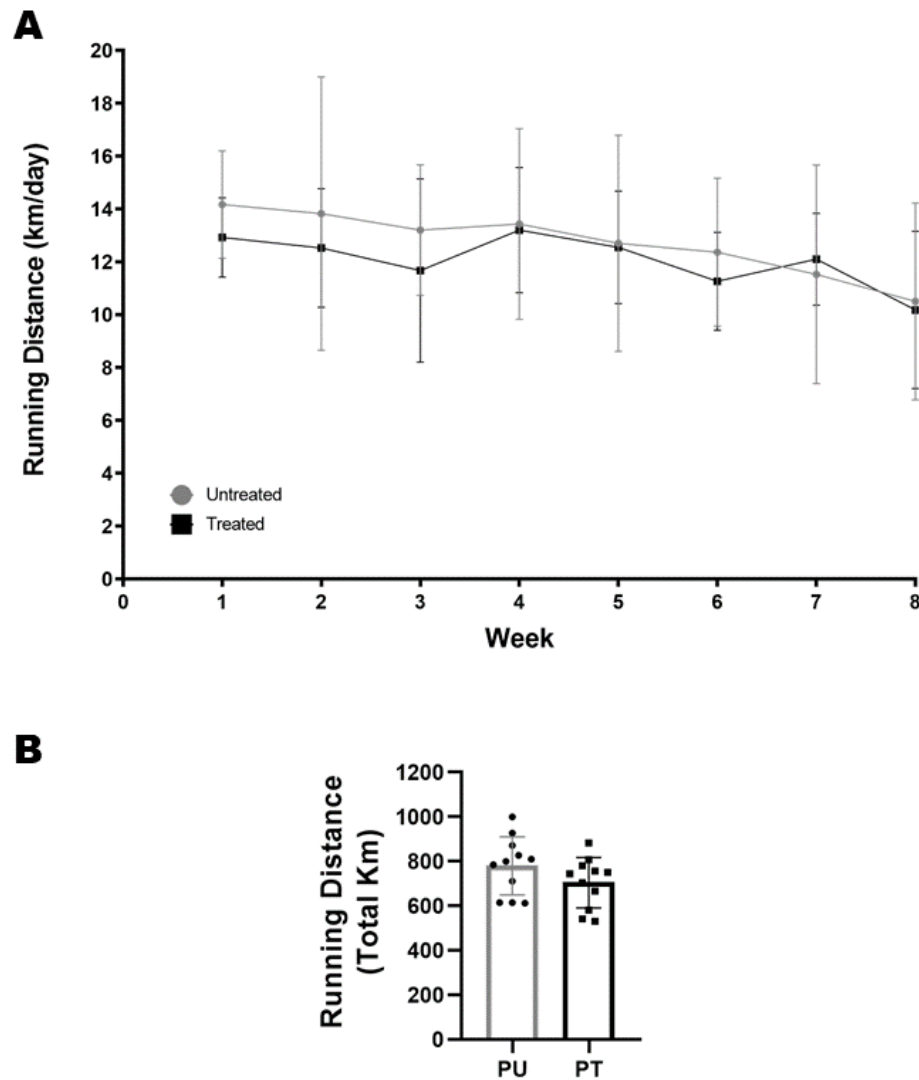


Figure 2.5 Antibiotic Induced Dysbiosis of the Gut Microbiome Does Not Impair Exercise Activity. Running volume during PoWeR training. (A) weekly running volume (km/day) of the PoWeR untreated and treated groups, (B) Mean total distance run during PoWeR training between PoWeR untreated and treated groups n=11 per group. Bars represent means, dots represent individual mice, filled circles on A represent group averages for the corresponding week and error bars = standard deviation.



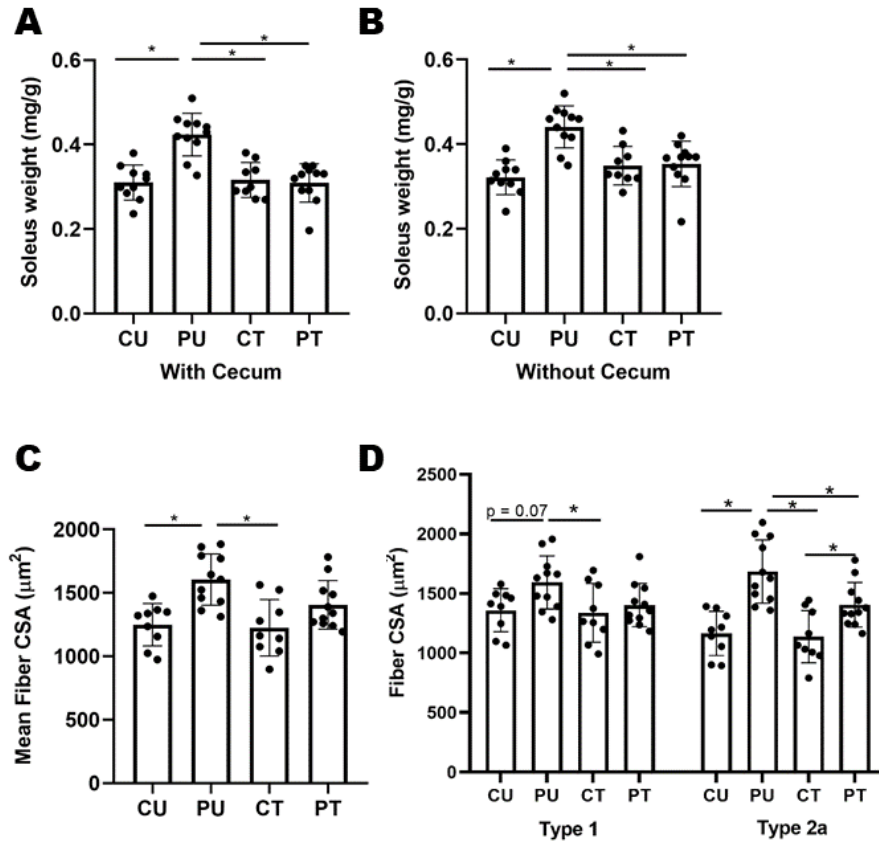


Figure 2.6 Antibiotic Induced Dysbiosis of the Gut Microbiome Results in a Blunted Hypertrophic Response in the Soleus. Analysis of the soleus muscle after PoWeR training with or without dysbiosis. (A) Normalized soleus wet weight to body weight including the cecum, (B) Normalized soleus wet weight to body weight excluding the cecum, (C) Soleus mean cross-sectional area ( $7\mu\text{m}$  sections), (D) Type 1 and type 2a skeletal muscle cross sectional area fiber cross-sectional area ( $7\mu\text{m}$  sections).  $n=8-11$  per group. Bars represent means, dots represent individual mice, error bars = standard deviation.  $*=p < 0.05$ .

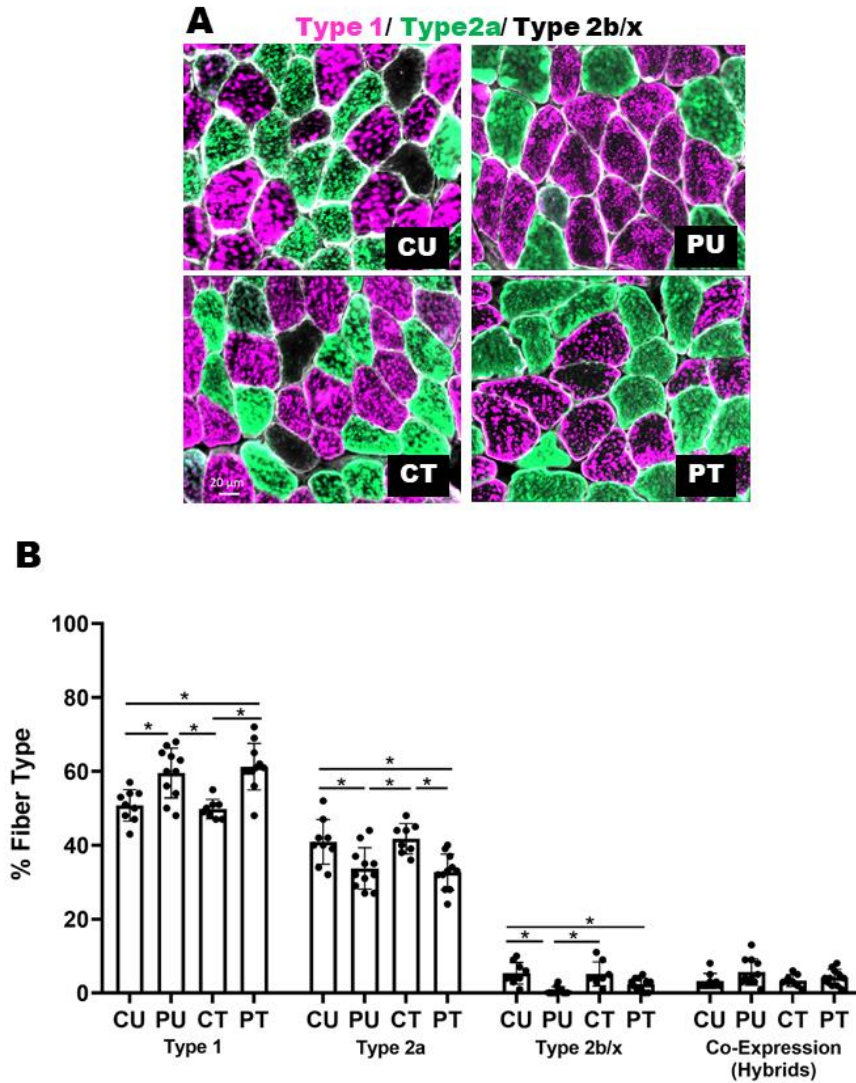


Figure 2.7 Antibiotic Induced Dysbiosis of the Gut Microbiome Does Not Impair Skeletal Muscle Fiber-Type Shift in the Soleus

Analysis of the fiber-type distribution in the soleus muscle after PoWeR training. (A) Representative image of soleus cross section, (B) Fiber type distribution for type 1, type 2a, type 2b/x and co-expression (hybrid) skeletal muscle fibers. n=7 -11 per group. Bars represent means, dots represent individual mice, error bars = standard deviation. \*= p <0.05.

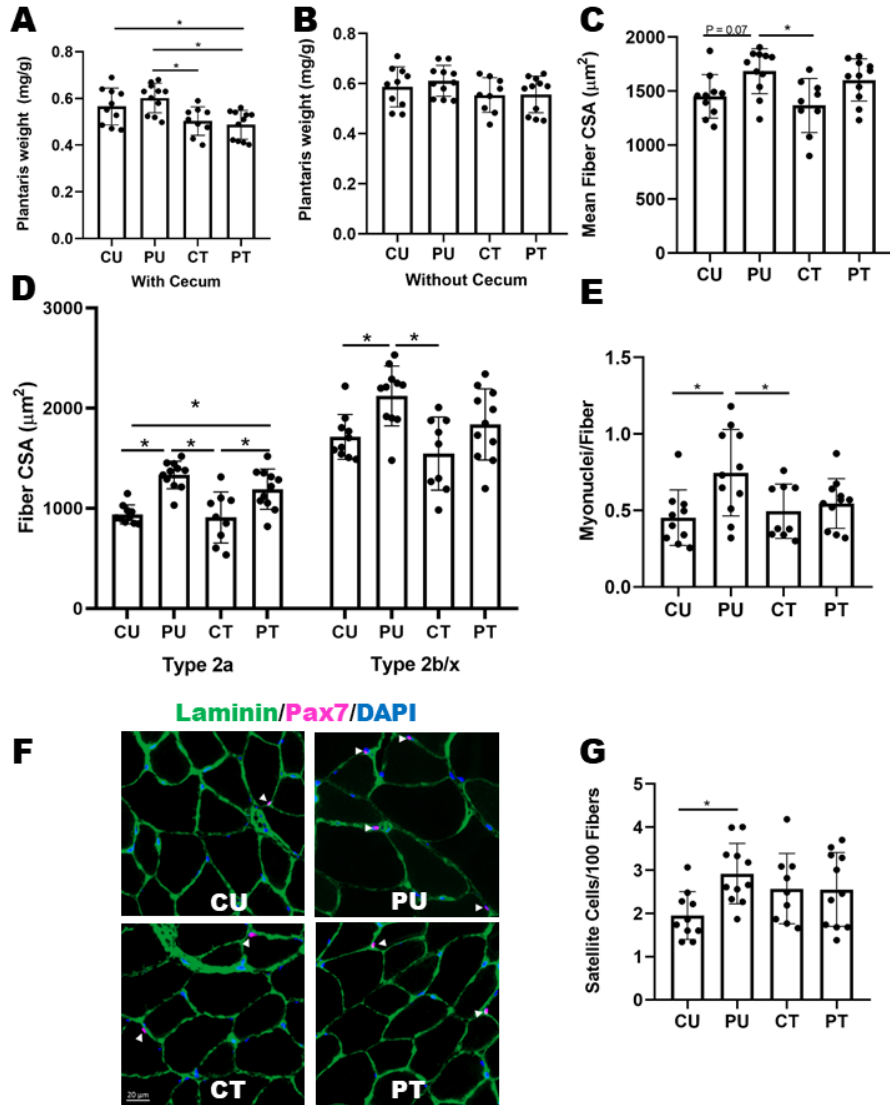


Figure 2.8 Antibiotic Induced Dysbiosis of the Gut Microbiome Results in Blunted Hypertrophy, Myonuclei Accretion and Altered Satellite Cell Abundance in the Plantaris

Analysis of the plantaris muscle after PoWeR training. (A) Normalized plantaris wet weight to body weight including the cecum, (B) Normalized plantaris wet weight to body weight excluding the cecum, (C) Plantaris mean fiber cross-sectional area ( $7\mu\text{m}$  sections), (D) Type 2a and type 2b/x skeletal muscle cross sectional area fiber cross-sectional area ( $7\mu\text{m}$  sections), (E) Number of myonuclei per fiber, (F) Representative image of Pax7<sup>+</sup> myonuclei (G) Satellite cells per 100 muscle fibers. n=9 -11 per group. Bars represent means, dots represent individual mice, error bars = standard deviation. \* = p < 0.05.

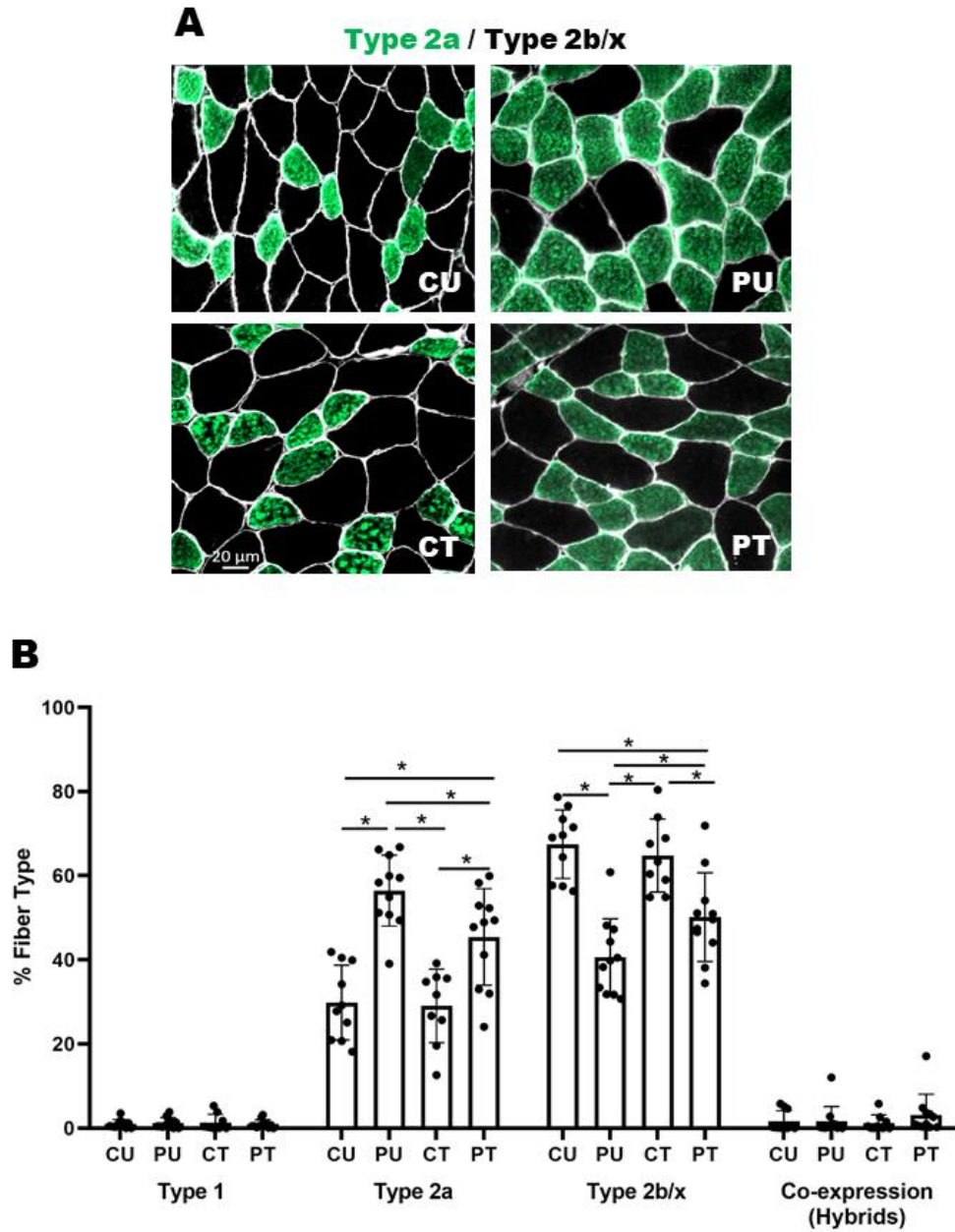


Figure 2.9 Antibiotic Induced Dysbiosis of the Gut Microbiome Results in a Blunted Fiber-Type Shift in the Plantaris

Analysis of the fiber-type distribution in the plantaris muscle after PoWeR training. (A) Representative image of plantaris cross section, (B) Fiber type distribution for type 1, type 2a, type 2b/x and co-expression (hybrid) skeletal muscle fibers. n=9 -11 per group. Bars represent means, dots represent individual mice, error bars = standard deviation. \* =  $p < 0.05$ .

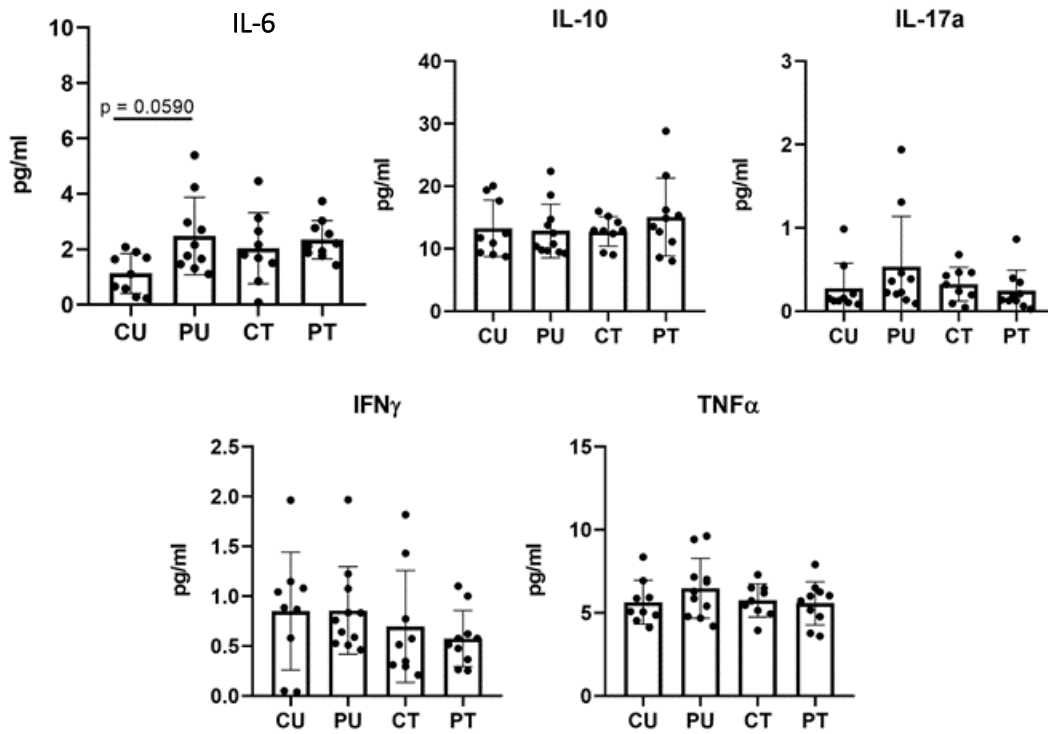


Figure 2.10 10 Weeks of Antibiotics Administration and PoWeR Training did Not Augment Inflammation

Serum concentrations of inflammatory markers taken after nine weeks of training and antibiotic administration.  $n = 9 - 11$  per group. Bars represent means, dots represent individual mice, error bars = standard deviation. IL-6, IL-10 and TNF- $\alpha$  were log transformed.

## CHAPTER 3. THE GUT MICROBIOME FROM AN EXERCISE TRAINED HOST AMELIORATES SKELETAL MUSCLE ATROPHY.

### Introduction

The loss of skeletal muscle mass occurs rapidly, with decreases in muscle cross sectional area (CSA) observed within the first week of week of hospitalization due to critical illnesses [347], immobilization [348] or space flight [145]. The loss in muscle mass and strength is associated with all-cause mortality, increased risk for hospitalization and decline in quality of life. Furthermore, after the age of 75, muscle mass begins to decrease roughly 1% per year with concomitant decreases in strength of about 3% per year [349]. While exercise has been demonstrated to promote many positive adaptations in muscle health, the implementation of physical activity may not be realistic in many situations such as immobilization and disease. Pharmacological interventions can be utilized to attenuate the loss of muscle mass in disease states [350], yet they are not without contraindications. For example, pharmacologic interventions to treat muscle loss was shown to induce liver damage in one out of 21 patients undergoing treatment with oxymetholone [18]. In a group of 106 men receiving testosterone supplementations to increase muscle mass, 23 experienced cardiovascular related events [19]. Nutrition represents yet another intervention to combat muscle wasting; however, there is a currently lack of nutritional supplementation for those populations who are most at risk for severe muscle loss [351]. Other reports have indicated that in the absence of exercise, nutritional interventions alone are not able to effectively restore muscle mass or strength in older adults [16, 17]. Therefore, additional strategies to treat or prevent the decline in muscle mass and function are needed.

Recently the gut microbiome has been shown to influence skeletal muscle hypertrophy, fiber-type shift, myonuclear accretion, grip strength and exercise capacity [199, 205, 352], suggesting the gut microbiome can regulate skeletal muscle phenotype and function. Exercise has also been shown to modulate both the composition and function of the microbiome [180, 302]. How exercise can modulate the composition and function of the microbiome remains unknown. There is some evidence that exercise is able increase

the production of microbially-derived short chain fatty acid such as acetate, butyrate and propionate [353]. Interestingly, butyrate was recently shown to prevent skeletal muscle atrophy and decrease the expression of *atrogen-1* and *MuRF1* in skeletal muscles of mice [199, 200].

Studies in mice have shown that exercise training results in compositional changes to the microbiome that are associated with a protective effect against sepsis [354] and myocardial infraction [355]. While the findings from these studies are very promising, they failed to determine if the benefits observed were solely derived from the exercise alone or the effects of the exercise on the gut microbiome. In a pivotal study which transplanted the microbiome from exercise-trained mice into exercise naïve recipient mice, Allen and co-workers demonstrated the microbiome of an exercise-trained host was shown to be protective in a mouse model of colitis [305]. These results were the first evidence of the therapeutic potential of the microbiome from exercise-trained host. The aim of this study was to determine if the microbiome of an exercise-trained host could mitigate skeletal muscle atrophy induced by 10 days of limb immobilization. We hypothesized that mice receiving the gut microbiome of an exercise-trained host would experience less atrophy compared to mice receiving the gut microbiome from sedentary control animals.

## Methods

### 3.1.1 Mice

*Recipient Mice:* Twelve-week-old female C57BL/6J mice were purchased from The Jackson Laboratory and then allowed to acclimate for four weeks after arrival to the animal facility. Montonye and co-workers found that during the first week of acclimation in a new facility, there was significant shifts in both the composition and function of mice microbiomes [315]. It was shown that the microbiome stabilized between seven and 28 day after arrival to a new facility [315]. Therefore, to ensure a stable and acclimatized microbiome in the recipient mice, the experimental procedures began four weeks after arrival. During the first week of acclimation, mice were randomly split into two groups (n=9 mice per group) and designated as Rex (recipient of exercised host) or Rsed (recipient

of sedentary host) and housed in groups of three referred to as Rex-1, -2 or -3 and Rsed-1, -2 and -3.

*Donor Mice:* Cecal contents were harvested from donor mice who had previously underwent 8-weeks of processive weighted wheel running (PoWeR) (Dex, donor exercised) or remained as sedentary control (Dsed, donor sedentary) [352]. We used the same design for Dex and Dsed groups as used for the recipient groups by making a combined cecal slurry for cecal microbial transplant (CMT) from three Dex or Dsed mice which produced Dex-1, -2 and -3 and Dsed-1, -2 and -3 groups (Figure 3.1 B). Body weight and food consumption was recorded each week for the duration of the study.

Mice were monitored daily, and cages were changed once per week. To minimize the potential for a drift in the microbial composition between individual cages of the same group, old bedding from each group was pooled, mixed with clean bedding, and then distributed to clean cages of the group.

### 3.1.2 PEG Bowel Clearing and Cecal Microbial Transfer

After the four-week acclimation period Rex and Rsed mice were gavaged with polyethylene glycol (PEG) (SLBZ3934, Sigma-Aldrich, St. Louis MO) to clear the gastrointestinal track, as previously described [356, 357]. Briefly, PEG was dissolved in autoclaved miliQ water at a concentration of 425g/L. Mice were sedated with isoflourane and gavaged (FTP-20-30-50 plastic feeding tubes 20gsx30mm, Instech Laboratories, Plymouth Meeting PA) with a 200µl bolus of PEG. This was repeated every 20 minutes, so that each mouse received a total of 800µl of PEG in 60 minutes. After the final dose of PEG, mice were placed in a clean sterile cage, void of bedding and food for six hours prior to the first CMT.

*Cecal Microbial Slurry:* Cecal contents from nine Dex and nine Dsed were used to make the cecal slurry. The cecal contents of three mice were pooled to generate three sub-groups (Figure 3.1 B). This was implemented to create biological triplicates, to decrease the inter-individual variability that exists in microbiome transfer studies [358]. The Dex groups were matched to control for running volume such that each Dex group had similar total running volume. A small aliquot of the cecal slurry from each Dex and Dsed sub-group was set aside for metagenomic sequencing. The cecal contents were mixed, placed in a sterile 15



ml tube with and 5 ml of sterile PBS added. The cecal concentration was approximately 150 mg/ml. The slurry was then vortex vigorously and centrifuge at 500 rpms for eight minutes to pellet non-soluble microbial cell fraction. Sterile conditions were used to prepare each slurry but under aerobic conditions. The resultant slurry was then distributed into 2ml aliquots and immediately stored at -80 °C.

### 3.1.3 Cecal Microbial Transfer:

Six hours after the final bolus of PEG, mice were administered their first CMT. Mice were sedated with isoflurane and gavage with a 200 µl bolus of cecal slurry. Twenty-four and 48 hours after the first CMT, mice received their second and third bolus. The mice then received a CMT once per week for the next four weeks, prior to the immobilization. Mice received a total of seven CMT throughout the study.

### 3.1.4 Limb Immobilization

The unilateral limb immobilization procedure was performed as previously described with minor modifications [144]. Briefly, a capless 0.6 ml centrifuge tube was cut 1 cm down from the opening and attached to small paper clip (ACC72320, No. 3, ACCO Brands, Inc., Lincolnshire, IL) with the adhesive side of a 0.5 cm x 3 cm Velcro strip (Velcro 90198, Velcro USA, Inc., Manchester, NH). The mice were sedated with isoflurane and the right hind leg was carefully placed into the tube in a slightly plantarflexed position. The foot was secured to the paper clip by using an additional 0.5 cm x 3 cm Velcro strip. Two strips of tape were then applied to the cast in order to provide reinforcement. Each day of the 10-day immobilization period, mice were checked to determine if the cast had been removed. If a cast was removed the mouse was sedated with isoflurane and the cast re-applied as described above. One mouse in Rex-1 group removed the cast on the final day of immobilization.

### 3.1.5 Immunohistochemistry

Immunohistochemistry (IHC) analysis was performed as previously described by us [56, 314] on the soleus and plantaris muscles to determine skeletal muscle fiber cross-sectional

area, fiber-type composition, and myonuclei abundance. Excised soleus muscles were immediately weighed, with one limb snap-frozen in O.C.T using liquid nitrogen-cooled isopentane with muscles from the other limb snap-frozen in liquid nitrogen and then stored in  $-80^{\circ}\text{C}$  for biochemical and molecular analyses. Muscle samples were mounted and cut into  $7\mu\text{m}$  sections. Muscle sections were air-dried overnight at room temperature. After drying, the sections were incubated in a cocktail of iso-type specific anti-mouse primary antibodies against myosin heavy chain MyHC-1 (IgG2B, BA.D5), MyHC-2a (IgG1, SC.71) and MyHC-2b (IgM, BF.F3) from Developmental Studies Hybridoma Bank (DSHB Iowa City, IA) in addition Rabbit anti-Laminin (1:100, Sigma #L9393( was used to delineate the fiber border). Type-2x fibers were not stained and counted based on the lack of staining. Primary antibodies were diluted 1:100 in PBS with slides incubated for in  $4^{\circ}\text{C}$  overnight. Sections were subsequently washed three times with PBS and incubated with secondary antibodies (1:250, goat anti-mouse IgG2b Alexa Flour 647, #A21242; 1:250 IgG1 Alexa Flour 488, #A21121; 1:250, IgM Alexa Flour 555, #A21426) from Invitrogen (Carlsbad, CA, USA). Goat anti-rabbit IgG, AMCA was used for the secondary for laminin (Vector Laboratories, CL-1000). Slides were incubated with secondary antibodies for 90 minutes at room temperature. Sections were then washed three times in PBS and mounted using PBS:glycerol solution at a 1:1 ratio.

### 3.1.6 Image Capture and Analysis

IHC sections were captured at 20X magnification using an upright fluorescence microscope (AxioImager M1, Zeiss, Oberochen, Germany). Quantification of skeletal muscle cross-sectional area, fiber-type specific cross-sectional area and fiber-type distribution was quantified using MyoVision automated analysis software [322].

### 3.1.7 Microbial DNA Extraction and Sequencing

Microbial DNA was extracted from the cecal contents as previously described [352]. Briefly, upon euthanasia, the cecum was excised and the contents were carefully removed with a small spatula. The contents were placed in a 1.5 ml centrifuge tube and immediately flash frozen in liquid nitrogen. DNA was isolated from cecal content using the PureLink Microbiome DNA purification kit (ThermoFisher Scientific, Waltham, MA), ThermoFisher Scientific) according to the manufacturer's instructions.

### 3.1.8 Metagenomic Sequencing

Metagenomic sequencing was performed on extracted microbial DNA using HiSeq X Ten (Illumina) with a read length of 150 bp paired end reads and a sequencing depth of three Gigabase per sample. Taxonomic classification was performed with MetaPhlan3 [359]. Briefly, samples were processed for quality control using KneadData which trims low quality reads, and removes host-derived sequences. Processed sequences were then sent through the ChocoPhlan 3 pipeline to align and organize microbial genomes to the reference database (Uniprot [360] and NCBI Resource Coordinators and Coordinators [361]). Raw reads were mapped to the database using bowtie2. To obtain the functional profiling of the microbial communities, sequences processed by MetaPhlan3 were run through HUMAnN3 (the HMP Unified Metabolic Analysis Network)[359]. The functional profile was performed using pangenomes annotated with Uniref90 IDs that were generated from MetaPhlan3. For compositional analysis, ATIMA (Agile Toolkit for Incisive Microbial Analysis, Alkek Center for Metagenomic and Microbiome Research, Baylor College of Medicine) software was used to determine  $\alpha$ - and  $\beta$ -diversity and taxa abundance metrics. Rarefaction depth was set to 457,953 reads and resulted in 23/24 samples retained. This depth was chosen in order to include as many samples for analysis and avoid having skewed groups to compare. One sample in the Rsed group was excluded due to having extremely low reads (444). At the chosen rarefaction depth 10,532,919 reads were retained which was 15.5% of total reads. Mean abundance was set to  $\geq 0.05\%$ . MaAsLin2 (Multivariable Association Discovery in Population-scale Meta-Omics Studies) [362] was used to compare functional and metabolite data. To identify potential metabolites, outputs from HUMAnN2 analyses were processed through MelonnPan (Model-based Genomically Informed High-dimensional predictor of Microbial Community Metabolic Profiles) [363].

#### Statistics

To test for differences between body weight and food consumption during the experimental period, a repeated measures ANOVA was used. When comparing the non-immobilized and

immobilized leg of Rsed and Rex, a matching (non-casted to casted leg) 2-way ANOVA was used. If a main effect or interaction was found, a SIDAK multiple comparison test was used. When comparing the % difference in atrophy between the Rsed and Rex, paired, Welch's t-test was used. A difference in bacterial species abundance between groups was analyzed with a Mann-Whitney U test with an alpha set to  $p \leq 0.05$  and an FDR set to  $p < 0.10$ .

## Results

### 3.1.9 No Adverse Effects of CMT or Immobilization on Body Weight and Food Consumption

During the study, the Rsed and Rex were significantly heavier in weeks 5,6,7 and 8 (Rex only) compared to weeks 1 and 2 (Figure 3.1 D). However, there were no differences in body weight between Rsed and Rex at any time during the study. In addition, there were no differences in food consumption (Figure 3.1 E). The running volume of the Dex sub-groups were similar; Dex-1 =  $796.6 \pm 81.33$  km; Dex-2 =  $837.2 \pm 78.05$  km; Dex-3 =  $813 \pm 193.4$  km (Figure 3.1 F). During the 10-day immobilization period, one mouse from Rex-1 removed the cast on the final day of immobilization.

### 3.1.10 The Gut Microbiome from an Exercise Trained Host Blunts Skeletal Muscle Atrophy in the Soleus

Immobilization of the hind limb resulted in significant atrophy in the soleus of both the Rsed and Rex groups, when looking at both normalized muscle wet (Figure 3.2 A), mean fiber cross-sectional area (CSA) and fiber-type specific CSA. (Figure 3.2 B-E). There was no difference in normalized muscle weight or mean fiber CSA when comparing the immobilized leg of Rsed to Rex. However, when comparing the percent change in mean fiber CSA between the non-immobilized and immobilized leg of each group, there was a significant difference ( $p = 0.006$ ) in the magnitude of reduction  $-42.71 \pm 13.9$  and  $-27.72 \pm 4.46\%$  for Rsed and Rex, respectively (Figure 3.2 F). Similarly, the percent decrease in Type-1 fiber CSA was significantly different ( $p = 0.039$ ) between Rsed and Rex ( $-38.47 \pm 10.01\%$  vs  $-22.08 \pm 18.53\%$ , respectively) (Figure 3.2 G). There was a trend ( $p = 0.06$ ) for the percent decrease in Type-2a fiber CSA for Rsed compared to Rex ( $-42.62 \pm 10.11\%$  vs  $-33.82 \pm 13.0\%$ , respectively) (Figure 3.2 H).

### 3.1.11 The Gut Microbiome from an Exercise Trained Host Preserves Type2a fibers in the Soleus

The fiber-type composition of the soleus showed no change in the abundance of Type-1 fibers when comparing the non-immobilized to the immobilized leg for both Rsed and Rex groups (Figure 3.2 I). The Rsed group had significantly less ( $p = 0.047$ ) Type-2a fibers in the immobilized leg compared to the non-immobilized leg; this difference was not observed in the Rex group (Figure 3.2 J). When looking at the abundance of Type-2b+x fibers, there was a significant increase in the immobilized leg compared to the non-immobilized leg for both Rsed and Rex groups ( $p = 0.016$  and  $p = 0.009$ , respectively) (Figure 3.2 K).

### 3.1.12 Changes in Microbial Composition and Function after CMT

To broadly characterize the microbial composite resulting from CMT, we determine  $\alpha$ - and  $\beta$ -diversity. Following CMT, there were no differences in  $\alpha$ -diversity between Rsed and Rex as assessed by the Shannon and Simpson Index (Figure 3.3 A). However, the Rex had significantly more observed OTUs compared to the Rsed (adj.  $p = 0.0059$ ), suggesting samples in Rex had more low abundant taxa compared to Rsed (Figure 3.3 A). This is also demonstrated by the Choa1 measure, which indicated some samples in Rex contained more rare species (Figure 3.3A) suggesting Rex had greater species richness compared to Rsed. A comparison of Dsed and Dex microbial composition showed no differences in  $\alpha$ -diversity between the donor groups (Figure 3.3 B).

The  $\beta$ -diversity analysis demonstrated that there was a clear difference between the Rsed & Rex as measured by weighted Bray-Curtis ( $p = 0.001$ ) (Figure 3.4 A); however, there was no difference in  $\beta$ -diversity of Dsed and Dex groups (Figure 3.4 B). Principle component analysis showed no difference between Dsed and Rsed groups (Figure 3.5 A) but did reveal a significant ( $p = 0.005$ ) differences in  $\beta$ -diversity between the Dex and Rex groups (Figure 3.5 B). These results indicate there was higher dissimilarity between the Dex and Rex groups. If the comparison between donor and recipient groups was restricted to the top 10 most abundant species, which accounted for ~80% of the total identified

microbes, there was no differences between the donors and their respective recipients (Figure 3.5 C-D).

I next sought to identify species that were successfully transferred from Dex to Rex that were not observed in Dsed or Rsed. Initial comparisons were performed at the genus levels (Figure 3.6 A) and species levels (Figure 3.6B). Composition differences at the species level revealed *Muribaculaceae Bacterium DSM 103720* to be only present in Dex and Rex groups suggesting it was an exercise-influenced microbe that engrafted from donor to recipient (Figure 3.7 B). In addition to *Muribaculaceae Bacterium DSM 103720* there were seven other species identified that were significantly (adj.  $p < 0.05$ ) different between Rsed and Rex (Figure 3.7 B & Table 3.1). Interestingly, *Akkermanisa muciniphilia* was present in both Dsed and Dex, however it was significantly (adj.  $p = 0.00274$ ) more abundant in Rex compared to Rsed (Figure 3.7 B). Although not significant, a similar trend was also seen for the species *Bacteroides thetaiotamicron*. Further analysis found *Faecalibaculum\_rodentium*, *Parasutterella\_excrementihominis*, *Turicimonas\_muris*, *Ileibacterium\_valens*, unclassified *Proteobacteria\_bacterium\_CAG\_139*, *Clostridium\_cocleatum* and *Olsenella\_scotoligenes* species were all significantly higher in Rex compared to Rsed (Table 3.1). This may indicate the transfer of *Muribaculaceae Bacterium DSM 103720* caused compositional shifts in specific microbe abundance in the Rex group.

To identify functional pathways that were associated with either Rsed or Rex, I ran normalized (total sum scaling) pathway abundance data through Maaslin2. Multiple pathways relating to nucleotide, amino acid and carbohydrate metabolism were significantly associated with Rex compared to Rsed (Figure 3.8 A-C). Figure 3.8 A-C show which pathways related to microbial function were significantly associated with Rex (Green) and Rsed (Purple). The strength of the association can be seen by the coefficient value which can be a proxy for the effect size [362]. Figure 3.8 A reveals that the Rex microbiome was significantly associated with pathways that are involved in nucleotide biosynthesis and degradation.

Figure 3.8 B represents pathways significantly associated with amino acid metabolism between Rsed and Rex. An interesting observation found in this analysis was

that Rsed was associated with greater tryptophan and glutamate biosynthesis, while Rex was associated with higher histidine biosynthesis and degradation. This suggests that the microbiomes of each group have a propensity for specific amino acids which produce discrete metabolites. Histidine can be metabolized by certain microbes into imidazole propionate which has been shown to activate TORC-1 [319]. Therefore, these results suggest that receiving the microbiome of an exercise-trained host may shift the preference for specific amino acids which could influence (both compositionally and functionally) the community of surrounding microbes ultimately altering the production of microbial derived metabolites.

Figure 3.8 C shows which pathways related to carbohydrate metabolism are associated with Rsed and Rex. One of the top pathways associated with Rex was fucose degradation (fucose degradation and the super-pathway of fucose and rhamnose degradation). Fucose and rhamnose is metabolized to lactaldehyde which is further metabolized into lactate or propane-1,2-diol. Lactate and propane-1,2-diol can participate in the formation propionate which is a SCFA known to increase with exercise [205, 364]. Additional pathways relating to formate metabolism (N10 formyl tetrahydrofolate biosynthesis and X6 hydroxymethyl dihydropterin diphosphate biosynthesis III) and CO<sub>2</sub> production (Calvin-Benson-Bassham Cycle, Reductive TCA cycle) were also significantly associated with Rex (Figure 3.8 C). Formate can participate in the production of butyrate and acetate [364]. These results suggest that the microbiome in Rex may be metabolizing carbohydrate precursors to generate SCFAs.

Next, to obtain further insight into differences between the microbiomes of Rsed and Rex, an additional analysis using MelonnPan was performed to identify potential microbially-derived metabolites. MelonnPan is a computation program where abundance files are input to predict metabolite composition [363]. Figure 3.9 A show the Representative Training Sample Index (RSTI) for each sample. The RSTI is an indicator of the accuracy of metabolite prediction, where the higher value RSTI (0-1) indicate a stronger prediction [363]. The average RSTI scores were  $0.359 \pm 0.145$  and  $0.337 \pm 0.17$  for Rsed and Rex, respectively. There were 36 predicted metabolites to be significantly associated with either Rsed or Rex (Figure 3.9 B). Specifically, metabolites related to lipids

and bile acids were found to be significantly associated with Rex. Not significant by the cut off used previously ( $p < 0.01$  and adj.  $p < 0.1$ ) a known microbial produced product of histidine metabolism, imidazole propionate, was trending ( $p = 0.056$ , adj.  $p = 0.117$ ) to be significantly associated with Rex (Figure 3.9 B). Taken together with the histidine metabolism pathways shown in Figure 3.8, the predictive metabolite analysis revealed the possibility that the microbiome of Rex could be engaging in the production of imidazole propionate through metabolizing histidine.

## Discussion

The purpose of this study was to determine if the gut microbiome from an exercise trained host could attenuate skeletal muscle atrophy induced by limb immobilization. The major finding from this study is that the gut microbiome from an exercise-trained mouse can blunt soleus muscle atrophy as assessed by the percent decrease in mean fiber CSA and fiber-type specific CSA between the non-immobilized and immobilized limb. The gut microbiome from an exercised mouse was also found to preserve the abundance of Type-2a fibers in the Rex group compared to Rsed group, suggesting that an exercise-trained microbiome can influence skeletal muscle fiber-type transition induced with muscle atrophy. These findings provide new evidence demonstrating unique properties of the gut microbiome of an exercise-trained individual and add to the growing literature supporting the existence of a skeletal muscle-microbiome axis [197, 199, 201, 248, 352].

To elucidate a mechanism metagenomic sequencing was performed on the cecal contents taken from the donors and recipients. The metagenomic analysis revealed significant difference in the composition and function of the gut microbiome between Rsed and Rex. These differences are consistent with the literature which has shown exercise can modulate the gut microbiome [365]. Compositional differences between Rsed and Rex indicated discrete microbes that were highly abundant in one group and either extremely low or not found in the other group. Analysis of  $\beta$ -diversity further revealed that Rsed and Rex were significantly different compositionally, suggesting the transfer of the donor microbiome caused significant shifts in the microbiota. Interestingly, when comparing the Dex and Rex groups, there were also significant differences in microbial composition, a



difference not found when comparing Dsed and Rsed. When taking into consideration the top 10 most abundant species, there were no observable differences between Dex and Rex. This finding indicates that lowly abundant species most likely accounted for the differences between Dex and Rex. This finding indicates there are species sensitive to exercise that were present in Dex but did not engraft in Rex, thus suggesting these species require ongoing exercise to maintain their abundance within the gut microbiome. As reported by Grosicki and colleagues, the genus *Veillonella* increased 143-fold in an individual who just completed a 161-km run [206]. Scheiman and co-workers also determined that *Veillonella* abundance was higher immediately post-marathon race compared to later time points [205]. These data provide compelling evidence that specific gut microbes are responsive to exercise as shown by a transient increase in their abundance following exercise. This finding has important implications for future studies, performing microbial transfer from an exercise-trained host into a non-exercising recipient may require the recipients to exercise to maintain microbial composition of the donor. While speculative, this finding suggests that soluble factors generated during exercise, possibly from skeletal muscle, positively influence the activity of specific gut microbes [366]. Additionally, the systemic effects of exercise may also impact the gut microbiome through the redistribution of blood to the gastrointestinal tract, changes in pH, increases in core temperature and mechanical perturbations of the gastrointestinal tract that accompany some forms of exercise. Future studies will need to determine how exercise directly affects the growth of the gut microbiota and if these compositional changes are associated with concomitant functional changes.

The most intriguing finding from the study was the identification of the Dex-specific microbe *Muribaculaceae bacterium DSM 103720* which was successfully transferred to all Rex mice. While it remains to be tested, *Muribaculaceae bacterium DSM 103720* may further influence the composition of the gut microbiome by directly affecting the growth and/or function of other microbes. In support of such a scenario, the abundance of *Akkermanisa muciniphila*, *Ileibacterium valens* and *Faecalibacterium rodentium* were significantly higher (and within the top 20 most abundant taxa) in the Rex compared to Rsed group. The gut microbiota represents a highly dynamic and connected community and the microbes share core bioenergetic machinery, such as the electron transport chain,

hemes, quinones and amino acids in the extracellular space, termed the “Pantryome”, which influences the functional capabilities of individual microbial species [367]. As an example, Daisley and co-workers suggest the Pantryome helps to create a reservoir of resources whereby if a primary degrader produces products with insufficient carbon-based energy, the secondary degraders may utilize what is in the pantryome in order to carry out their respective roles [367]. In support a pantryome, Li and co-workers showed the synthesis of the metabolite isoalloLCA was dependent upon the activity of three different bacteria, revealing a network of microbes drives the generation of precursor molecules needed for the final product [368]. This finding highlights the interconnectedness of the microbial community of the gut microbiome in which the production and consumption of intermediates that ultimately result in metabolites that can affect the host [369].

The composition analysis presented here, suggest that the transfer of *Muribaculaceae bacterium DSM 103720* from Dex to Rex, promoted the growth of additional bacteria, that was not observed in the Rsed group. *Akkermanisa muciniphila*, *Ileibacterium valens* and *Faecalibacterium rodentium* were significantly higher in Rex compared to Rsed. In addition, although not significant, *Bacteroides thetaiotamicron* was almost 50% more abundant in Rex compared to Rsed (Table 3.1). These bacteria are known to produce or are associated with SCFAs [370-372]. Additionally, *Akkermansia muciniphila* and *Bacteroides thetaiotamicron* can degrade fucose which is abundant in host mucosal surfaces [373, 374]. Fucose degradation was one of the pathways significantly associated with Rex, which could indicate enhanced SCFA production.

A deeper analysis of the metagenomic analysis revealed a significant association in histidine biosynthesis and degradation in Rex compared to Rsed. The analysis from MelonnPan also indicated that the metabolite imidazole propionate was trending to be significantly associated with Rex. Ammonia lyase is an enzyme that catalyzes the elimination of the alpha-amino group converting histidine to urocanic acid [375]. Urocanic acid is subsequently reduced to imidazole propionate by the microbial enzyme urocanate reductase [376]. Imidazole propionate was first shown to contribute to insulin resistance by activating TORC-1 in a p62 phosphorylation dependent mechanism, leading to desensitized insulin receptor substrate [319]. These findings indicate that imidazole

propionate has a negative effect on host health by impairing glucose metabolism. Most recently a study found protective effects of imidazole propionate against irradiation induced toxicity of the pulmonary system by attenuating pyroptosis in the lung [377]. These authors also found that treating mice with L-histidine resulted in an increase in *Ileibacterium valenes*, *Akkermanisa munciniphilia*, both of which were significantly higher in Rex compared to Rsed. These results provide a potential mechanism where transplanting the gut microbiome from an exercised-trained host results in an increase in imidazole propionate, driven by enhanced histidine and SCFA metabolism, that could ameliorate skeletal muscle atrophy through TORC-1 stimulation.

The proposed mechanism contrasts with previously published literature which has demonstrated negative health implications of imidazole propionate regarding glucose metabolism [319, 378, 379]; though these negative implications are primarily observed in patients with type 2 diabetes. Although not detected with MelonnPan, the metagenomic analysis revealed pathways related to SCFA production were higher in Rex. The potential of SCFAs to regulate host health and skeletal muscle is an active area of research [242, 380]. SCFAs are also associated with improvements in insulin sensitivity and increase energy expenditure [381]. The results from this study suggest an interconnection of microbial-derived metabolites. Both the production of imidazole propionate and SCFAs may act in synergy, such as seen with different hormones [382]. Synergism between SCFA and phenolic metabolites was demonstrated by Zheng and co-workers. These authors showed that butyric acid in combination with three phenolic acids had a greater capacity to reduce TNF- $\alpha$  and NK- $\kappa\beta$  signaling in Caco-2 cells [383]. These results highlight that microbial-derived metabolites may work in tandem and/or potentiate one another's effect on the host.

An important consideration regarding the effect of imidazole propionate and other metabolites may be context dependent. This has been seen elsewhere when looking at branch chained amino acids (BCAA). In terms of skeletal muscle hypertrophy, especially mTOR activation, BCAAs can stimulate protein synthesis and are considered to enhance anabolic activity [384]. In contrast, studies have demonstrated potential negative consequences of BCAA in terms of glucose metabolism, suggesting that BCAA activation

of TORC-1 leads to phosphorylation and subsequent inhibition of insulin receptor substrate [385, 386]. This paradox may be explained by other factors such as lifestyle, diet, disease and age could influence how metabolites (both microbial-derived and host-derived) regulate physiology. For example, Molinaro and co-workers concluded that imidazole propionate is associated with a pro-inflammatory microbiota. One of the microbes they found to be pro inflammatory was *Veillonella atypica* [379]. This microbe has recently been shown to be abundant in elite endurance athletes and improved exercise time to exhaustion when administered to mice [205, 206]. In the context of highly trained athletes, *Veillonella* is thought to be highly beneficial to endurance activity, whereas in a sedentary lifestyle, the absence of exercise could shift the function of this microbe towards an inflammatory phenotype. This reinforces the idea that the function of a particular microbe may be due in part to the behavior of the host and the surrounding community of microbiota within an environment. Therefore, stating that a microbe or a microbial derived metabolite is harmful or beneficial depends on numerous factors such as host lifestyle, diet, age and/or community of microbes that comprise the microbiome.

### Limitations

The results from this study are not without limitations. Due to laboratory constraints, the cecal slurry used to transfer into recipient mice was prepared under aerobic conditions. Aerobic conditions likely killed microbes which are highly sensitive to oxygen, thus altering the composition of the cecal contents that were present for transfer. Recently Hunt and co-workers demonstrated that the integrated transcriptomic and proteomic response to different atrophy conditions varies across conditions [387]. Therefore, the ability of gut microbiome of exercise-trained mice to ameliorate muscle atrophy may in fact be specific for atrophy induced by limb immobilization and not necessarily applicable to other forms atrophy caused by denervation, muscle wasting diseases such as cancer cachexia or aging. MaAsLin2 was used to determine significant association between gene features and groups. Due to linear models being bias towards larger samples size, the results from this analysis may not have accurately encompassed all of the significant relationships [362]. The metabolite prediction software, MelonnPan, was originally trained using microbiome and metabolites collect from humans [363]. The input used in the current experiment came

from the microbiome of mice, which could limit the accuracy of the MelonnPan's performance. A future study should focus on determining the serum concentration of imidazole propionate with the prediction it will be higher in Rex mice compared to Rsed mice, and determining how imidazole propionate effects skeletal muscle alone or in conjunction with SCFAs. It will also be important to demonstrate that the microbiome of Rex mice can generate these metabolites.

In conclusion this is the first study to demonstrate that the microbiome from an exercised-trained host can mitigate skeletal muscle atrophy in a host undergoing limb immobilization. The potential mechanism mediating this finding is thought to be due to the synergistic effect of the microbial derived metabolites imidazole propionate and SCFAs. This is driven by the addition of *Muribaculaceae bacterium DSM 103720*, which acts as an influencer to other microbes, facilitating their growth and subsequent metabolism of fucose and histidine. While the findings await further confirmation, the results provide a potential new therapeutic strategy to combat the loss of skeletal muscle and additional evidence of the skeletal muscle-gut microbiome axis.

Taxa	P-Value	FDR-Adj. P	Mean of Exercised	Mean of Sedentary
Family Lachnospiraceae(Lachnospiraceae unclassifiedLachnospiraceae bacterium A2)	0.000	0.003	0.000	0.189
Family Lachnospiraceae(Lachnospiraceae unclassifiedLachnospiraceae bacterium A4)	0.000	0.003	0.000	0.090
Family Muribaculaceae(Muribaculaceae unclassified Muribaculaceae bacterium DSM 103720)	0.000	0.003	0.081	0.000
Genus Acutalibacter(Acutalibacter muris)	0.000	0.003	0.000	0.126
Genus Akkermansia(Akkermansia muciniphila)	0.000	0.003	0.261	0.001
Genus Anaerotruncus(Anaerotruncus sp G3 2012)	0.000	0.003	0.001	0.023
Family Lachnospiraceae(Lachnospiraceae unclassifiedLachnospiraceae bacterium 3 1)	0.001	0.003	0.000	0.007
Phylum Firmicutes (Firmicutes_unclassifiedFirmicutes_unclassifiedFirmicutes_unclassified Firmicutes_unclassifiedFirmicutes bacterium ASF500)	0.001	0.003	0.000	0.001
Genus Faecalibaculum(Faecalibaculum rodentium)	0.001	0.004	0.027	0.000
Genus Parasutterella(Parasutterella excrementihominis)	0.001	0.004	0.013	0.001
Genus Turicimonas(Turicimonas muris)	0.001	0.004	0.002	0.000
Genus Ileibacterium(Ileibacterium valens)	0.002	0.005	0.152	0.001
Phylum Proteobacteria (Proteobacteria_unclassifiedProteobacteria_unclassified Proteobacteria_unclassifiedProteobacteria_unclassifiedProteobacteria bacterium CAG 139)	0.002	0.005	0.001	0.000
Family Lachnospiraceae(Lachnospiraceae unclassifiedLachnospiraceae bacterium 28 4)	0.002	0.007	0.000	0.088
Genus Erysipelatoclostridium(Clostridium cocleatum)	0.003	0.008	0.002	0.000
Genus Lactobacillus(Lactobacillus johnsonii)	0.011	0.029	0.016	0.051
Genus Limnochorda(Limnochorda pilosa)	0.015	0.037	0.000	0.001
Family Lachnospiraceae(Lachnospiraceae unclassifiedLachnospiraceae bacterium 3 2)	0.036	0.078	0.002	0.007
Genus Olsenella(Olsenella scatoligenes)	0.036	0.078	0.002	0.001
Genus Eubacterium(Eubacterium sp 14 2)	0.060	0.123	0.000	0.003

Table 3.1 Top 20 Significantly Different Taxa Between Recipient Groups

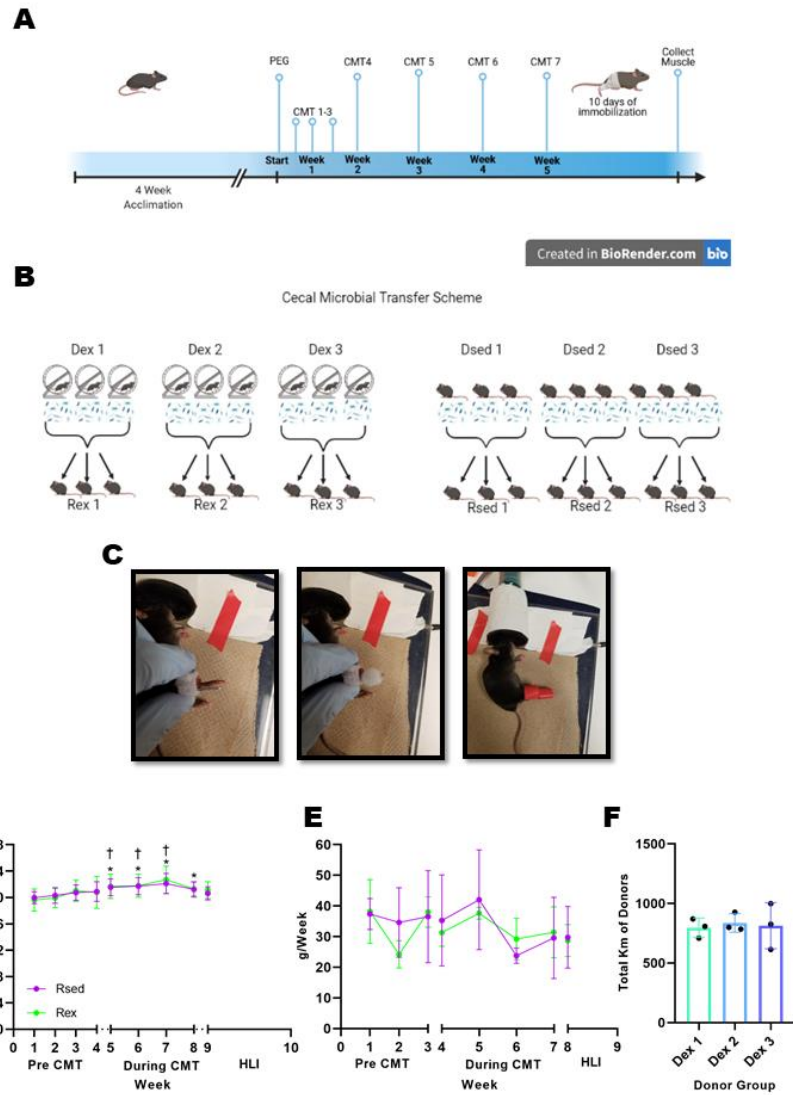


Figure 3.1 No Adverse Effects of CMT or Immobilization on Body Weight or Food Consumption

A) Overview of experimental design, B) Schematic for cecal microbial transfer, C) Representative images of immobilization technique; D) Body weights during experimental period; E) Food consumption during experimental period; F) Total running volume of each group of exercise trained donors during 8-weeks of PoWeR training. † =  $p < 0.05$  when comparing Rsed body weights in week 1 to weeks 5-7. \* =  $p < 0.05$  when comparing Rex body weights in week 1 to weeks 5-8 and week 2 to week 8.

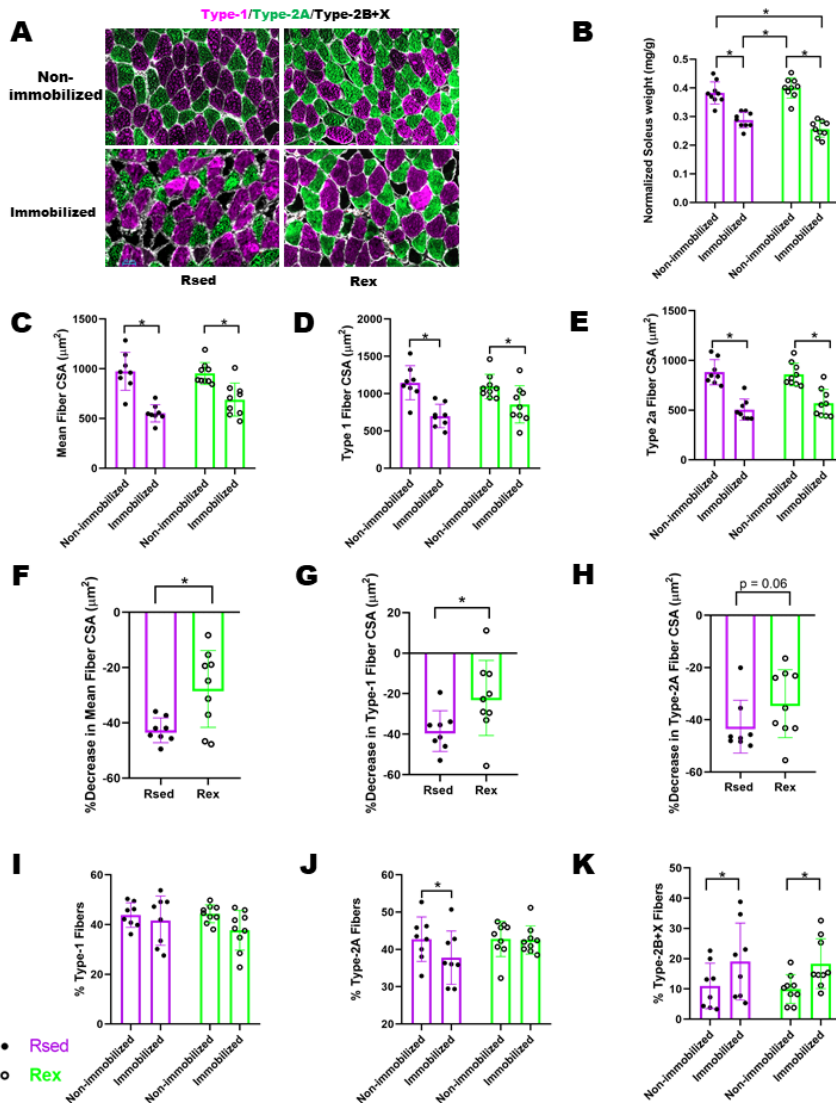


Figure 3.2 The Gut Microbiome from an Exercised Trained Host Blunts Skeletal Muscle Atrophy in the Soleus  
 A) representative images of soleus muscle, B) Normalized wet weight to body weight, C) Comparison of mean fiber cross-sectional area (CSA) in non-immobilized and immobilized limbs, D) Comparison of Type-1 fiber mean fiber CSA in non-immobilized and immobilized limbs, E) Comparison of Type-2A fiber mean fiber CSA in non-immobilized and immobilized limbs, F) The percent difference in mean fiber CSA between non-immobilized and immobilized limb for each recipient group, G) The percent difference in mean Type-1 fiber CSA between non-immobilized and immobilized limb for each recipient group, H) The percent difference in mean Type-2A fiber CSA between non-immobilized and immobilized limb for each recipient group, I) Percent Type-1 fiber abundance in non-immobilized and immobilized limbs, J) Percent Type-2A fiber abundance in non-immobilized and immobilized limbs, K) Percent Type-2B+X fiber abundance in non-immobilized and immobilized limbs. \* =  $p < 0.05$ .



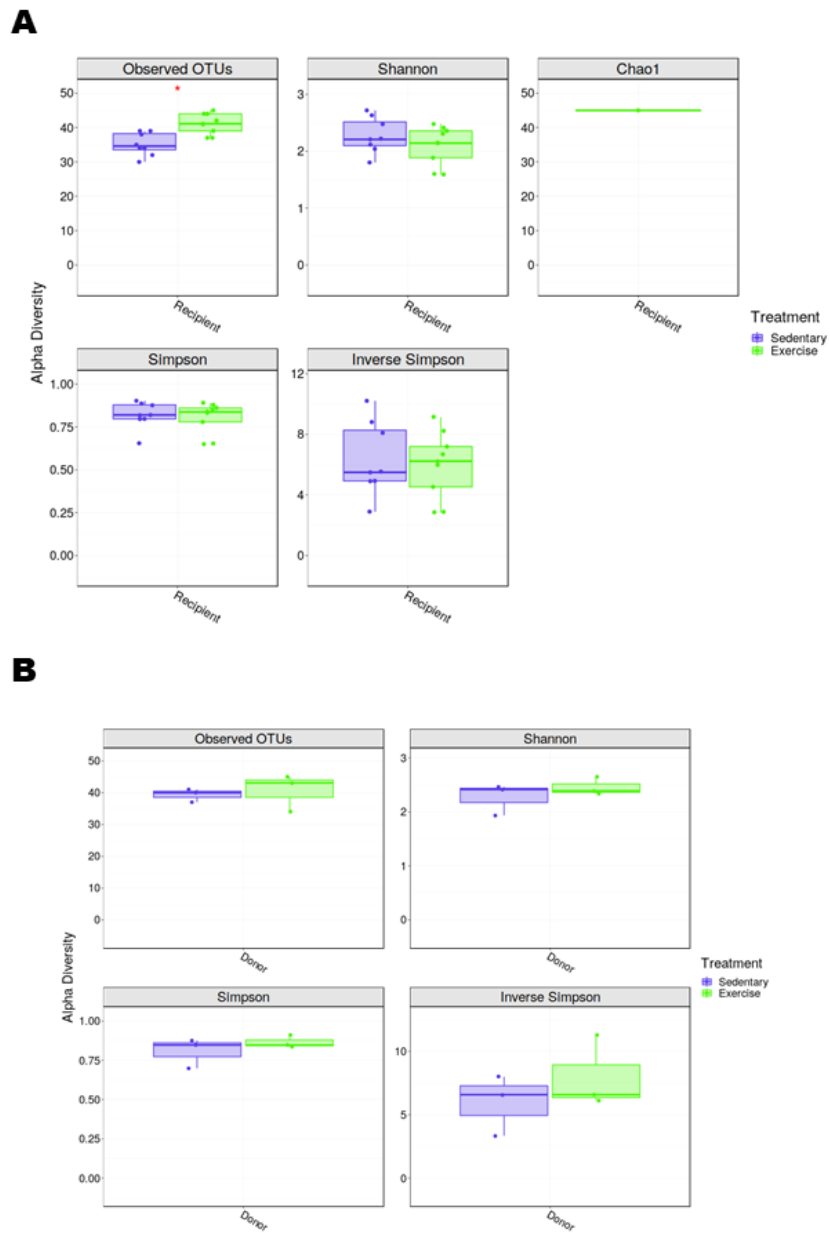


Figure 3.3 Alpha Diversity Measures in Recipient and Donor Mice  
 Box plots displaying  $\alpha$ -diversity measures on A) recipients only and B) donors only. \* =  
 adj.  $p = 0.0059$ .

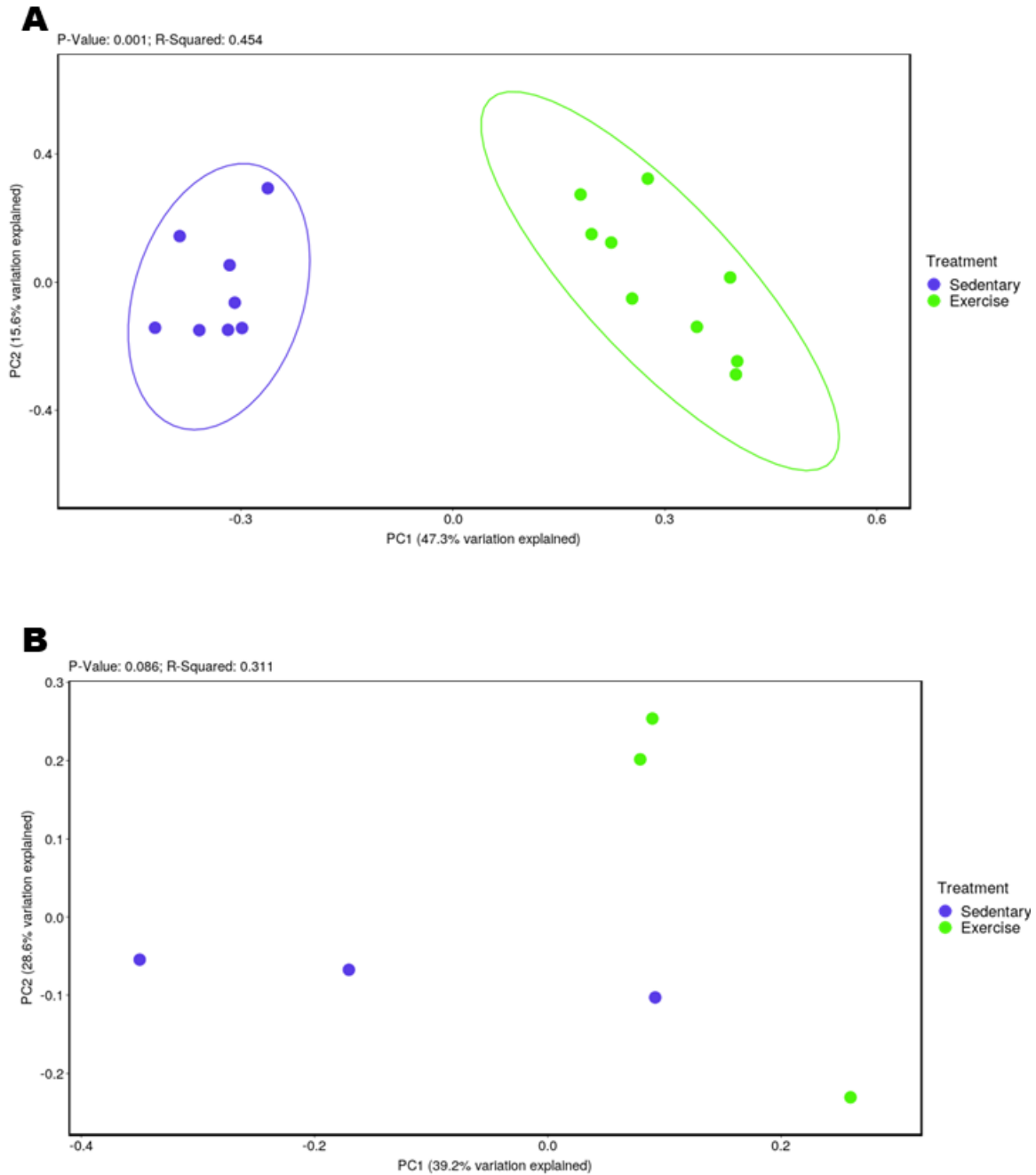


Figure 3.4 Beta Diversity Measures in Recipient and Donor Mice  
 A) Principal component analysis showing the effects of CMT on recipient groups at the end-point of the experiment. B) Principal component analysis of the donors. Distance metric Weighed Bray-Curtis.

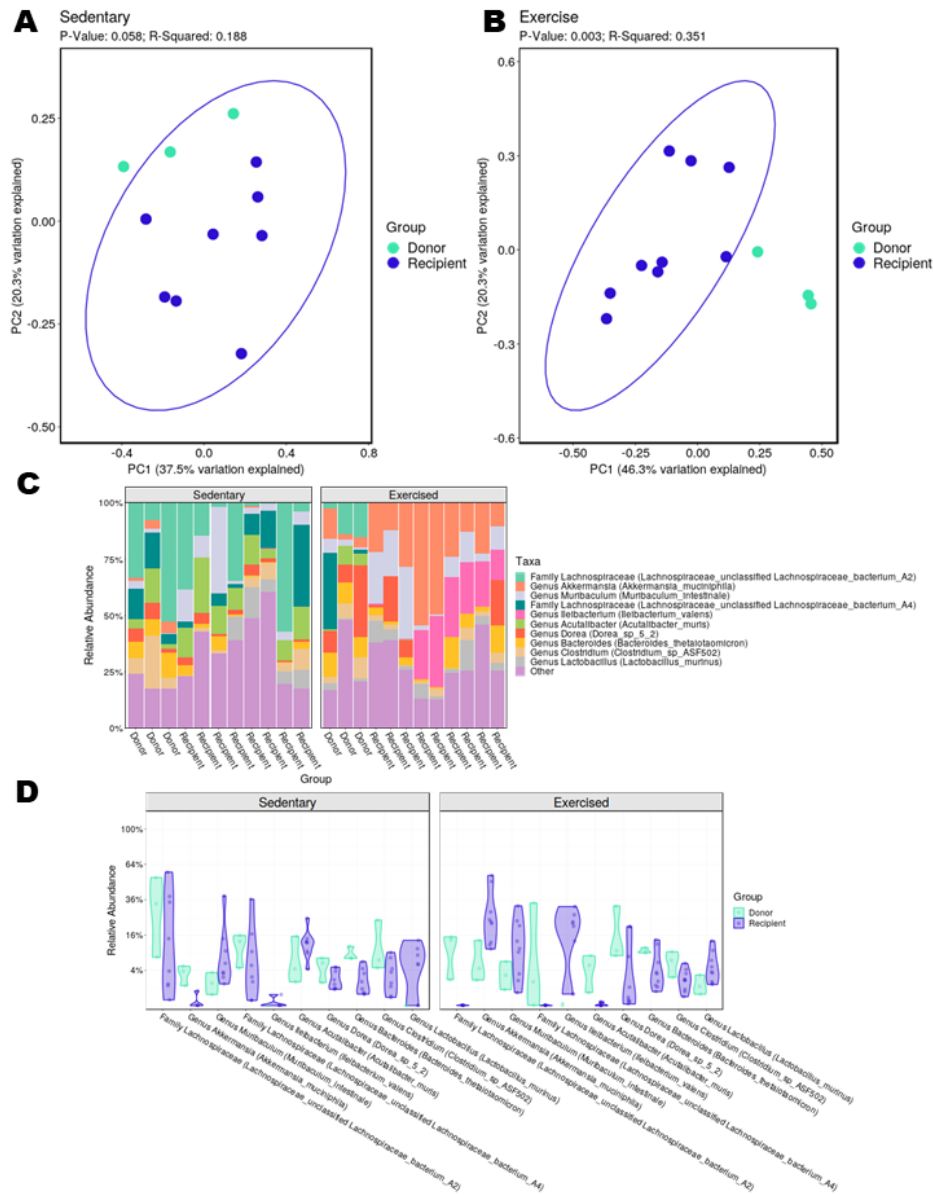


Figure 3.5 Comparison of Donor and Recipient Microbiomes  
 A) Principal component analysis comparing sedentary donors and their respective recipients, B) Principal component analysis comparing exercise trained donors and their respective recipients, distance metric Weighted Bray-Curtis, C) Stacked bar plots representing the top 10 most abundant species between donors and their respective recipients, D) Violin plots comparisons between the top 10 most abundant taxa between the donors and their respective recipients.

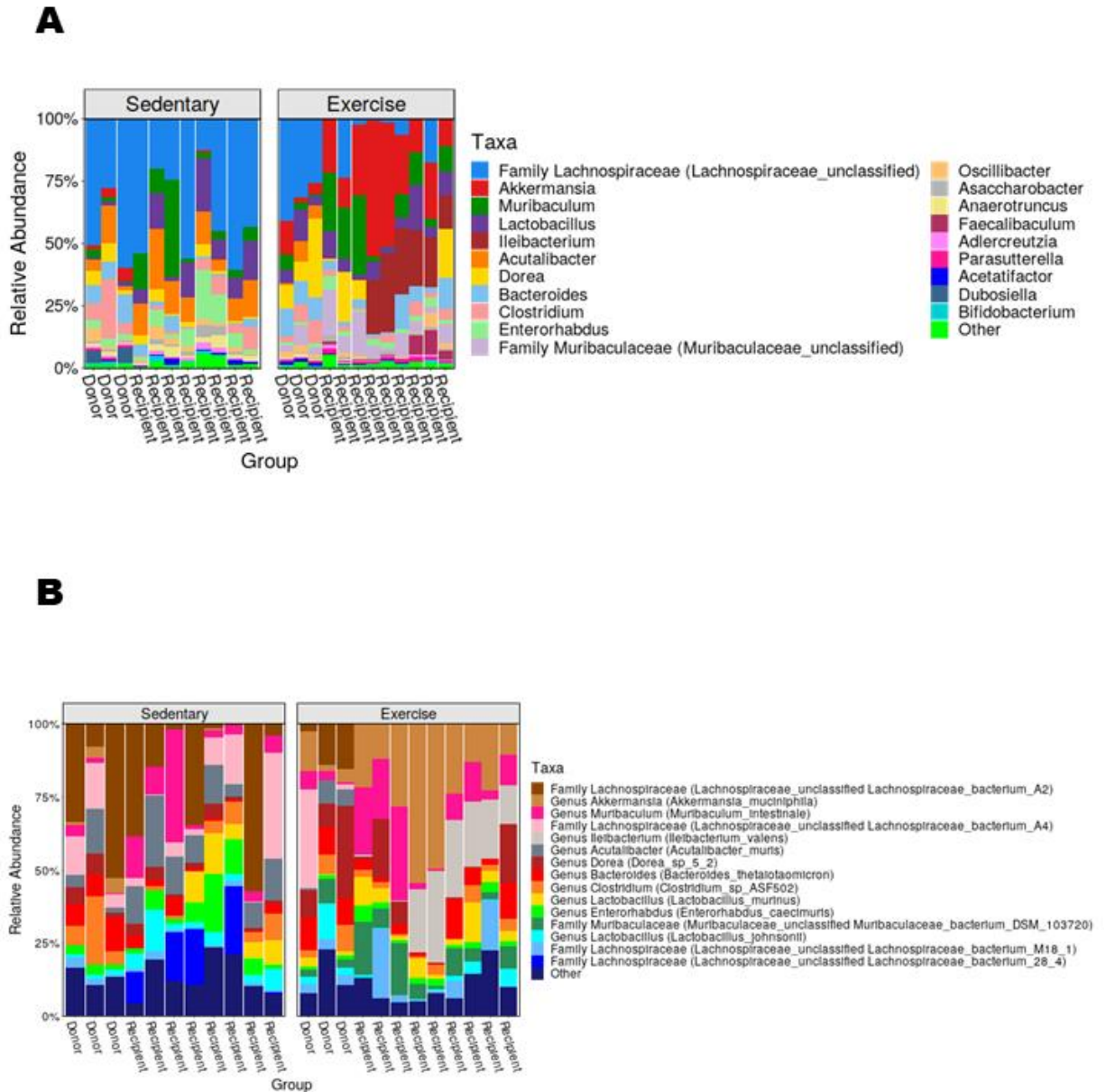


Figure 3.6 Genera and Species Comparison Between Donors and Recipients  
Stacked bar plots showing differences in the top 20 most abundant genre (A) and top 15 most abundant species (B).

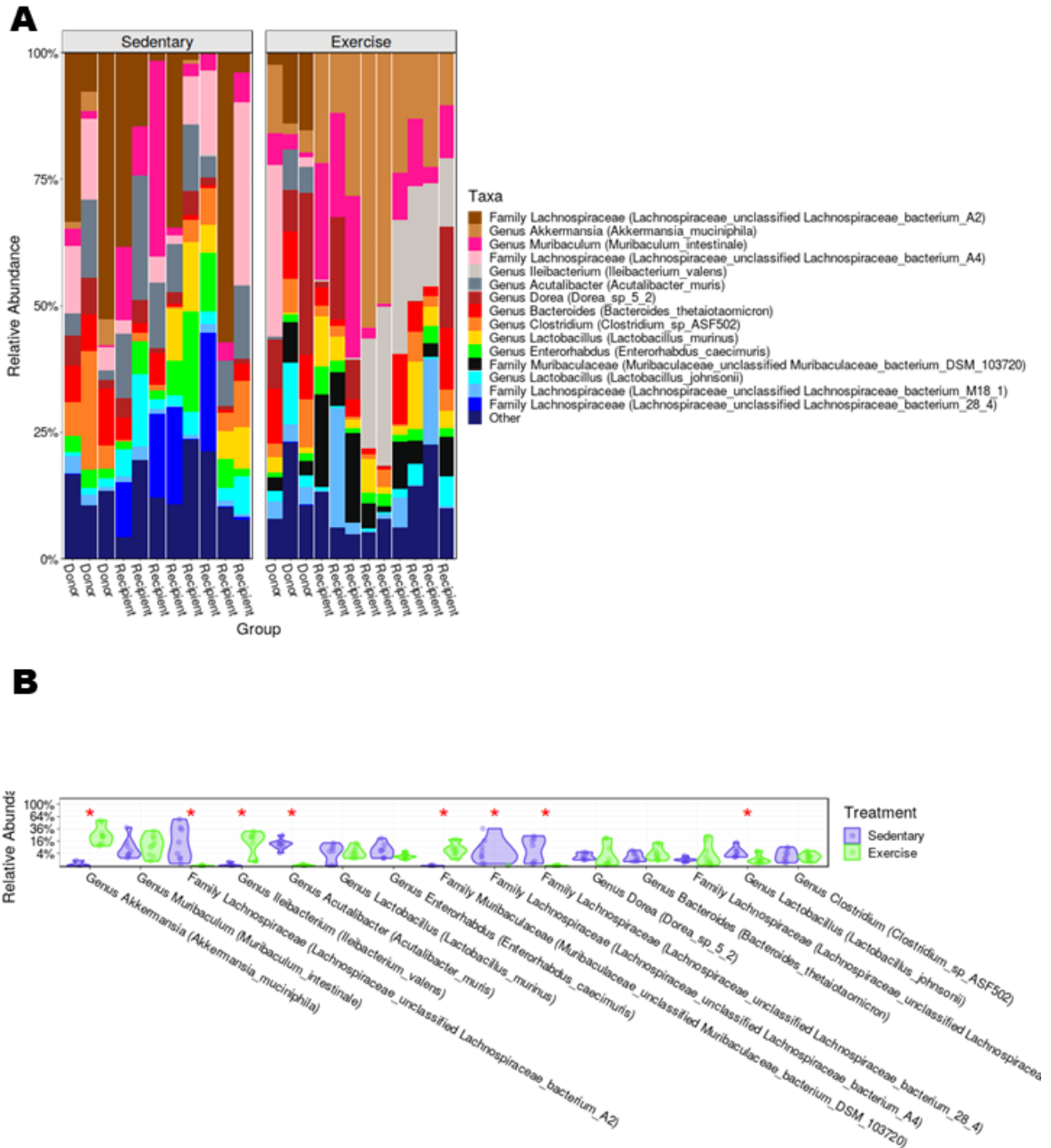


Figure 3.7 Species Comparison Between Recipients Groups

A) Stacked bar plot showing top 15 most abundant species between donors and recipients, separated by training status of the donor, B) Violin plots comparing the top 15 most abundant species between Rsed and Rex. \* Adj.  $p < 0.1$ ,  $p < 0.05$ . *Muribaculaceae bacterium DSM 103720* is colored black to highlight its abundance profile.

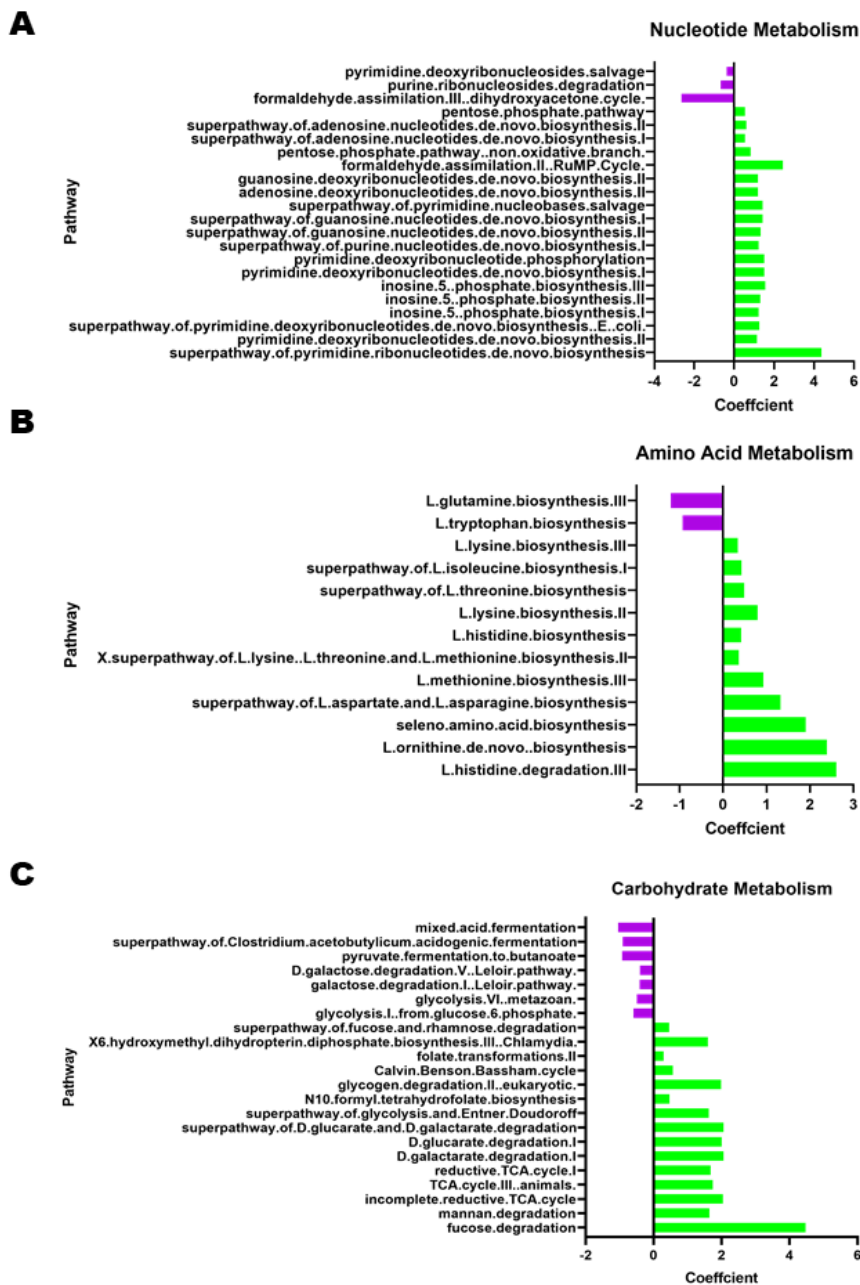


Figure 3.8 Gene Pathway Analysis  
 Comparison of gene pathways significantly associated with Rsed or Rex A) nucleotide Metabolism, B) Amino acid metabolism, C) Carbohydrate metabolism. Pathways listed are significant adj.  $p < 0.1$  and  $p < 0.05$ . Coefficient refers to effect estimate.

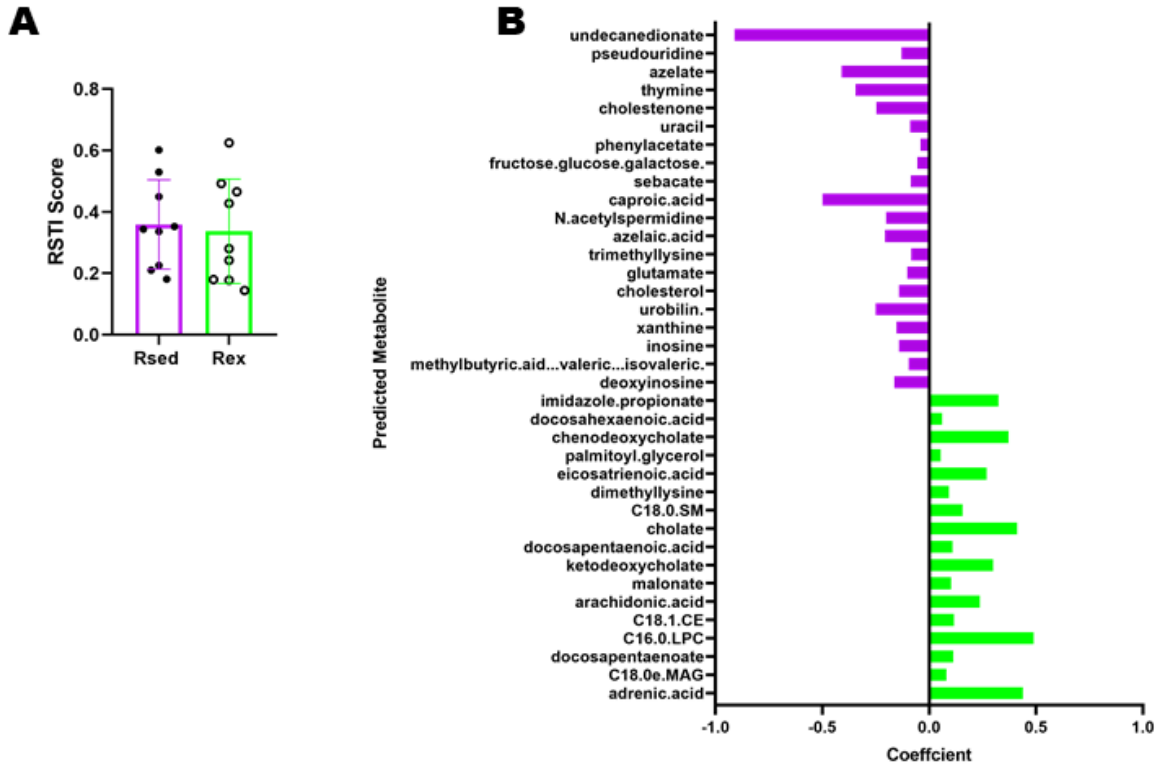


Figure 3.9 Predictive Metabolite Analysis  
 A) Representative Training Sample Index (RSTI) scores, B) Predictive metabolite significantly associated with Rsed or Rex. Pathways listed are significant at  $p < 0.05$ . Coefficient refers to effect estimate.

## CHAPTER 4. DISCUSSION

Major Findings from Dysbiosis of the Gut Microbiome Impairs Mouse Skeletal Muscle Adaption to Exercise.

This was the first study to demonstrate that antibiotic-induced dysbiosis impaired the ability of skeletal muscle to adapt to exercise. This effect was seen in both the hypertrophic response in the soleus (Figure 2.6) and fiber-type shift in the plantaris muscles (Figure 2.9). This study also revealed that antibiotic-induced dysbiosis interfered with satellite cell fusion in the plantaris muscle, an observation not seen in the soleus (Figure 2.8). These results demonstrate the influence of the gut microbiome on skeletal muscle is specific to each muscle, likely reflecting the difference in fiber-type composition between the soleus and plantaris muscles (Chapter 1.1.2).

The analysis of satellite cell abundance in the plantaris muscle revealed that satellite cells in the antibiotic-treated runners did not adequately fuse into the muscle as observed in the non-treated runners. This finding raises the intriguing possibility that the microbiome may regulate skeletal muscle stem cell i.e., satellite cell, dynamics in skeletal muscle. In support of this possibility is the results using germ-free mice in which the expression of myogenic regulatory factors, *MyoD* and *MyoG*, were downregulated compared to SPF mice [199]. The *MyoD* knockout mouse was shown to have defective satellite cells that exhibited dysregulated differentiation, fusion and formed large aggregates [388]. If the gut microbiome modulates myogenic regulatory factor expression through a yet-to-be described mechanism, then it is plausible that dysbiosis could have disrupted such a mechanism resulting in diminished satellite cell fusion to myofibers during adaptation to PoWeR training (see Figure 2.8). While speculative, but none-the-less exciting, these results indicate the gut microbiome can influence the fate of satellite cells, as seen in other stem cell populations [389].

Another finding from this study was that antibiotic administration did not interfere with exercise performance (Figure 2.5). This finding was significant due to the fact that prior studies utilizing germ-free mice or high doses of antibiotics reported exercise intolerance [202, 317]. The dose of antibiotics utilized in our study was much lower



compared to doses previously used (in both concentration and amount of antibiotics) [250, 317] yet we were able to effectively induce dysbiosis (Figures 2.2 & 2.3) with no signs of adverse effects. This result was critical to the study because the exercise stimulus, i.e., the amount of running, promoting muscle adaptation was the same between the two running groups, thus allowing us to make stronger conclusions regarding the role of the gut microbiome on skeletal muscle adaptation. Additionally, future studies investigating the role of the gut microbiome in muscle adaptation can use the dose of antibiotics we used without compromising exercise capacity or muscle function.

### Major Findings from The Gut Microbiome from an Exercise-Trained Host Ameliorates Skeletal Muscle Atrophy

The results from this study demonstrate that the gut microbiome from an exercise-trained host significantly attenuated skeletal muscle atrophy in the soleus muscle induced by hind-limb immobilization (Figure 3.2). This is a novel finding in the field of skeletal muscle-gut microbiome research, as it offers a clear therapeutic potential of the microbiome from an exercise-trained host to reduce the degree of atrophy caused by disuse. These results are in line with a recent paper which also showed the gut microbiome can mitigate skeletal muscle atrophy through the administration of the SCFA butyrate [200]. In addition to affecting muscle atrophy, I also found that recipients of the exercise-trained gut microbiome (Rex), had higher abundance of Type-2A fibers in the immobilized leg compared to recipients of gut microbiome from sedentary mice (Rsed) (Figure 3.2). This finding indicates the gut microbiome from an exercised-trained host can also modulate fiber-type composition. These findings are in support of my previous research (discussed in Chapter 2 and 4.1)[352] and other research which has shown the gut microbiome can influence fiber-type composition of a muscle [197].

To understand how the gut microbiome from an exercise-trained host regulates skeletal muscle atrophy, the cecal contents from donor and recipient mice were sent for metagenomic sequencing. Initial analysis revealed that the Rex group had significantly more observed taxonomical units (OTUs) compared to Rsed, however, there was no differences in  $\alpha$ -diversity (Figure 3.3A). These findings suggest that collectively, Rex had more low abundant species (increased species richness) compared to Rsed, with no

changes in species evenness. The analysis did not focus on these lowly abundant species but that does not negate their potential importance for future studies [390].  $\beta$ -diversity analysis showed a clear distinction between Rsed and Rex, indicating these two groups had significantly different microbiomes (Figure 3.4 A). When  $\beta$ -diversity analysis was performed comparing the donor and their respective recipient, it was found that there was significant difference between Dex and Rex, a finding not observed when comparing Dsed and Rsed (Figure 3.5 A). Currently there is not a definitive explanation for why these Dsed and Rex are different, but I propose this difference is due to the absence of exercise in the recipient group. The donors in Dex had undergone eight weeks of progressive weighted wheel running (PoWeR) prior to cecal collection. These mice were running approximately 10-12km a night against a load that was roughly 25% of their body weight (Figure 2.5). The Rex group remained sedentary throughout the experimental period which may have affected exercise-dependent microbial species. This conclusion is supported by a recent study that demonstrated rapid shifts in microbial abundance before, immediately after, and 10 days post-100 mile ultramarathon [206]. The physical act of exercise may be a potent stimulus for specific microbes, causing a significant change in their abundance. Cessation of exercise may reverse these changes in abundance, which could also influence the surrounding pool of microbial-derived metabolites that could potentially interact with the host.

The metagenomic analysis revealed many different pathways that were significantly associated with Rex compared to Rsed (Figure 3.8 A-C), suggesting the transfer of an exercise-trained microbiome significantly altered the functional capacity of the recipient microbiome. This interpretation is supported by the compositional data showing 1) the microbe *Muribaculaceae bacterium DSM 103720* which was only observed in Dex successfully transferred to all Rex and 2) microbes that were of low abundance in Rsed were significantly more abundant in Rex (Table 3.1). Therefore, I conclude that the microbiome from an exercise-trained host containing *Muribaculaceae bacterium DSM 103720* significantly changed both the composition and function of the recipient microbiome. The functional changes are reflected in specific pathways related to carbohydrate and amino acid metabolism, indicating an increase fucose, rhamnose and histidine metabolism, which could drive the production of the imidazole propionate and

propionate, respectively. This conclusion is supported by the predicted metabolite analysis, showing imidazole propionate is significantly associated with Rex (Figure 3.9 B). In skeletal muscle, imidazole propionate and propionate have been shown to activate TORC-1 [200, 319], increase the protein levels of PGC-1 $\alpha$  [391], lower the expression of atrogenes [199] and serve as an alternative fuel source [205]. I propose a mechanism that connects these two microbial derived metabolites which caused the attenuated atrophic response seen in the Rex group induced by hind-limb immobilization. This predicted pathway needs to be validated by additional experiments; however, this hypothesis posits that microbial-derived metabolites work in tandem to elicit a response in skeletal muscle.

### The Gut Microbiome and Skeletal Muscle Mass

The results from my dissertation provide evidence that the gut microbiome contributes to the regulation of skeletal muscle mass. This was seen in both an anabolic condition where, hypertrophy was blunted with dysbiosis, and a catabolic condition, where the microbiome, which was modulated by exercise, had the capacity to attenuate skeletal muscle atrophy. The result from this work agrees with other studies showing that skeletal muscle mass can be modulated by the gut microbiome. For example, Lahiri and co-workers found that skeletal muscle from germ-free mice are atrophic [199]. Upon colonization, germ-free mice showed an increase in skeletal muscle mass [199]. These results have been seen in other germ-free animals such as piglets. Skeletal muscle taken from germ-free piglets had a significantly smaller fibers compared to piglets with a microbiome [392]. Performing a fecal transplant into the germ-free piglets shifted the fiber size distribution towards larger fibers [392]. Administration of antibiotics to mice to deplete the gut microbiome resulted in significant atrophy in the leg muscles [338]. These authors further determined the muscle atrophy was not driven by the antibiotics themselves, rather aberrant bile acid signaling, which led to a decrease in phosphorylation of rpS6 through extracellular signal-regulated protein kinase (ERK) [338]. The results from my dissertation further demonstrate that skeletal muscle mass can be modulated by the gut microbiome. I also provide novel evidence that skeletal muscle fiber-type specific hypertrophy is differentially regulated by the gut microbiome. For example, in the plantaris muscle, both the Type-2A fibers hypertrophied in the untreated and treated

runners (Figure 2.8). Looking at the Type-2B+X fibers, only the untreated runners showed significant hypertrophy. This is the first time these results have been shown, demonstrating a high degree of specificity in the interaction between the gut microbiome and skeletal muscle.

### The Gut Microbiome and Skeletal Muscle Fiber-type

The result from this study also found that skeletal muscle fiber-type composition is sensitive to changes in the gut microbiome. In support of this finding, Yan and co-workers took the feces from two different species of pigs, which had distinct fiber-type compositions, and transferred the microbiome into germ-free mice. These authors found that the recipient mice exhibited similar skeletal muscle fiber-type composition as the donor pigs [197]. Bäckhead and co-workers determined the skeletal muscle of germ-free mice had significantly higher expression of phosphorylated AMP-activated protein kinase (AMPK), phosphorylated acetyl-coA carboxylase (ACC) and carnitine palmitoyltransferase (CPT) compared to conventionalized mice [193]. These data suggest that germ-free muscle had a higher capacity for lipid oxidation and possibly higher mitochondrial content. Although skeletal muscle fiber-type composition was not measured, the results are still indicative of a higher abundance of oxidative fibers in germ-free muscle. These experiments were performed in the gastrocnemius muscle which in the mouse is typically considered more glycolytic, mostly comprised of Type-2B and Type-2X fibers [393]. The data from germ-free mice suggest there may have been a shift towards the more oxidative Type-2A fibers. In comparison, when the microbiome was disrupted with antibiotics, Qui and co-workers did not find any changes in fiber-type composition [338]. Currently, there is not a defined mechanism for how the gut microbiome exerts an effect on fiber-type composition, though speculations in fiber-type composition changes may be mediated by microbially derived SCFAs [242, 394]. Dietary acetic acid supplementation was shown to significantly increase the expression of AMPK and peroxisome proliferator-activated receptor-delta (PPAR- $\delta$ ), which was correlated to a significant increase in oxidative fibers in the soleus muscle of the mouse [391]. This potential mechanism is consistent with the finding showing PPAR- $\delta$  is a downstream target of AMPK with activation of PPAR- $\delta$  associated with an increase in oxidative (slow

twitch/Type-1) fibers [395]. Determining if SCFAs produced from the gut microbiome directly interact with skeletal muscle in-vivo remains to be directly tested. Future work will need to define such a pathway and demonstrate mechanistically how SCFA and/or other gut microbial-derived metabolite(s) regulate skeletal muscle mass and fiber-type composition.

## Future Directions

### 4.1.1 Alternative Strategies to Induce Dysbiosis

This study used antibiotics to induce dysbiosis and disrupt the gut microbiome. It would be interesting to use another method which causes disturbances to the gut microbiome such as dietary manipulations. Diet exerts a strong stimulus to change both the function and composition of the microbiome [211]. A high-fat diet, in particular, has been shown to cause a pro-inflammatory microbiome [326] that is associated with cardiovascular disease, colon cancer and obesity [396-398]. It would be interesting to determine if a high-fat diet induced a dysbiotic state of the gut microbiome that resulted in impaired skeletal muscle adaptations to exercise. Furthermore, such a study could determine if exercise might help resolve dysbiosis of the gut microbiome caused by a high-fat diet. The extent of the beneficial effects of exercise on the gut microbiome are still being discovered. More research is needed to ascertain the extent by which exercise causes changes to the gut microbiome that result in beneficial effects to the host.

### 4.1.2 Identifying Gut Microbial Derived Metabolites that Regulate Promote Skeletal Muscle Hypertrophy.

This study did not identify a mechanism for how the gut microbiome regulates skeletal muscle adaptations to exercise. Future research should begin to address this gap in knowledge. Recently, Han and co-workers showed that there are 833 metabolites associated with microbial metabolism [399]. Knowledge of how exercise modulates this pool of metabolites remains incomplete. As discussed in Chapter 1, there are many potential gut microbial-derived metabolites that may be modulating skeletal muscle. SCFAs are the most studied in relation to skeletal muscle [199, 200, 205, 317] but this

does not preclude novel metabolites that arise from exercise modulation of the microbiome. Future studies need to incorporate strategies that can clearly distinguish between gut microbial metabolites from host-derived metabolites, and if these compounds have the capacity to regulate skeletal muscle.

Utilizing stable isotope tracing, future experiments can begin to determine which compounds produced from the microbiome contribute to the regulation of skeletal muscle adaptations to exercise. This can be performed by administering  $^{13}\text{C}$ -inulin, a fermentable fiber specifically metabolized by intestinal bacteria, to rodents to track the flux of labeled carbons to muscle. Lund and co-workers recently validated this method in-vivo and demonstrated that the microbiome provides carbons which ultimately participated in histone acetylation within intestinal epithelial cells [253]. Performing this experiment in exercising hosts, along with non-exercising controls, provides a potential method to identify which gut microbial-derived metabolite(s) interact with muscle and how such metabolites may change with exercise. Another important aspect of such an experiment would be the ability to better define how exercise is able to influence microbial metabolism. Understanding how exercise alters the metabolic output from the gut microbiome is an important consideration when describing the crosstalk between the gut microbiome and host.

#### 4.1.3 Validating and Testing Imidazole Propionate and Propionate

I propose that imidazole propionate and propionate are acting synergistically to blunt skeletal muscle atrophy induced by hind-limb immobilization. The gut microbiome was found to produce over 800 different metabolites, and it has been recently shown that the microbial-derived metabolites butyric acid in combination with either benzoic acid, phenylacetic acid or phenylpropionic acid, potentiated a decrease in TNF- $\alpha$  induced secretion of Il-8 [383]. These results suggest gut microbial-derived metabolites may act synergistically with one another to elicit a response in the host. To test the proposed mechanism an in-vitro model using myotubes could be employed along with imidazole propionate treatment in combination with propionate. Using myotubes I could test the hypothesis that imidazole propionate in combination with propionate stimulates skeletal

muscle protein synthesis and increases oxidative metabolism. If the results from such an in-vitro experiment support my hypothesis, I could subsequently move to an in-vivo model to determine if they can be recapitulated. This method of administering microbial metabolites directly, termed postbiotic, may be preferred over trying to directly alter certain microbes with dietary sources (prebiotic) or by consuming a high number of a few species (probiotic) [400]. Currently the efficacy of probiotics is limited and has risks via aberrant interactions with resident microbes which may lead to adverse events in the host [401]. Prebiotics refer to anything that the gut microbiota can metabolize which effects the composition and function of the microbiome [402]. Prebiotics have been shown to be a powerful method to modulate the microbiome at the single strain level [403]. A potential contraindication of prebiotics is that the compositional and functional changes may not result in universal benefits to the population [401]. The inter-individual response to prebiotics may limit the extent to which this approach can be used clinically. Therefore, identifying the gut microbial-derived metabolites that exert beneficial effects to the host may be the most advantageous route for therapeutic use.

Upon the identification of the specific pathways that connects gut microbial-derived metabolite(s) to skeletal muscle, additional experiments could be performed to validate the findings. If for example, the candidate metabolite(s) bind to a specific receptor on skeletal muscle, the expression of the receptor could be genetically manipulated. SCFAs fatty acids bind to G-coupled protein receptor (GCPR) known as free fatty acid receptor (FFAR 1,2, 3 and 4) which are expressed in tissues such as the heart, immune, adipose and skeletal muscle [244, 404]. Tang and co-workers demonstrated that the SCFA butyrate upregulated the expression of FFAR2 in myotubes leading to enhanced phosphorylation of TORC-1[200]. Future experiments utilizing transgenic mice could directly modulate the expression of FFAR2 in skeletal muscle to determine the if this pathway is one way by which SCFAs produced by the gut microbiome regulate a hypertrophic response in skeletal muscle.

An additional metabolite that was found to be significantly associated with Rex was bile acids, specifically chenodeoxycholate and cholate (Figure 3.9 B). Secondary bile

acids produced from the gut microbiome have been shown to ameliorate antibiotic induced skeletal muscle atrophy by increasing the release of fibroblast growth factor 15 (FGF15) from intestinal epithelial cells [338]. Secondary bile acids were also shown to act as a ligand for the GCPR TGR5, which is expressed in skeletal muscle. Sasaki and co-workers showed that direct oral administration of the secondary bile acid tauroolithocholic acids (TLCA) resulted in significant skeletal muscle hypertrophy [263]. However, no study has yet demonstrated that secondary bile acids produced from the gut microbiome bind to TGR5 receptors in skeletal muscle. Thus, a possible mechanism for how the exercise-trained gut microbiome might mitigate skeletal muscle atrophy may involve bile acid metabolites such as TLCA.

#### 4.1.4 Other Models of Atrophy

It has been recently shown that different models of atrophy elicit distinct transcriptomic and proteomic signatures [387]. Taking this into consideration, a future study should focus on other models of atrophy to determine if the gut microbiome from an exercise-trained host exerts the same beneficial response. Such knowledge will be important for determining the therapeutic potential of the microbiome to broadly treat the various conditions known to cause a loss of skeletal muscle mass. Extending the findings of my study into other models of atrophy has the potential to impact other conditions, such as space exploration and systemic diseases, where the underlying mechanism promoting muscle atrophy have been shown to differ [145].

#### 4.1.5 Characterizing *Muribaculaceae bacterium DSM 103720*

As mentioned previously, the microbe *Muribaculaceae bacterium DSM 103720* was observed in Dex and Rex, while absent from Dsed and Rsed. This indicates *Muribaculaceae bacterium DSM 103720* responded to exercise training in the Dex group and was able to proliferate in Rex. *Muribaculaceae bacterium DSM 103720* is not well-characterized but other members belonging to the same genus were shown to be enriched with genes relating to complex carbohydrate degradation and protein translation [405, 406]. Chung and co-workers reported that *Muribaculum* (Taxonomic Level-Family)



contained many genes involved in protein translation, which was consistent at the metatranscriptomic level [406]. These authors found that the higher abundance of translation-related pathways resulted in an increase in transcripts associated with ribosomal proteins. A detailed inspection of the current metagenomic analysis revealed that out of the 10 species contributing to the tRNA charging pathway, *Muribaculaceae bacterium DSM 103720* contributed almost 25% of the total pathway (data not shown). The metagenomic analysis in the current study is in line with previous research suggesting *Muribaculaceae bacterium DSM 103720* has a high capacity for complex carbohydrate utilization and protein translation. More experiments need to determine if and how this impact surrounding microbes and host which harbor this species.

The change in the abundance of other microbes due to the presence of *Muribaculaceae bacterium DSM 103720* may also be matched with an increase in their function leading to enhanced metabolite production. In support of this scenario, Wu and co-workers demonstrated that genetic depletion of hypoxia inducible factor 2A alpha (HIF-2 $\alpha$ ) in the intestines, decreased lactate levels, which suppressed the levels of *Bacteroides vulgatus*. The decrease in *Bacteroides vulgatus* abundance was shown to cause a greater increase in *Ruminococcus torques*, that led to an increase in taurine-conjugated cholic acid (TCA) [407]. It was not described how *Bacteroides vulgatus* modulates *Ruminococcus torques*, but it does demonstrate that microbes can influence the abundance of fellow microbes within an environment, which impacts the pool of available metabolites. The reliance of gut microbes upon one another is thought to reflect the fact that some microbes lose certain genes over evolution (auxotroph), which then cause them to rely on other microbes to produce nutrients required for their survival and ability to grow [367]. Thus, the presence of a particular microbe, such as *Muribaculaceae bacterium DSM 103720*, may lead to the production of essential nutrients or components of translation that other species, such as *Akkermanisa munciniphila*, *Faecalibaculum rodentium*, *Parasutterella excrementihominis* and *Ileibacterium valens* need for their viability within the gut.

A future set of experiments could begin to characterize *Muribaculaceae bacterium DSM 103720*. As demonstrated by Hoffman and colleagues, utilization of fecal

cell suspensions led to the characterization of a novel microbe (JB12), an *Acutlibacter* species from the family *Ruminococcaceae* [408]. This technique involves isolating microbes from feces and suspending them in growth media, removing the influence of the host or other environmental factors [220]. *Muribaculaceae* is a strict anaerobe of the *Bacteroidales* order; other members of this order have been successfully isolated from cell suspensions, streaked on agar isolates and supplied with a mucus media [405]. Collecting the feces from exercise-trained mice and performing a series of growth experiments can lead to the isolation of a species like *Muribaculaceae bacterium DSM 103720* (which can be validated by whole genome sequencing). The complete metabolic fingerprint of *Muribaculaceae bacterium* can then be identified by incubation of isolates in pure culture and collecting media at a time point that reflects optimal growth. Additional fecal cell suspensions with feces from exercise naïve mouse can be used to directly add *Muribaculaceae bacterium* into these cultures. Metabolomics can then be performed on fecal cell suspensions with or without the addition of *Muribaculaceae bacterium* to determine how this microbe specifically shapes the gut microbiome and shape the metabolite profile.

The fecal cell suspension also offers another means to interrogate if exercise leads to the production of novel gut microbial metabolites. Our group determined that performing fecal cell suspension supplemented with  $^{13}\text{C}$ -inulin, allowed for the quantification of microbial-derived metabolites [220]. This experiment can be performed using feces from exercise-trained and untrained hosts to determine how exercise alters the metabolic output. Subsequently, metabolites that appear to be associated with a microbiome from an exercise-trained host can be directly studied to determine their potential to regulate skeletal muscle mass.

## Conclusion

In conclusion, the work performed during my dissertation has demonstrated that the gut microbiome contributes to skeletal muscle plasticity, as seen in both a hypertrophic and atrophic setting. The mechanism(s) involved are not fully elucidated. Future experiments will work to unravel how the gut microbiome specifically regulates skeletal muscle plasticity. Additional experiments are needed to understand the complex interaction

between microbes within an environment and how they influence the behavior of the surrounding species. Finally, this work has brought to attention that microbial metabolites may not be working independently from one another and in fact act as a consortium.

## REFERENCES

1. Janssen, I., et al., *Skeletal muscle mass and distribution in 468 men and women aged 18-88 yr.* J Appl Physiol (1985), 2000. **89**(1): p. 81-8.
2. Partridge, T.A., *Cells that participate in regeneration of skeletal muscle.* Gene Ther, 2002. **9**(11): p. 752-3.
3. Lieber, R.L., et al., *Skeletal muscle mechanics, energetics and plasticity.* J Neuroeng Rehabil, 2017. **14**(1): p. 108.
4. Woszczyna, M.N. and T.A. Rando, *A Muscle Stem Cell Support Group: Coordinated Cellular Responses in Muscle Regeneration.* Dev Cell, 2018. **46**(2): p. 135-143.
5. Pedersen, B.K., *Muscles and their myokines.* J Exp Biol, 2011. **214**(Pt 2): p. 337-46.
6. Vechetti, I.J., Jr., et al., *The role of extracellular vesicles in skeletal muscle and systematic adaptation to exercise.* J Physiol, 2020.
7. Gomez-Pinilla, F., et al., *Differential regulation by exercise of BDNF and NT-3 in rat spinal cord and skeletal muscle.* Eur J Neurosci, 2001. **13**(6): p. 1078-84.
8. Vechetti, I.J., Jr., et al., *Mechanical overload-induced muscle-derived extracellular vesicles promote adipose tissue lipolysis.* FASEB J, 2021. **35**(6): p. e21644.
9. Goates, S., et al., *Economic Impact of Hospitalizations in US Adults with Sarcopenia.* J Frailty Aging, 2019. **8**(2): p. 93-99.
10. Koliaki, C., et al., *Sarcopenic Obesity: Epidemiologic Evidence, Pathophysiology, and Therapeutic Perspectives.* Curr Obes Rep, 2019. **8**(4): p. 458-471.
11. Anker, S.D., et al., *Wasting as independent risk factor for mortality in chronic heart failure.* Lancet, 1997. **349**(9058): p. 1050-3.
12. Kouw, I.W.K., et al., *One Week of Hospitalization Following Elective Hip Surgery Induces Substantial Muscle Atrophy in Older Patients.* J Am Med Dir Assoc, 2019. **20**(1): p. 35-42.
13. Lo, Y.C., et al., *Medical costs of a low skeletal muscle mass are modulated by dietary diversity and physical activity in community-dwelling older Taiwanese: a longitudinal study.* Int J Behav Nutr Phys Act, 2017. **14**(1): p. 31.
14. Janssen, I., et al., *The healthcare costs of sarcopenia in the United States.* J Am Geriatr Soc, 2004. **52**(1): p. 80-5.
15. von Haehling, S. and S.D. Anker, *Prevalence, incidence and clinical impact of cachexia: facts and numbers-update 2014.* J Cachexia Sarcopenia Muscle, 2014. **5**(4): p. 261-3.
16. Arentson-Lantz, E.J., et al., *Countering disuse atrophy in older adults with low volume leucine supplementation.* J Appl Physiol (1985), 2020.
17. Fiatarone, M.A., et al., *Exercise training and nutritional supplementation for physical frailty in very elderly people.* N Engl J Med, 1994. **330**(25): p. 1769-75.
18. Supasyndh, O., et al., *Effect of oral anabolic steroid on muscle strength and muscle growth in hemodialysis patients.* Clin J Am Soc Nephrol, 2013. **8**(2): p. 271-9.
19. Basaria, S., et al., *Adverse events associated with testosterone administration.* N Engl J Med, 2010. **363**(2): p. 109-22.

20. Bamman, M.M., B.M. Roberts, and G.R. Adams, *Molecular Regulation of Exercise-Induced Muscle Fiber Hypertrophy*. Cold Spring Harb Perspect Med, 2018. **8**(6).
21. Bowen, T.S., G. Schuler, and V. Adams, *Skeletal muscle wasting in cachexia and sarcopenia: molecular pathophysiology and impact of exercise training*. J Cachexia Sarcopenia Muscle, 2015. **6**(3): p. 197-207.
22. Schiaffino, S., et al., *Molecular Mechanisms of Skeletal Muscle Hypertrophy*. J Neuromuscul Dis, 2021. **8**(2): p. 169-183.
23. Ryall, J.G., *Metabolic reprogramming as a novel regulator of skeletal muscle development and regeneration*. FEBS J, 2013. **280**(17): p. 4004-13.
24. Hargreaves, M., *Skeletal muscle metabolism during exercise in humans*. Clin Exp Pharmacol Physiol, 2000. **27**(3): p. 225-8.
25. Hargreaves, M. and L.L. Spriet, *Skeletal muscle energy metabolism during exercise*. Nat Metab, 2020. **2**(9): p. 817-828.
26. Sharma, N.S., A.K. Saluja, and S. Banerjee, *"Nutrient-sensing" and self-renewal: O-GlcNAc in a new role*. J Bioenerg Biomembr, 2018. **50**(3): p. 205-211.
27. Ly, C.H., G.S. Lynch, and J.G. Ryall, *A Metabolic Roadmap for Somatic Stem Cell Fate*. Cell Metab, 2020.
28. Haws, S.A., C.M. Leech, and J.M. Denu, *Metabolism and the Epigenome: A Dynamic Relationship*. Trends Biochem Sci, 2020. **45**(9): p. 731-747.
29. Diehl, K.L. and T.W. Muir, *Chromatin as a key consumer in the metabolite economy*. Nat Chem Biol, 2020. **16**(6): p. 620-629.
30. Hagos, E.G. and S.T. Dougan, *Time-dependent patterning of the mesoderm and endoderm by Nodal signals in zebrafish*. BMC Dev Biol, 2007. **7**: p. 22.
31. Chal, J. and O. Pourquie, *Making muscle: skeletal myogenesis in vivo and in vitro*. Development, 2017. **144**(12): p. 2104-2122.
32. Braun, T. and M. Gautel, *Transcriptional mechanisms regulating skeletal muscle differentiation, growth and homeostasis*. Nat Rev Mol Cell Biol, 2011. **12**(6): p. 349-61.
33. Buckingham, M., *Making muscle in mammals*. Trends Genet, 1992. **8**(4): p. 144-8.
34. Kalcheim, C. and R. Ben-Yair, *Cell rearrangements during development of the somite and its derivatives*. Curr Opin Genet Dev, 2005. **15**(4): p. 371-80.
35. Bryson-Richardson, R.J. and P.D. Currie, *The genetics of vertebrate myogenesis*. Nat Rev Genet, 2008. **9**(8): p. 632-46.
36. Montarras, D., et al., *Developmental patterns in the expression of Myf5, MyoD, myogenin, and MRF4 during myogenesis*. New Biol, 1991. **3**(6): p. 592-600.
37. Tajbakhsh, S., et al., *Gene targeting the myf-5 locus with nlacZ reveals expression of this myogenic factor in mature skeletal muscle fibres as well as early embryonic muscle*. Dev Dyn, 1996. **206**(3): p. 291-300.
38. Marcelle, C., M.R. Stark, and M. Bronner-Fraser, *Coordinate actions of BMPs, Wnts, Shh and noggin mediate patterning of the dorsal somite*. Development, 1997. **124**(20): p. 3955-63.
39. Ben-Yair, R., N. Kahane, and C. Kalcheim, *LGN-dependent orientation of cell divisions in the dermomyotome controls lineage segregation into muscle and dermis*. Development, 2011. **138**(19): p. 4155-66.

40. Kahane, N., Y. Cinnamon, and C. Kalcheim, *The origin and fate of pioneer myotomal cells in the avian embryo*. Mech Dev, 1998. **74**(1-2): p. 59-73.
41. Williams, B.A. and C.P. Ordahl, *Pax-3 expression in segmental mesoderm marks early stages in myogenic cell specification*. Development, 1994. **120**(4): p. 785-96.
42. Pourquie, O., et al., *Control of somite patterning by signals from the lateral plate*. Proc Natl Acad Sci U S A, 1995. **92**(8): p. 3219-23.
43. Ott, M.O., et al., *Early expression of the myogenic regulatory gene, myf-5, in precursor cells of skeletal muscle in the mouse embryo*. Development, 1991. **111**(4): p. 1097-107.
44. Bajard, L., et al., *A novel genetic hierarchy functions during hypaxial myogenesis: Pax3 directly activates Myf5 in muscle progenitor cells in the limb*. Genes Dev, 2006. **20**(17): p. 2450-64.
45. Giordani, J., et al., *Six proteins regulate the activation of Myf5 expression in embryonic mouse limbs*. Proc Natl Acad Sci U S A, 2007. **104**(27): p. 11310-5.
46. Gustafsson, M.K., et al., *Myf5 is a direct target of long-range Shh signaling and Gli regulation for muscle specification*. Genes Dev, 2002. **16**(1): p. 114-26.
47. Sato, T., et al., *A Pax3/Dmrt2/Myf5 regulatory cascade functions at the onset of myogenesis*. PLoS Genet, 2010. **6**(4): p. e1000897.
48. Mauro, A., *Satellite cell of skeletal muscle fibers*. J Biophys Biochem Cytol, 1961. **9**: p. 493-5.
49. Lepper, C. and C.M. Fan, *Inducible lineage tracing of Pax7-descendant cells reveals embryonic origin of adult satellite cells*. Genesis, 2010. **48**(7): p. 424-36.
50. Schultz, E., *A quantitative study of the satellite cell population in postnatal mouse lumbrical muscle*. Anat Rec, 1974. **180**(4): p. 589-95.
51. Schultz, E., M.C. Gibson, and T. Champion, *Satellite cells are mitotically quiescent in mature mouse muscle: an EM and radioautographic study*. J Exp Zool, 1978. **206**(3): p. 451-6.
52. Relaix, F., et al., *Perspectives on skeletal muscle stem cells*. Nat Commun, 2021. **12**(1): p. 692.
53. Yablonka-Reuveni, Z., *The skeletal muscle satellite cell: still young and fascinating at 50*. J Histochem Cytochem, 2011. **59**(12): p. 1041-59.
54. Seale, P., et al., *Pax7 is required for the specification of myogenic satellite cells*. Cell, 2000. **102**(6): p. 777-86.
55. Murach, K.A., et al., *Starring or Supporting Role? Satellite Cells and Skeletal Muscle Fiber Size Regulation*. Physiology (Bethesda), 2018. **33**(1): p. 26-38.
56. Fry, C.S., et al., *Myogenic Progenitor Cells Control Extracellular Matrix Production by Fibroblasts during Skeletal Muscle Hypertrophy*. Cell Stem Cell, 2017. **20**(1): p. 56-69.
57. Ceafalan, L.C., et al., *Skeletal muscle regeneration involves macrophage-myoblast bonding*. Cell Adh Migr, 2018. **12**(3): p. 228-235.
58. Yartseva, V., et al., *Heterogeneity of Satellite Cells Implicates DELTA1/NOTCH2 Signaling in Self-Renewal*. Cell Rep, 2020. **30**(5): p. 1491-1503 e6.
59. Ryall, J.G., et al., *The NAD(+)-dependent SIRT1 deacetylase translates a metabolic switch into regulatory epigenetics in skeletal muscle stem cells*. Cell Stem Cell, 2015. **16**(2): p. 171-83.

60. Gillette, T.G. and J.A. Hill, *Readers, writers, and erasers: chromatin as the whiteboard of heart disease*. *Circ Res*, 2015. **116**(7): p. 1245-53.
61. Reik, W., W. Dean, and J. Walter, *Epigenetic reprogramming in mammalian development*. *Science*, 2001. **293**(5532): p. 1089-93.
62. Sincennes, M.C., C.E. Brun, and M.A. Rudnicki, *Concise Review: Epigenetic Regulation of Myogenesis in Health and Disease*. *Stem Cells Transl Med*, 2016. **5**(3): p. 282-90.
63. Dai, Z., V. Ramesh, and J.W. Locasale, *The evolving metabolic landscape of chromatin biology and epigenetics*. *Nat Rev Genet*, 2020. **21**(12): p. 737-753.
64. Yucel, N., et al., *Glucose Metabolism Drives Histone Acetylation Landscape Transitions that Dictate Muscle Stem Cell Function*. *Cell Rep*, 2019. **27**(13): p. 3939-3955 e6.
65. Lieber, R.L., *Skeletal muscle adaptability. I: Review of basic properties*. *Dev Med Child Neurol*, 1986. **28**(3): p. 390-7.
66. Gans, C. and W.J. Bock, *The functional significance of muscle architecture--a theoretical analysis*. *Ergeb Anat Entwicklungsgesch*, 1965. **38**: p. 115-42.
67. Lieber, R.L. and J. Friden, *Functional and clinical significance of skeletal muscle architecture*. *Muscle Nerve*, 2000. **23**(11): p. 1647-66.
68. Grotmol, S., et al., *Spatial distribution of fiber types within skeletal muscle fascicles from Standardbred horses*. *Anat Rec*, 2002. **268**(2): p. 131-6.
69. Henderson, C.A., et al., *Overview of the Muscle Cytoskeleton*. *Compr Physiol*, 2017. **7**(3): p. 891-944.
70. Csapo, R., M. Gumpenberger, and B. Wessner, *Skeletal Muscle Extracellular Matrix - What Do We Know About Its Composition, Regulation, and Physiological Roles? A Narrative Review*. *Front Physiol*, 2020. **11**: p. 253.
71. Gillies, A.R. and R.L. Lieber, *Structure and function of the skeletal muscle extracellular matrix*. *Muscle Nerve*, 2011. **44**(3): p. 318-31.
72. Maas, H. and T.G. Sandercock, *Force transmission between synergistic skeletal muscles through connective tissue linkages*. *J Biomed Biotechnol*, 2010. **2010**: p. 575672.
73. Purslow, P.P., *The Structure and Role of Intramuscular Connective Tissue in Muscle Function*. *Front Physiol*, 2020. **11**: p. 495.
74. Halper, J. and M. Kjaer, *Basic components of connective tissues and extracellular matrix: elastin, fibrillin, fibulins, fibrinogen, fibronectin, laminin, tenascins and thrombospondins*. *Adv Exp Med Biol*, 2014. **802**: p. 31-47.
75. Mukund, K. and S. Subramaniam, *Skeletal muscle: A review of molecular structure and function, in health and disease*. *Wiley Interdiscip Rev Syst Biol Med*, 2020. **12**(1): p. e1462.
76. Luther, P.K., *The vertebrate muscle Z-disc: sarcomere anchor for structure and signalling*. *J Muscle Res Cell Motil*, 2009. **30**(5-6): p. 171-85.
77. Geeves, M.A., R. Fedorov, and D.J. Manstein, *Molecular mechanism of actomyosin-based motility*. *Cell Mol Life Sci*, 2005. **62**(13): p. 1462-77.
78. Huxley, H. and J. Hanson, *Changes in the cross-striations of muscle during contraction and stretch and their structural interpretation*. *Nature*, 1954. **173**(4412): p. 973-6.

79. Wang, Z., et al., *The molecular basis for sarcomere organization in vertebrate skeletal muscle*. Cell, 2021. **184**(8): p. 2135-2150 e13.
80. Raeker, M.O., et al., *Membrane-myofibril cross-talk in myofibrillogenesis and in muscular dystrophy pathogenesis: lessons from the zebrafish*. Front Physiol, 2014. **5**: p. 14.
81. Boppart, M.D. and Z.S. Mahmassani, *Integrin signaling: linking mechanical stimulation to skeletal muscle hypertrophy*. Am J Physiol Cell Physiol, 2019. **317**(4): p. C629-C641.
82. Craig, S.W. and J.V. Pardo, *Gamma actin, spectrin, and intermediate filament proteins colocalize with vinculin at costameres, myofibril-to-sarcolemma attachment sites*. Cell Motil, 1983. **3**(5-6): p. 449-62.
83. Vassilopoulos, S., *Unconventional roles for membrane traffic proteins in response to muscle membrane stress*. Curr Opin Cell Biol, 2020. **65**: p. 42-49.
84. Peter, A.K., et al., *The costamere bridges sarcomeres to the sarcolemma in striated muscle*. Prog Pediatr Cardiol, 2011. **31**(2): p. 83-88.
85. Anastasi, G., et al., *Costameric proteins in human skeletal muscle during muscular inactivity*. J Anat, 2008. **213**(3): p. 284-95.
86. Hoffman, E.P., R.H. Brown, Jr., and L.M. Kunkel, *Dystrophin: the protein product of the Duchenne muscular dystrophy locus*. Cell, 1987. **51**(6): p. 919-28.
87. Koenig, M., et al., *The molecular basis for Duchenne versus Becker muscular dystrophy: correlation of severity with type of deletion*. Am J Hum Genet, 1989. **45**(4): p. 498-506.
88. Lieber, R.L. and B.I. Binder-Markey, *Biochemical and structural basis of the passive mechanical properties of whole skeletal muscle*. J Physiol, 2021. **599**(16): p. 3809-3823.
89. Schiaffino, S., et al., *Developmental myosins: expression patterns and functional significance*. Skelet Muscle, 2015. **5**: p. 22.
90. Schiaffino, S. and C. Reggiani, *Fiber types in mammalian skeletal muscles*. Physiol Rev, 2011. **91**(4): p. 1447-531.
91. Zierath, J.R. and J.A. Hawley, *Skeletal muscle fiber type: influence on contractile and metabolic properties*. PLoS Biol, 2004. **2**(10): p. e348.
92. Wang, Y. and J.E. Pessin, *Mechanisms for fiber-type specificity of skeletal muscle atrophy*. Curr Opin Clin Nutr Metab Care, 2013. **16**(3): p. 243-50.
93. Scott, W., J. Stevens, and S.A. Binder-Macleod, *Human skeletal muscle fiber type classifications*. Phys Ther, 2001. **81**(11): p. 1810-6.
94. Rubenstein, A.B., et al., *Single-cell transcriptional profiles in human skeletal muscle*. Sci Rep, 2020. **10**(1): p. 229.
95. Schiaffino, S., et al., *Mechanisms regulating skeletal muscle growth and atrophy*. FEBS J, 2013. **280**(17): p. 4294-314.
96. McCarthy, J.J. and K.A. Murach, *Anabolic and Catabolic Signaling Pathways That Regulate Skeletal Muscle Mass*. Nutrition and Enhanced Sports Performance: Muscle Building, Endurance, and Strength, 2nd Edition, 2019: p. 275-290.
97. Kirby, T.J., *Mechanosensitive pathways controlling translation regulatory processes in skeletal muscle and implications for adaptation*. J Appl Physiol (1985), 2019. **127**(2): p. 608-618.



98. Attwaters, M. and S.M. Hughes, *Cellular and molecular pathways controlling muscle size in response to exercise*. FEBS J, 2021.
99. Anthony, T.G., *Mechanisms of protein balance in skeletal muscle*. Domest Anim Endocrinol, 2016. **56 Suppl**: p. S23-32.
100. Saxton, R.A. and D.M. Sabatini, *mTOR Signaling in Growth, Metabolism, and Disease*. Cell, 2017. **169**(2): p. 361-371.
101. Vainshtein, A. and M. Sandri, *Signaling Pathways That Control Muscle Mass*. Int J Mol Sci, 2020. **21**(13).
102. Mayer, C. and I. Grummt, *Ribosome biogenesis and cell growth: mTOR coordinates transcription by all three classes of nuclear RNA polymerases*. Oncogene, 2006. **25**(48): p. 6384-91.
103. Mayer, C., et al., *mTOR-dependent activation of the transcription factor TIF-IA links rRNA synthesis to nutrient availability*. Genes Dev, 2004. **18**(4): p. 423-34.
104. Giguere, V., *Canonical signaling and nuclear activity of mTOR-a teamwork effort to regulate metabolism and cell growth*. FEBS J, 2018. **285**(9): p. 1572-1588.
105. Iadevaia, V., R. Liu, and C.G. Proud, *mTORC1 signaling controls multiple steps in ribosome biogenesis*. Semin Cell Dev Biol, 2014. **36**: p. 113-20.
106. Hsieh, A.C., et al., *The translational landscape of mTOR signalling steers cancer initiation and metastasis*. Nature, 2012. **485**(7396): p. 55-61.
107. Hannan, K.M., et al., *mTOR-dependent regulation of ribosomal gene transcription requires S6K1 and is mediated by phosphorylation of the carboxy-terminal activation domain of the nucleolar transcription factor UBF*. Mol Cell Biol, 2003. **23**(23): p. 8862-77.
108. Ruvinsky, I., et al., *Ribosomal protein S6 phosphorylation is a determinant of cell size and glucose homeostasis*. Genes Dev, 2005. **19**(18): p. 2199-211.
109. Kantidakis, T., et al., *mTOR associates with TFIIC, is found at tRNA and 5S rRNA genes, and targets their repressor Maf1*. Proc Natl Acad Sci U S A, 2010. **107**(26): p. 11823-8.
110. Figueiredo, V.C., J.F. Markworth, and D. Cameron-Smith, *Considerations on mTOR regulation at serine 2448: implications for muscle metabolism studies*. Cell Mol Life Sci, 2017. **74**(14): p. 2537-2545.
111. Hay, N. and N. Sonenberg, *Upstream and downstream of mTOR*. Genes Dev, 2004. **18**(16): p. 1926-45.
112. Mamane, Y., et al., *mTOR, translation initiation and cancer*. Oncogene, 2006. **25**(48): p. 6416-22.
113. Baar, K. and K. Esser, *Phosphorylation of p70(S6k) correlates with increased skeletal muscle mass following resistance exercise*. Am J Physiol, 1999. **276**(1): p. C120-7.
114. Bodine, S.C., et al., *Akt/mTOR pathway is a crucial regulator of skeletal muscle hypertrophy and can prevent muscle atrophy in vivo*. Nat Cell Biol, 2001. **3**(11): p. 1014-9.
115. Laplante, M. and D.M. Sabatini, *mTOR signaling in growth control and disease*. Cell, 2012. **149**(2): p. 274-93.
116. Yang, H., et al., *The structure of mTOR complexes at a glance*. Precision Cancer Medicine, 2018. **1**.

117. Kaizuka, T., et al., *Tti1 and Tel2 are critical factors in mammalian target of rapamycin complex assembly*. J Biol Chem, 2010. **285**(26): p. 20109-16.
118. Kleinert, M., et al., *Mammalian target of rapamycin complex 2 regulates muscle glucose uptake during exercise in mice*. J Physiol, 2017. **595**(14): p. 4845-4855.
119. Thorpe, L.M., H. Yuzugullu, and J.J. Zhao, *PI3K in cancer: divergent roles of isoforms, modes of activation and therapeutic targeting*. Nat Rev Cancer, 2015. **15**(1): p. 7-24.
120. Dibble, C.C. and L.C. Cantley, *Regulation of mTORC1 by PI3K signaling*. Trends Cell Biol, 2015. **25**(9): p. 545-55.
121. Garami, A., et al., *Insulin activation of Rheb, a mediator of mTOR/S6K/4E-BP signaling, is inhibited by TSC1 and 2*. Mol Cell, 2003. **11**(6): p. 1457-66.
122. Yang, H., et al., *Mechanisms of mTORC1 activation by RHEB and inhibition by PRAS40*. Nature, 2017. **552**(7685): p. 368-373.
123. Shin, H.R. and R. Zoncu, *The Lysosome at the Intersection of Cellular Growth and Destruction*. Dev Cell, 2020. **54**(2): p. 226-238.
124. Goodman, C.A., *Role of mTORC1 in mechanically induced increases in translation and skeletal muscle mass*. J Appl Physiol (1985), 2019. **127**(2): p. 581-590.
125. Dowling, R.J., et al., *mTORC1-mediated cell proliferation, but not cell growth, controlled by the 4E-BPs*. Science, 2010. **328**(5982): p. 1172-6.
126. Sancak, Y., et al., *PRAS40 is an insulin-regulated inhibitor of the mTORC1 protein kinase*. Mol Cell, 2007. **25**(6): p. 903-15.
127. Oshiro, N., et al., *The proline-rich Akt substrate of 40 kDa (PRAS40) is a physiological substrate of mammalian target of rapamycin complex 1*. J Biol Chem, 2007. **282**(28): p. 20329-39.
128. Fonseca, B.D., et al., *La-related Protein 1 (LARP1) Represses Terminal Oligopyrimidine (TOP) mRNA Translation Downstream of mTOR Complex 1 (mTORC1)*. J Biol Chem, 2015. **290**(26): p. 15996-6020.
129. Cockman, E., P. Anderson, and P. Ivanov, *TOP mRNPs: Molecular Mechanisms and Principles of Regulation*. Biomolecules, 2020. **10**(7).
130. Land, S.C. and A.R. Tee, *Hypoxia-inducible factor 1alpha is regulated by the mammalian target of rapamycin (mTOR) via an mTOR signaling motif*. J Biol Chem, 2007. **282**(28): p. 20534-43.
131. Weidemann, A. and R.S. Johnson, *Biology of HIF-1alpha*. Cell Death Differ, 2008. **15**(4): p. 621-7.
132. Billin, A.N., et al., *HIF prolyl hydroxylase inhibition protects skeletal muscle from eccentric contraction-induced injury*. Skelet Muscle, 2018. **8**(1): p. 35.
133. Valentino, T., et al., *Evidence of myomiR regulation of the pentose phosphate pathway during mechanical load-induced hypertrophy*. Physiol Rep, 2021. **9**(23): p. e15137.
134. Hoshino, D., et al., *Trans-omic Analysis Reveals ROS-Dependent Pentose Phosphate Pathway Activation after High-Frequency Electrical Stimulation in C2C12 Myotubes*. iScience, 2020. **23**(10): p. 101558.
135. Reddy, A., et al., *pH-Gated Succinate Secretion Regulates Muscle Remodeling in Response to Exercise*. Cell, 2020. **183**(1): p. 62-75 e17.

136. De Souza, R.W., et al., *High-intensity resistance training with insufficient recovery time between bouts induce atrophy and alterations in myosin heavy chain content in rat skeletal muscle*. *Anat Rec (Hoboken)*, 2011. **294**(8): p. 1393-400.
137. Cohen, S., J.A. Nathan, and A.L. Goldberg, *Muscle wasting in disease: molecular mechanisms and promising therapies*. *Nat Rev Drug Discov*, 2015. **14**(1): p. 58-74.
138. Trombetti, A., et al., *Age-associated declines in muscle mass, strength, power, and physical performance: impact on fear of falling and quality of life*. *Osteoporos Int*, 2016. **27**(2): p. 463-71.
139. Li, R., et al., *Associations of Muscle Mass and Strength with All-Cause Mortality among US Older Adults*. *Med Sci Sports Exerc*, 2018. **50**(3): p. 458-467.
140. Lecker, S.H., et al., *Multiple types of skeletal muscle atrophy involve a common program of changes in gene expression*. *FASEB J*, 2004. **18**(1): p. 39-51.
141. Caron, A.Z., et al., *A novel hindlimb immobilization procedure for studying skeletal muscle atrophy and recovery in mouse*. *J Appl Physiol (1985)*, 2009. **106**(6): p. 2049-59.
142. Fitts, R.H., et al., *Models of disuse: a comparison of hindlimb suspension and immobilization*. *J Appl Physiol (1985)*, 1986. **60**(6): p. 1946-53.
143. Onda, A., et al., *New mouse model of skeletal muscle atrophy using spiral wire immobilization*. *Muscle Nerve*, 2016. **54**(4): p. 788-91.
144. You, J.S., et al., *The role of mTOR signaling in the regulation of protein synthesis and muscle mass during immobilization in mice*. *Dis Model Mech*, 2015. **8**(9): p. 1059-69.
145. Cadena, S.M., et al., *Skeletal muscle in MuRF1 null mice is not spared in low-gravity conditions, indicating atrophy proceeds by unique mechanisms in space*. *Sci Rep*, 2019. **9**(1): p. 9397.
146. Xia, Q., et al., *The Role of Autophagy in Skeletal Muscle Diseases*. *Front Physiol*, 2021. **12**: p. 638983.
147. Gomes, M.D., et al., *Atrogin-1, a muscle-specific F-box protein highly expressed during muscle atrophy*. *Proc Natl Acad Sci U S A*, 2001. **98**(25): p. 14440-5.
148. Bodine, S.C., et al., *Identification of ubiquitin ligases required for skeletal muscle atrophy*. *Science*, 2001. **294**(5547): p. 1704-8.
149. Sartori, R., V. Romanello, and M. Sandri, *Mechanisms of muscle atrophy and hypertrophy: implications in health and disease*. *Nat Commun*, 2021. **12**(1): p. 330.
150. Baehr, L.M., J.D. Furlow, and S.C. Bodine, *Muscle sparing in muscle RING finger 1 null mice: response to synthetic glucocorticoids*. *J Physiol*, 2011. **589**(Pt 19): p. 4759-76.
151. Cohen, S., et al., *Ubiquitylation by Trim32 causes coupled loss of desmin, Z-bands, and thin filaments in muscle atrophy*. *J Cell Biol*, 2012. **198**(4): p. 575-89.
152. Paul, P.K., et al., *Targeted ablation of TRAF6 inhibits skeletal muscle wasting in mice*. *J Cell Biol*, 2010. **191**(7): p. 1395-411.
153. Nagpal, P., et al., *The ubiquitin ligase Nedd4-1 participates in denervation-induced skeletal muscle atrophy in mice*. *PLoS One*, 2012. **7**(10): p. e46427.
154. Sandri, M., et al., *Foxo transcription factors induce the atrophy-related ubiquitin ligase atrogin-1 and cause skeletal muscle atrophy*. *Cell*, 2004. **117**(3): p. 399-412.
155. O'Neill, B.T., et al., *FoxO Transcription Factors Are Critical Regulators of Diabetes-Related Muscle Atrophy*. *Diabetes*, 2019. **68**(3): p. 556-570.

156. McPherron, A.C., A.M. Lawler, and S.J. Lee, *Regulation of skeletal muscle mass in mice by a new TGF-beta superfamily member*. *Nature*, 1997. **387**(6628): p. 83-90.
157. Han, H.Q., et al., *Myostatin/activin pathway antagonism: molecular basis and therapeutic potential*. *Int J Biochem Cell Biol*, 2013. **45**(10): p. 2333-47.
158. Ross, S. and C.S. Hill, *How the Smads regulate transcription*. *Int J Biochem Cell Biol*, 2008. **40**(3): p. 383-408.
159. Zimmers, T.A., et al., *Induction of cachexia in mice by systemically administered myostatin*. *Science*, 2002. **296**(5572): p. 1486-8.
160. Goodman, C.A., et al., *Smad3 induces atrogen-1, inhibits mTOR and protein synthesis, and promotes muscle atrophy in vivo*. *Mol Endocrinol*, 2013. **27**(11): p. 1946-57.
161. Zhou, X., et al., *Reversal of cancer cachexia and muscle wasting by ActRIIB antagonism leads to prolonged survival*. *Cell*, 2010. **142**(4): p. 531-43.
162. Lee, S.J. and A.C. McPherron, *Regulation of myostatin activity and muscle growth*. *Proc Natl Acad Sci U S A*, 2001. **98**(16): p. 9306-11.
163. Webster, J.M., et al., *Inflammation and Skeletal Muscle Wasting During Cachexia*. *Front Physiol*, 2020. **11**: p. 597675.
164. Jepson, M.M., et al., *The effects of endotoxaemia on protein metabolism in skeletal muscle and liver of fed and fasted rats*. *Biochem J*, 1986. **235**(2): p. 329-36.
165. Langen, R.C., et al., *NF-kappaB activation is required for the transition of pulmonary inflammation to muscle atrophy*. *Am J Respir Cell Mol Biol*, 2012. **47**(3): p. 288-97.
166. Balage, M., et al., *Presence of low-grade inflammation impaired postprandial stimulation of muscle protein synthesis in old rats*. *J Nutr Biochem*, 2010. **21**(4): p. 325-31.
167. Draganidis, D., et al., *Inflammaging and Skeletal Muscle: Can Protein Intake Make a Difference?* *J Nutr*, 2016. **146**(10): p. 1940-1952.
168. Cani, P.D., *Human gut microbiome: hopes, threats and promises*. *Gut*, 2018. **67**(9): p. 1716-1725.
169. Almeida, A., et al., *A new genomic blueprint of the human gut microbiota*. *Nature*, 2019. **568**(7753): p. 499-504.
170. Li, J., et al., *An integrated catalog of reference genes in the human gut microbiome*. *Nat Biotechnol*, 2014. **32**(8): p. 834-41.
171. Tanaka, M. and J. Nakayama, *Development of the gut microbiota in infancy and its impact on health in later life*. *Allergol Int*, 2017. **66**(4): p. 515-522.
172. Gosalbes, M.J., et al., *Meconium microbiota types dominated by lactic acid or enteric bacteria are differentially associated with maternal eczema and respiratory problems in infants*. *Clin Exp Allergy*, 2013. **43**(2): p. 198-211.
173. Yang, I., et al., *The Infant Microbiome: Implications for Infant Health and Neurocognitive Development*. *Nurs Res*, 2016. **65**(1): p. 76-88.
174. Backhed, F., et al., *Dynamics and Stabilization of the Human Gut Microbiome during the First Year of Life*. *Cell Host Microbe*, 2015. **17**(5): p. 690-703.
175. Yatsunencko, T., et al., *Human gut microbiome viewed across age and geography*. *Nature*, 2012. **486**(7402): p. 222-7.

176. Ferretti, P., et al., *Mother-to-Infant Microbial Transmission from Different Body Sites Shapes the Developing Infant Gut Microbiome*. Cell Host Microbe, 2018. **24**(1): p. 133-145 e5.
177. Howard, B.M., et al., *Characterizing the gut microbiome in trauma: significant changes in microbial diversity occur early after severe injury*. Trauma Surg Acute Care Open, 2017. **2**(1): p. e000108.
178. Nicholson, S.E., et al., *Moderate Traumatic Brain Injury Alters the Gastrointestinal Microbiome in a Time-Dependent Manner*. Shock, 2019. **52**(2): p. 240-248.
179. Maurice, C.F., H.J. Haiser, and P.J. Turnbaugh, *Xenobiotics shape the physiology and gene expression of the active human gut microbiome*. Cell, 2013. **152**(1-2): p. 39-50.
180. Allen, J.M., et al., *Exercise Alters Gut Microbiota Composition and Function in Lean and Obese Humans*. Med Sci Sports Exerc, 2018. **50**(4): p. 747-757.
181. Carmody, R.N., et al., *Diet dominates host genotype in shaping the murine gut microbiota*. Cell Host Microbe, 2015. **17**(1): p. 72-84.
182. Bharwani, A., et al., *Structural & functional consequences of chronic psychosocial stress on the microbiome & host*. Psychoneuroendocrinology, 2016. **63**: p. 217-27.
183. Sittipo, P., J.W. Shim, and Y.K. Lee, *Microbial Metabolites Determine Host Health and the Status of Some Diseases*. Int J Mol Sci, 2019. **20**(21).
184. Lavelle, A. and H. Sokol, *Gut microbiota-derived metabolites as key actors in inflammatory bowel disease*. Nat Rev Gastroenterol Hepatol, 2020. **17**(4): p. 223-237.
185. Schroeder, B.O. and F. Backhed, *Signals from the gut microbiota to distant organs in physiology and disease*. Nat Med, 2016. **22**(10): p. 1079-1089.
186. Wilmanski, T., et al., *Blood metabolome predicts gut microbiome alpha-diversity in humans*. Nat Biotechnol, 2019. **37**(10): p. 1217-1228.
187. Menni, C., et al., *Serum metabolites reflecting gut microbiome alpha diversity predict type 2 diabetes*. Gut Microbes, 2020: p. 1-11.
188. Routy, B., et al., *Gut microbiome influences efficacy of PD-1-based immunotherapy against epithelial tumors*. Science, 2018. **359**(6371): p. 91-97.
189. Sharon, G., et al., *Human Gut Microbiota from Autism Spectrum Disorder Promote Behavioral Symptoms in Mice*. Cell, 2019. **177**(6): p. 1600-1618 e17.
190. Ridaura, V.K., et al., *Gut microbiota from twins discordant for obesity modulate metabolism in mice*. Science, 2013. **341**(6150): p. 1241214.
191. Sampson, T.R., et al., *Gut Microbiota Regulate Motor Deficits and Neuroinflammation in a Model of Parkinson's Disease*. Cell, 2016. **167**(6): p. 1469-1480 e12.
192. Das, N.K., et al., *Microbial Metabolite Signaling Is Required for Systemic Iron Homeostasis*. Cell Metab, 2020. **31**(1): p. 115-130 e6.
193. Backhed, F., et al., *Mechanisms underlying the resistance to diet-induced obesity in germ-free mice*. Proc Natl Acad Sci U S A, 2007. **104**(3): p. 979-84.
194. Everard, A., et al., *Responses of gut microbiota and glucose and lipid metabolism to prebiotics in genetic obese and diet-induced leptin-resistant mice*. Diabetes, 2011. **60**(11): p. 2775-86.

195. Bindels, L.B., et al., *Restoring specific lactobacilli levels decreases inflammation and muscle atrophy markers in an acute leukemia mouse model*. PLoS One, 2012. **7**(6): p. e37971.
196. Chen, Y.M., et al., *Lactobacillus plantarum TWK10 Supplementation Improves Exercise Performance and Increases Muscle Mass in Mice*. Nutrients, 2016. **8**(4): p. 205.
197. Yan, H., et al., *Gut microbiota can transfer fiber characteristics and lipid metabolic profiles of skeletal muscle from pigs to germ-free mice*. Sci Rep, 2016. **6**: p. 31786.
198. Fielding, R.A., et al., *Muscle strength is increased in mice that are colonized with microbiota from high-functioning older adults*. Exp Gerontol, 2019. **127**: p. 110722.
199. Lahiri, S., et al., *The gut microbiota influences skeletal muscle mass and function in mice*. Sci Transl Med, 2019. **11**(502).
200. Tang, G., et al., *Butyrate ameliorate skeletal muscle atrophy in Diabetic Nephropathy via enhancing gut barrier function and FFA2-mediated PI3K/AKT/mTOR signals*. Br J Pharmacol, 2021.
201. Lv, W.Q., et al., *Human gut microbiome impacts skeletal muscle mass via gut microbial synthesis of the short-chain fatty acid butyrate among healthy menopausal women*. J Cachexia Sarcopenia Muscle, 2021.
202. Hsu, Y.J., et al., *Effect of intestinal microbiota on exercise performance in mice*. J Strength Cond Res, 2015. **29**(2): p. 552-8.
203. Huang, W.C., et al., *Lactobacillus plantarum PS128 Improves Physiological Adaptation and Performance in Triathletes through Gut Microbiota Modulation*. Nutrients, 2020. **12**(8).
204. Lee, M.C., et al., *Effectiveness of human-origin Lactobacillus plantarum PL-02 in improving muscle mass, exercise performance and anti-fatigue*. Sci Rep, 2021. **11**(1): p. 19469.
205. Scheiman, J., et al., *Meta-omics analysis of elite athletes identifies a performance-enhancing microbe that functions via lactate metabolism*. Nat Med, 2019. **25**(7): p. 1104-1109.
206. Grosicki, G.J., R.P. Durk, and J.R. Bagley, *Rapid gut microbiome changes in a world-class ultramarathon runner*. Physiol Rep, 2019. **7**(24): p. e14313.
207. Jaago, M., et al., *Drastic Effects on the Microbiome of a Young Rower Engaged in High-Endurance Exercise After a Month Usage of a Dietary Fiber Supplement*. Front Nutr, 2021. **8**: p. 654008.
208. Sudo, N., et al., *Postnatal microbial colonization programs the hypothalamic-pituitary-adrenal system for stress response in mice*. J Physiol, 2004. **558**(Pt 1): p. 263-75.
209. Clarke, G., et al., *Minireview: Gut microbiota: the neglected endocrine organ*. Mol Endocrinol, 2014. **28**(8): p. 1221-38.
210. Rastelli, M., P.D. Cani, and C. Knauf, *The Gut Microbiome Influences Host Endocrine Functions*. Endocr Rev, 2019. **40**(5): p. 1271-1284.
211. Cani, P.D., et al., *Microbial regulation of organismal energy homeostasis*. Nat Metab, 2019. **1**(1): p. 34-46.
212. Markle, J.G., et al., *Microbiome manipulation modifies sex-specific risk for autoimmunity*. Gut Microbes, 2014. **5**(4): p. 485-93.

213. Plottel, C.S. and M.J. Blaser, *Microbiome and malignancy*. Cell Host Microbe, 2011. **10**(4): p. 324-35.
214. Weger, B.D., et al., *The Mouse Microbiome Is Required for Sex-Specific Diurnal Rhythms of Gene Expression and Metabolism*. Cell Metab, 2019. **29**(2): p. 362-382 e8.
215. Mallott, E.K., et al., *Reproductive hormones mediate changes in the gut microbiome during pregnancy and lactation in Phayre's leaf monkeys*. Sci Rep, 2020. **10**(1): p. 9961.
216. Markle, J.G., et al., *Sex differences in the gut microbiome drive hormone-dependent regulation of autoimmunity*. Science, 2013. **339**(6123): p. 1084-8.
217. Schwarzer, M., et al., *Lactobacillus plantarum strain maintains growth of infant mice during chronic undernutrition*. Science, 2016. **351**(6275): p. 854-7.
218. Yan, J., et al., *Gut microbiota induce IGF-1 and promote bone formation and growth*. Proc Natl Acad Sci U S A, 2016. **113**(47): p. E7554-E7563.
219. Whon, T.W., et al., *Male castration increases adiposity via small intestinal microbial alterations*. EMBO Rep, 2021. **22**(1): p. e50663.
220. Deng, P., et al., *Untargeted Stable Isotope Probing of the Gut Microbiota Metabolome Using (13)C-Labeled Dietary Fibers*. J Proteome Res, 2021. **20**(5): p. 2904-2913.
221. Koh, A. and F. Backhed, *From Association to Causality: the Role of the Gut Microbiota and Its Functional Products on Host Metabolism*. Mol Cell, 2020. **78**(4): p. 584-596.
222. Johnson, E.L., et al., *Sphingolipids produced by gut bacteria enter host metabolic pathways impacting ceramide levels*. Nat Commun, 2020. **11**(1): p. 2471.
223. Krautkramer, K.A., J. Fan, and F. Backhed, *Gut microbial metabolites as multi-kingdom intermediates*. Nat Rev Microbiol, 2021. **19**(2): p. 77-94.
224. Caspani, G., et al., *Gut microbial metabolites in depression: understanding the biochemical mechanisms*. Microb Cell, 2019. **6**(10): p. 454-481.
225. Tang, W.H.W., D.Y. Li, and S.L. Hazen, *Dietary metabolism, the gut microbiome, and heart failure*. Nat Rev Cardiol, 2019. **16**(3): p. 137-154.
226. Shats, I., et al., *Bacteria Boost Mammalian Host NAD Metabolism by Engaging the Deamidated Biosynthesis Pathway*. Cell Metab, 2020. **31**(3): p. 564-579 e7.
227. Olesen, S.V., et al., *An NAD(+)-Dependent Sirtuin Depropionylase and Deacetylase (Sir2La) from the Probiotic Bacterium Lactobacillus acidophilus NCFM*. Biochemistry, 2018. **57**(26): p. 3903-3915.
228. Oh, T.G., et al., *A Universal Gut-Microbiome-Derived Signature Predicts Cirrhosis*. Cell Metab, 2020. **32**(5): p. 878-888 e6.
229. Oliphant, K. and E. Allen-Vercoe, *Macronutrient metabolism by the human gut microbiome: major fermentation by-products and their impact on host health*. Microbiome, 2019. **7**(1): p. 91.
230. Nogal, A., A.M. Valdes, and C. Menni, *The role of short-chain fatty acids in the interplay between gut microbiota and diet in cardio-metabolic health*. Gut Microbes, 2021. **13**(1): p. 1-24.
231. Ragsdale, S.W. and E. Pierce, *Acetogenesis and the Wood-Ljungdahl pathway of CO(2) fixation*. Biochim Biophys Acta, 2008. **1784**(12): p. 1873-98.

232. Reichardt, N., et al., *Phylogenetic distribution of three pathways for propionate production within the human gut microbiota*. ISME J, 2014. **8**(6): p. 1323-35.
233. Vital, M., A.C. Howe, and J.M. Tiedje, *Revealing the bacterial butyrate synthesis pathways by analyzing (meta)genomic data*. mBio, 2014. **5**(2): p. e00889.
234. Louis, P. and H.J. Flint, *Formation of propionate and butyrate by the human colonic microbiota*. Environ Microbiol, 2017. **19**(1): p. 29-41.
235. Cummings, J.H., et al., *Short chain fatty acids in human large intestine, portal, hepatic and venous blood*. Gut, 1987. **28**(10): p. 1221-7.
236. Bloemen, J.G., et al., *Short chain fatty acids exchange across the gut and liver in humans measured at surgery*. Clin Nutr, 2009. **28**(6): p. 657-61.
237. Krautkramer, K.A., et al., *Diet-Microbiota Interactions Mediate Global Epigenetic Programming in Multiple Host Tissues*. Mol Cell, 2016. **64**(5): p. 982-992.
238. Hoffman, J.D., et al., *Dietary inulin alters the gut microbiome, enhances systemic metabolism and reduces neuroinflammation in an APOE4 mouse model*. PLoS One, 2019. **14**(8): p. e0221828.
239. Unger, M.M., et al., *Short chain fatty acids and gut microbiota differ between patients with Parkinson's disease and age-matched controls*. Parkinsonism Relat Disord, 2016. **32**: p. 66-72.
240. Malczewski, A.B., et al., *Microbiome-derived metabolome as a potential predictor of response to cancer immunotherapy*. J Immunother Cancer, 2020. **8**(2).
241. McNabney, S.M. and T.M. Henagan, *Short Chain Fatty Acids in the Colon and Peripheral Tissues: A Focus on Butyrate, Colon Cancer, Obesity and Insulin Resistance*. Nutrients, 2017. **9**(12).
242. Frampton, J., et al., *Short-chain fatty acids as potential regulators of skeletal muscle metabolism and function*. Nat Metab, 2020. **2**(9): p. 840-848.
243. Poll, B.G., M.U. Cheema, and J.L. Pluznick, *Gut Microbial Metabolites and Blood Pressure Regulation: Focus on SCFAs and TMAO*. Physiology (Bethesda), 2020. **35**(4): p. 275-284.
244. Layden, B.T., et al., *Short chain fatty acids and their receptors: new metabolic targets*. Transl Res, 2013. **161**(3): p. 131-40.
245. Gao, Z., et al., *Butyrate improves insulin sensitivity and increases energy expenditure in mice*. Diabetes, 2009. **58**(7): p. 1509-17.
246. Li, Q., et al., *Altered short chain fatty acid profiles induced by dietary fiber intervention regulate AMPK levels and intestinal homeostasis*. Food Funct, 2019. **10**(11): p. 7174-7187.
247. Zhou, H., et al., *Short-chain fatty acids can improve lipid and glucose metabolism independently of the pig gut microbiota*. J Anim Sci Biotechnol, 2021. **12**(1): p. 61.
248. Liu, Y., et al., *Gut Microbiome Fermentation Determines the Efficacy of Exercise for Diabetes Prevention*. Cell Metab, 2020. **31**(1): p. 77-91 e5.
249. Sukkar, A.H., et al., *Regulation of energy expenditure and substrate oxidation by short-chain fatty acids*. J Endocrinol, 2019. **242**(2): p. R1-R8.
250. Okamoto, T., et al., *Microbiome potentiates endurance exercise through intestinal acetate production*. Am J Physiol Endocrinol Metab, 2019. **316**(5): p. E956-E966.
251. Yu, Y., et al., *Gut dysbiosis is associated with the reduced exercise capacity of elderly patients with hypertension*. Hypertens Res, 2018. **41**(12): p. 1036-1044.



252. Fellows, R., et al., *Microbiota derived short chain fatty acids promote histone crotonylation in the colon through histone deacetylases*. Nat Commun, 2018. **9**(1): p. 105.
253. Lund, P.J., et al., *Stable Isotope Tracing in vivo Reveals A Metabolic Bridge Linking the Microbiota to Host Histone Acetylation*. bioRxiv, 2021: p. 2021.07.05.450926.
254. Von Walden, F., et al., *The myonuclear DNA methylome in response to an acute hypertrophic stimulus*. Epigenetics, 2020. **15**(11): p. 1151-1162.
255. Chiang, J.Y., *Regulation of bile acid synthesis*. Front Biosci, 1998. **3**: p. d176-93.
256. Ridlon, J.M., D.J. Kang, and P.B. Hylemon, *Bile salt biotransformations by human intestinal bacteria*. J Lipid Res, 2006. **47**(2): p. 241-59.
257. de Aguiar Vallim, T.Q., E.J. Tarling, and P.A. Edwards, *Pleiotropic roles of bile acids in metabolism*. Cell Metab, 2013. **17**(5): p. 657-69.
258. Wahlstrom, A., et al., *Intestinal Crosstalk between Bile Acids and Microbiota and Its Impact on Host Metabolism*. Cell Metab, 2016. **24**(1): p. 41-50.
259. Sayin, S.I., et al., *Gut microbiota regulates bile acid metabolism by reducing the levels of tauro-beta-muricholic acid, a naturally occurring FXR antagonist*. Cell Metab, 2013. **17**(2): p. 225-35.
260. Tian, Y., et al., *The microbiome modulating activity of bile acids*. Gut Microbes, 2020. **11**(4): p. 979-996.
261. Chaudhari, S.N., et al., *A microbial metabolite remodels the gut-liver axis following bariatric surgery*. Cell Host Microbe, 2021. **29**(3): p. 408-424 e7.
262. Watanabe, M., et al., *Bile acids induce energy expenditure by promoting intracellular thyroid hormone activation*. Nature, 2006. **439**(7075): p. 484-9.
263. Sasaki, T., et al., *The exercise-inducible bile acid receptor Tgr5 improves skeletal muscle function in mice*. J Biol Chem, 2018. **293**(26): p. 10322-10332.
264. Sasaki, T., et al., *Muscle-specific TGR5 overexpression improves glucose clearance in glucose-intolerant mice*. J Biol Chem, 2021. **296**: p. 100131.
265. Thomas, C., et al., *TGR5-mediated bile acid sensing controls glucose homeostasis*. Cell Metab, 2009. **10**(3): p. 167-77.
266. Abrigo, J., et al., *Cholic acid and deoxycholic acid induce skeletal muscle atrophy through a mechanism dependent on TGR5 receptor*. J Cell Physiol, 2021. **236**(1): p. 260-272.
267. Aguirre, N., L.J. van Loon, and K. Baar, *The role of amino acids in skeletal muscle adaptation to exercise*. Nestle Nutr Inst Workshop Ser, 2013. **76**: p. 85-102.
268. Church, D.D., et al., *Essential Amino Acids and Protein Synthesis: Insights into Maximizing the Muscle and Whole-Body Response to Feeding*. Nutrients, 2020. **12**(12).
269. Reidy, P.T. and B.B. Rasmussen, *Role of Ingested Amino Acids and Protein in the Promotion of Resistance Exercise-Induced Muscle Protein Anabolism*. J Nutr, 2016. **146**(2): p. 155-83.
270. Castell, L.M. and E.A. Newsholme, *The effects of oral glutamine supplementation on athletes after prolonged, exhaustive exercise*. Nutrition, 1997. **13**(7-8): p. 738-42.

271. Choi, B.S., et al., *Feeding diversified protein sources exacerbates hepatic insulin resistance via increased gut microbial branched-chain fatty acids and mTORC1 signaling in obese mice*. Nat Commun, 2021. **12**(1): p. 3377.
272. Storelli, G., et al., *Lactobacillus plantarum promotes Drosophila systemic growth by modulating hormonal signals through TOR-dependent nutrient sensing*. Cell Metab, 2011. **14**(3): p. 403-14.
273. Palego, L., et al., *Tryptophan Biochemistry: Structural, Nutritional, Metabolic, and Medical Aspects in Humans*. J Amino Acids, 2016. **2016**: p. 8952520.
274. Santiveri, C.M. and M.A. Jimenez, *Tryptophan residues: scarce in proteins but strong stabilizers of beta-hairpin peptides*. Biopolymers, 2010. **94**(6): p. 779-90.
275. Agus, A., J. Planchais, and H. Sokol, *Gut Microbiota Regulation of Tryptophan Metabolism in Health and Disease*. Cell Host Microbe, 2018. **23**(6): p. 716-724.
276. Hubbard, T.D., I.A. Murray, and G.H. Perdew, *Indole and Tryptophan Metabolism: Endogenous and Dietary Routes to Ah Receptor Activation*. Drug Metab Dispos, 2015. **43**(10): p. 1522-35.
277. Ehrlich, A.M., et al., *Indole-3-lactic acid associated with Bifidobacterium-dominated microbiota significantly decreases inflammation in intestinal epithelial cells*. BMC Microbiol, 2020. **20**(1): p. 357.
278. Whitfield-Cargile, C.M., et al., *The microbiota-derived metabolite indole decreases mucosal inflammation and injury in a murine model of NSAID enteropathy*. Gut Microbes, 2016. **7**(3): p. 246-61.
279. Walton, R.G., et al., *Human skeletal muscle macrophages increase following cycle training and are associated with adaptations that may facilitate growth*. Sci Rep, 2019. **9**(1): p. 969.
280. Schwarcz, R., *The kynurenine pathway of tryptophan degradation as a drug target*. Curr Opin Pharmacol, 2004. **4**(1): p. 12-7.
281. Atarashi, K., et al., *Induction of colonic regulatory T cells by indigenous Clostridium species*. Science, 2011. **331**(6015): p. 337-41.
282. Rhee, S.J., W.A. Walker, and B.J. Cherayil, *Developmentally regulated intestinal expression of IFN-gamma and its target genes and the age-specific response to enteric Salmonella infection*. J Immunol, 2005. **175**(2): p. 1127-36.
283. Agudelo, L.Z., et al., *Skeletal muscle PGC-1alpha1 modulates kynurenine metabolism and mediates resilience to stress-induced depression*. Cell, 2014. **159**(1): p. 33-45.
284. Agudelo, L.Z., et al., *Skeletal muscle PGC-1alpha1 reroutes kynurenine metabolism to increase energy efficiency and fatigue-resistance*. Nat Commun, 2019. **10**(1): p. 2767.
285. Muro, E., G.E. Atilla-Gokcumen, and U.S. Eggert, *Lipids in cell biology: how can we understand them better?* Mol Biol Cell, 2014. **25**(12): p. 1819-23.
286. Cohen, P. and S. Kajimura, *The cellular and functional complexity of thermogenic fat*. Nat Rev Mol Cell Biol, 2021.
287. Thompson, D., et al., *Physical activity and exercise in the regulation of human adipose tissue physiology*. Physiol Rev, 2012. **92**(1): p. 157-91.
288. Nakamura, M.T., B.E. Yudell, and J.J. Loor, *Regulation of energy metabolism by long-chain fatty acids*. Prog Lipid Res, 2014. **53**: p. 124-44.

289. Fagone, P. and S. Jackowski, *Membrane phospholipid synthesis and endoplasmic reticulum function*. J Lipid Res, 2009. **50 Suppl**: p. S311-6.
290. Jacquemyn, J., A. Cascalho, and R.E. Goodchild, *The ins and outs of endoplasmic reticulum-controlled lipid biosynthesis*. EMBO Rep, 2017. **18**(11): p. 1905-1921.
291. Brown, E.M., et al., *Bacteroides-Derived Sphingolipids Are Critical for Maintaining Intestinal Homeostasis and Symbiosis*. Cell Host Microbe, 2019. **25**(5): p. 668-680 e7.
292. Rienzi, S.C.D., et al., *The microbiome affects liver sphingolipids and plasma fatty acids in a murine model of the Western diet based on soybean oil: Hepatic sphingolipids and plasma FAs are altered by gut microbes*. J Nutr Biochem, 2021: p. 108808.
293. Chavez, J.A., et al., *Ceramides and glucosylceramides are independent antagonists of insulin signaling*. J Biol Chem, 2014. **289**(2): p. 723-34.
294. Morigny, P., et al., *High levels of modified ceramides are a defining feature of murine and human cancer cachexia*. J Cachexia Sarcopenia Muscle, 2020. **11**(6): p. 1459-1475.
295. Meeusen, J.W., et al., *Plasma Ceramides*. Arterioscler Thromb Vasc Biol, 2018. **38**(8): p. 1933-1939.
296. Danieli-Betto, D., et al., *Sphingosine 1-phosphate protects mouse extensor digitorum longus skeletal muscle during fatigue*. Am J Physiol Cell Physiol, 2005. **288**(6): p. C1367-73.
297. Strub, G.M., et al., *Sphingosine-1-phosphate produced by sphingosine kinase 2 in mitochondria interacts with prohibitin 2 to regulate complex IV assembly and respiration*. FASEB J, 2011. **25**(2): p. 600-12.
298. Gibala, M.J., *Regulation of skeletal muscle amino acid metabolism during exercise*. Int J Sport Nutr Exerc Metab, 2001. **11**(1): p. 87-108.
299. DeFronzo, R.A., *Lilly lecture 1987. The triumvirate: beta-cell, muscle, liver. A collusion responsible for NIDDM*. Diabetes, 1988. **37**(6): p. 667-87.
300. Lecker, S.H., A.L. Goldberg, and W.E. Mitch, *Protein degradation by the ubiquitin-proteasome pathway in normal and disease states*. J Am Soc Nephrol, 2006. **17**(7): p. 1807-19.
301. Rowland, L.A., N.C. Bal, and M. Periasamy, *The role of skeletal-muscle-based thermogenic mechanisms in vertebrate endothermy*. Biol Rev Camb Philos Soc, 2015. **90**(4): p. 1279-97.
302. Allen, J.M., et al., *Voluntary and forced exercise differentially alters the gut microbiome in C57BL/6J mice*. J Appl Physiol (1985), 2015. **118**(8): p. 1059-66.
303. Clarke, S.F., et al., *Exercise and associated dietary extremes impact on gut microbial diversity*. Gut, 2014. **63**(12): p. 1913-20.
304. Campbell, S.C., et al., *The Effect of Diet and Exercise on Intestinal Integrity and Microbial Diversity in Mice*. PLoS One, 2016. **11**(3): p. e0150502.
305. Allen, J.M., et al., *Exercise training-induced modification of the gut microbiota persists after microbiota colonization and attenuates the response to chemically-induced colitis in gnotobiotic mice*. Gut Microbes, 2018. **9**(2): p. 115-130.
306. Codella, R., L. Luzi, and I. Terruzzi, *Exercise has the guts: How physical activity may positively modulate gut microbiota in chronic and immune-based diseases*. Dig Liver Dis, 2018. **50**(4): p. 331-341.

307. Bleau, C., et al., *Crosstalk between intestinal microbiota, adipose tissue and skeletal muscle as an early event in systemic low-grade inflammation and the development of obesity and diabetes*. *Diabetes Metab Res Rev*, 2015. **31**(6): p. 545-61.
308. Bastiaanssen, T.F.S., et al., *Gutted! Unraveling the Role of the Microbiome in Major Depressive Disorder*. *Harv Rev Psychiatry*, 2020. **28**(1): p. 26-39.
309. Grosicki, G.J., R.A. Fielding, and M.S. Lustgarten, *Gut Microbiota Contribute to Age-Related Changes in Skeletal Muscle Size, Composition, and Function: Biological Basis for a Gut-Muscle Axis*. *Calcif Tissue Int*, 2018. **102**(4): p. 433-442.
310. Lustgarten, M.S., *The Role of the Gut Microbiome on Skeletal Muscle Mass and Physical Function: 2019 Update*. *Front Physiol*, 2019. **10**: p. 1435.
311. Ticinesi, A., et al., *Exercise and immune system as modulators of intestinal microbiome: implications for the gut-muscle axis hypothesis*. *Exerc Immunol Rev*, 2019. **25**: p. 84-95.
312. Ticinesi, A., et al., *Gut Microbiota, Muscle Mass and Function in Aging: A Focus on Physical Frailty and Sarcopenia*. *Nutrients*, 2019. **11**(7).
313. Ni Lochlainn, M., R.C.E. Bowyer, and C.J. Steves, *Dietary Protein and Muscle in Aging People: The Potential Role of the Gut Microbiome*. *Nutrients*, 2018. **10**(7).
314. Dungan, C.M., et al., *Elevated myonuclear density during skeletal muscle hypertrophy in response to training is reversed during detraining*. *Am J Physiol Cell Physiol*, 2019. **316**(5): p. C649-C654.
315. Montonye, D.R., et al., *Acclimation and Institutionalization of the Mouse Microbiota Following Transportation*. *Front Microbiol*, 2018. **9**: p. 1085.
316. Ericsson, A.C., et al., *The influence of caging, bedding, and diet on the composition of the microbiota in different regions of the mouse gut*. *Sci Rep*, 2018. **8**(1): p. 4065.
317. Nay, K., et al., *Gut bacteria are critical for optimal muscle function: a potential link with glucose homeostasis*. *Am J Physiol Endocrinol Metab*, 2019. **317**(1): p. E158-E171.
318. Suarez-Zamorano, N., et al., *Microbiota depletion promotes browning of white adipose tissue and reduces obesity*. *Nat Med*, 2015. **21**(12): p. 1497-1501.
319. Koh, A., et al., *Microbially Produced Imidazole Propionate Impairs Insulin Signaling through mTORC1*. *Cell*, 2018. **175**(4): p. 947-961 e17.
320. Murach, K.A., et al., *Muscle memory: myonuclear accretion, maintenance, morphology, and miRNA levels with training and detraining in adult mice*. *J Cachexia Sarcopenia Muscle*, 2020. **11**(6): p. 1705-1722.
321. McCarthy, J.J., et al., *Effective fiber hypertrophy in satellite cell-depleted skeletal muscle*. *Development*, 2011. **138**(17): p. 3657-66.
322. Wen, Y., et al., *MyoVision: software for automated high-content analysis of skeletal muscle immunohistochemistry*. *J Appl Physiol (1985)*, 2018. **124**(1): p. 40-51.
323. Hourigan, S.K., et al., *Comparison of Infant Gut and Skin Microbiota, Resistome and Virulome Between Neonatal Intensive Care Unit (NICU) Environments*. *Front Microbiol*, 2018. **9**: p. 1361.

324. Newman, T.M., et al., *Diet, obesity, and the gut microbiome as determinants modulating metabolic outcomes in a non-human primate model*. *Microbiome*, 2021. **9**(1): p. 100.
325. Cani, P.D., et al., *Metabolic endotoxemia initiates obesity and insulin resistance*. *Diabetes*, 2007. **56**(7): p. 1761-72.
326. Cani, P.D., et al., *Changes in gut microbiota control metabolic endotoxemia-induced inflammation in high-fat diet-induced obesity and diabetes in mice*. *Diabetes*, 2008. **57**(6): p. 1470-81.
327. Douzandeh-Mobarrez, B. and A. Kariminik, *Gut Microbiota and IL-17A: Physiological and Pathological Responses*. *Probiotics Antimicrob Proteins*, 2019. **11**(1): p. 1-10.
328. Schirmer, M., et al., *Linking the Human Gut Microbiome to Inflammatory Cytokine Production Capacity*. *Cell*, 2016. **167**(4): p. 1125-1136 e8.
329. Fayock, K., et al., *Antibiotic precautions in athletes*. *Sports Health*, 2014. **6**(4): p. 321-5.
330. Ericsson, A.C. and C.L. Franklin, *Manipulating the Gut Microbiota: Methods and Challenges*. *ILAR J*, 2015. **56**(2): p. 205-17.
331. Kennedy, E.A., K.Y. King, and M.T. Baldrige, *Mouse Microbiota Models: Comparing Germ-Free Mice and Antibiotics Treatment as Tools for Modifying Gut Bacteria*. *Front Physiol*, 2018. **9**: p. 1534.
332. Bayer, F., et al., *Antibiotic Treatment Protocols and Germ-Free Mouse Models in Vascular Research*. *Front Immunol*, 2019. **10**: p. 2174.
333. Song, X., et al., *Microbial bile acid metabolites modulate gut RORgamma(+) regulatory T cell homeostasis*. *Nature*, 2020. **577**(7790): p. 410-415.
334. Willing, B.P., S.L. Russell, and B.B. Finlay, *Shifting the balance: antibiotic effects on host-microbiota mutualism*. *Nat Rev Microbiol*, 2011. **9**(4): p. 233-43.
335. Tulstrup, M.V., et al., *Antibiotic Treatment Affects Intestinal Permeability and Gut Microbial Composition in Wistar Rats Dependent on Antibiotic Class*. *PLoS One*, 2015. **10**(12): p. e0144854.
336. Manickam, R., et al., *Metronidazole Causes Skeletal Muscle Atrophy and Modulates Muscle Chronometabolism*. *Int J Mol Sci*, 2018. **19**(8).
337. Hayao, K., et al., *Effects of Streptomycin Administration on Increases in Skeletal Muscle Fiber Permeability and Size Following Eccentric Muscle Contractions*. *Anat Rec (Hoboken)*, 2018. **301**(6): p. 1096-1102.
338. Qiu, Y., et al., *Depletion of gut microbiota induces skeletal muscle atrophy by FXR-FGF15/19 signalling*. *Ann Med*, 2021. **53**(1): p. 508-522.
339. Owen, A.M., et al., *Chronic muscle weakness and mitochondrial dysfunction in the absence of sustained atrophy in a preclinical sepsis model*. *Elife*, 2019. **8**.
340. Chen, H., et al., *A Forward Chemical Genetic Screen Reveals Gut Microbiota Metabolites That Modulate Host Physiology*. *Cell*, 2019. **177**(5): p. 1217-1231 e18.
341. White, J.P., et al., *G protein-coupled receptor 56 regulates mechanical overload-induced muscle hypertrophy*. *Proc Natl Acad Sci U S A*, 2014. **111**(44): p. 15756-61.
342. Cho, D.S. and J.D. Doles, *Single cell transcriptome analysis of muscle satellite cells reveals widespread transcriptional heterogeneity*. *Gene*, 2017. **636**: p. 54-63.

343. Murach, K.A., et al., *Making Mice Mighty: recent advances in translational models of load-induced muscle hypertrophy*. J Appl Physiol (1985), 2020. **129**(3): p. 516-521.
344. Rizzetto, L., et al., *Connecting the immune system, systemic chronic inflammation and the gut microbiome: The role of sex*. J Autoimmun, 2018. **92**: p. 12-34.
345. Razavi, A.C., et al., *Sex, gut microbiome, and cardiovascular disease risk*. Biol Sex Differ, 2019. **10**(1): p. 29.
346. Tuck, C.J., et al., *Nutritional profile of rodent diets impacts experimental reproducibility in microbiome preclinical research*. Sci Rep, 2020. **10**(1): p. 17784.
347. Puthuchery, Z.A., et al., *Acute skeletal muscle wasting in critical illness*. JAMA, 2013. **310**(15): p. 1591-600.
348. Wall, B.T., et al., *Substantial skeletal muscle loss occurs during only 5 days of disuse*. Acta Physiol (Oxf), 2014. **210**(3): p. 600-11.
349. Mitchell, W.K., et al., *Sarcopenia, dynapenia, and the impact of advancing age on human skeletal muscle size and strength; a quantitative review*. Front Physiol, 2012. **3**: p. 260.
350. Furrer, R. and C. Handschin, *Muscle Wasting Diseases: Novel Targets and Treatments*. Annu Rev Pharmacol Toxicol, 2019. **59**: p. 315-339.
351. Marshall, R.N., et al., *Nutritional Strategies to Offset Disuse-Induced Skeletal Muscle Atrophy and Anabolic Resistance in Older Adults: From Whole-Foods to Isolated Ingredients*. Nutrients, 2020. **12**(5).
352. Valentino, T.R., et al., *Dysbiosis of the gut microbiome impairs mouse skeletal muscle adaptation to exercise*. J Physiol, 2021. **599**(21): p. 4845-4863.
353. Ortiz-Alvarez, L., H. Xu, and B. Martinez-Tellez, *Influence of Exercise on the Human Gut Microbiota of Healthy Adults: A Systematic Review*. Clin Transl Gastroenterol, 2020. **11**(2): p. e00126.
354. Kim, D. and H. Kang, *Exercise training modifies gut microbiota with attenuated host responses to sepsis in wild-type mice*. FASEB J, 2019. **33**(4): p. 5772-5781.
355. Liu, Z., et al., *Moderate-Intensity Exercise Affects Gut Microbiome Composition and Influences Cardiac Function in Myocardial Infarction Mice*. Front Microbiol, 2017. **8**: p. 1687.
356. Wrzosek, L., et al., *Transplantation of human microbiota into conventional mice durably reshapes the gut microbiota*. Sci Rep, 2018. **8**(1): p. 6854.
357. Le Roy, T., et al., *Comparative Evaluation of Microbiota Engraftment Following Fecal Microbiota Transfer in Mice Models: Age, Kinetic and Microbial Status Matter*. Front Microbiol, 2018. **9**: p. 3289.
358. Walter, J., et al., *Establishing or Exaggerating Causality for the Gut Microbiome: Lessons from Human Microbiota-Associated Rodents*. Cell, 2020. **180**(2): p. 221-232.
359. Beghini, F., et al., *Integrating taxonomic, functional, and strain-level profiling of diverse microbial communities with bioBakery 3*. Elife, 2021. **10**.
360. UniProt, C., *UniProt: a worldwide hub of protein knowledge*. Nucleic Acids Res, 2019. **47**(D1): p. D506-D515.
361. Coordinators, N.R., *Database resources of the National Center for Biotechnology Information*. Nucleic Acids Res, 2014. **42**(Database issue): p. D7-17.

362. Mallick, H., et al., *Multivariable association discovery in population-scale metagenomics studies*. PLoS Comput Biol, 2021. **17**(11): p. e1009442.
363. Mallick, H., et al., *Predictive metabolomic profiling of microbial communities using amplicon or metagenomic sequences*. Nat Commun, 2019. **10**(1): p. 3136.
364. Louis, P., G.L. Hold, and H.J. Flint, *The gut microbiota, bacterial metabolites and colorectal cancer*. Nat Rev Microbiol, 2014. **12**(10): p. 661-72.
365. Monda, V., et al., *Exercise Modifies the Gut Microbiota with Positive Health Effects*. Oxid Med Cell Longev, 2017. **2017**: p. 3831972.
366. Olivera-Martinez, I. and K.G. Storey, *Wnt signals provide a timing mechanism for the FGF-retinoid differentiation switch during vertebrate body axis extension*. Development, 2007. **134**(11): p. 2125-35.
367. Daisley, B.A., et al., *Emerging connections between gut microbiome bioenergetics and chronic metabolic diseases*. Cell Rep, 2021. **37**(10): p. 110087.
368. Li, W., et al., *A bacterial bile acid metabolite modulates Treg activity through the nuclear hormone receptor NR4A1*. Cell Host Microbe, 2021. **29**(9): p. 1366-1377 e9.
369. Yang, J., et al., *Landscapes of bacterial and metabolic signatures and their interaction in major depressive disorders*. Sci Adv, 2020. **6**(49).
370. Feng, W., H. Ao, and C. Peng, *Gut Microbiota, Short-Chain Fatty Acids, and Herbal Medicines*. Front Pharmacol, 2018. **9**: p. 1354.
371. Zagato, E., et al., *Endogenous murine microbiota member Faecalibaculum rodentium and its human homologue protect from intestinal tumour growth*. Nat Microbiol, 2020. **5**(3): p. 511-524.
372. den Hartigh, L.J., et al., *Obese Mice Losing Weight Due to trans-10,cis-12 Conjugated Linoleic Acid Supplementation or Food Restriction Harbor Distinct Gut Microbiota*. J Nutr, 2018. **148**(4): p. 562-572.
373. Kostopoulos, I., et al., *Akkermansia muciniphila uses human milk oligosaccharides to thrive in the early life conditions in vitro*. Sci Rep, 2020. **10**(1): p. 14330.
374. Pacheco, A.R., et al., *Fucose sensing regulates bacterial intestinal colonization*. Nature, 2012. **492**(7427): p. 113-7.
375. Schwede, T.F., J. Retey, and G.E. Schulz, *Crystal structure of histidine ammonia-lyase revealing a novel polypeptide modification as the catalytic electrophile*. Biochemistry, 1999. **38**(17): p. 5355-61.
376. Venskutonyte, R., et al., *Structural characterization of the microbial enzyme urocanate reductase mediating imidazole propionate production*. Nat Commun, 2021. **12**(1): p. 1347.
377. Chen, Z., et al., *Gut Microbiota-Derived l-Histidine/Imidazole Propionate Axis Fights against the Radiation-Induced Cardiopulmonary Injury*. Int J Mol Sci, 2021. **22**(21).
378. Koh, A., et al., *Microbial Imidazole Propionate Affects Responses to Metformin through p38gamma-Dependent Inhibitory AMPK Phosphorylation*. Cell Metab, 2020. **32**(4): p. 643-653 e4.
379. Molinaro, A., et al., *Imidazole propionate is increased in diabetes and associated with dietary patterns and altered microbial ecology*. Nat Commun, 2020. **11**(1): p. 5881.

380. van der Hee, B. and J.M. Wells, *Microbial Regulation of Host Physiology by Short-chain Fatty Acids*. Trends Microbiol, 2021. **29**(8): p. 700-712.
381. Canfora, E.E., J.W. Jocken, and E.E. Blaak, *Short-chain fatty acids in control of body weight and insulin sensitivity*. Nat Rev Endocrinol, 2015. **11**(10): p. 577-91.
382. Mauras, N., et al., *Synergistic effects of testosterone and growth hormone on protein metabolism and body composition in prepubertal boys*. Metabolism, 2003. **52**(8): p. 964-9.
383. Zheng, S., et al., *Do short chain fatty acids and phenolic metabolites of the gut have synergistic anti-inflammatory effects? - New insights from a TNF-alpha-induced Caco-2 cell model*. Food Res Int, 2021. **139**: p. 109833.
384. Holecck, M., *Branched-chain amino acids in health and disease: metabolism, alterations in blood plasma, and as supplements*. Nutr Metab (Lond), 2018. **15**: p. 33.
385. Yoon, M.S., *The Emerging Role of Branched-Chain Amino Acids in Insulin Resistance and Metabolism*. Nutrients, 2016. **8**(7).
386. Cummings, N.E., et al., *Restoration of metabolic health by decreased consumption of branched-chain amino acids*. J Physiol, 2018. **596**(4): p. 623-645.
387. Hunt, L.C., et al., *Integrated genomic and proteomic analyses identify stimulus-dependent molecular changes associated with distinct modes of skeletal muscle atrophy*. Cell Rep, 2021. **37**(6): p. 109971.
388. Cornelison, D.D., et al., *MyoD(-/-) satellite cells in single-fiber culture are differentiation defective and MRF4 deficient*. Dev Biol, 2000. **224**(2): p. 122-37.
389. Kaiko, G.E., et al., *The Colonic Crypt Protects Stem Cells from Microbiota-Derived Metabolites*. Cell, 2016. **165**(7): p. 1708-1720.
390. de Cena, J.A., et al., *Low-Abundant Microorganisms: The Human Microbiome's Dark Matter, a Scoping Review*. Front Cell Infect Microbiol, 2021. **11**: p. 689197.
391. Pan, J.H., et al., *Acetic acid enhances endurance capacity of exercise-trained mice by increasing skeletal muscle oxidative properties*. Biosci Biotechnol Biochem, 2015. **79**(9): p. 1535-41.
392. Qi, R., et al., *The intestinal microbiota contributes to the growth and physiological state of muscle tissue in piglets*. Sci Rep, 2021. **11**(1): p. 11237.
393. Bloemberg, D. and J. Quadriatero, *Rapid determination of myosin heavy chain expression in rat, mouse, and human skeletal muscle using multicolor immunofluorescence analysis*. PLoS One, 2012. **7**(4): p. e35273.
394. Gizard, F., A. Fernandez, and F. De Vadder, *Interactions between gut microbiota and skeletal muscle*. Nutr Metab Insights, 2020. **13**: p. 1178638820980490.
395. Wang, Y.X., et al., *Regulation of muscle fiber type and running endurance by PPARdelta*. PLoS Biol, 2004. **2**(10): p. e294.
396. Yang, S., et al., *Gut Microbiota-Dependent Marker TMAO in Promoting Cardiovascular Disease: Inflammation Mechanism, Clinical Prognostic, and Potential as a Therapeutic Target*. Front Pharmacol, 2019. **10**: p. 1360.
397. Yang, J., et al., *High-Fat Diet Promotes Colorectal Tumorigenesis Through Modulating Gut Microbiota and Metabolites*. Gastroenterology, 2022. **162**(1): p. 135-149 e2.
398. Serino, M., et al., *Metabolic adaptation to a high-fat diet is associated with a change in the gut microbiota*. Gut, 2012. **61**(4): p. 543-53.



399. Han, S., et al., *A metabolomics pipeline for the mechanistic interrogation of the gut microbiome*. Nature, 2021. **595**(7867): p. 415-420.
400. Zolkiewicz, J., et al., *Postbiotics-A Step Beyond Pre- and Probiotics*. Nutrients, 2020. **12**(8).
401. Suez, J. and E. Elinav, *The path towards microbiome-based metabolite treatment*. Nat Microbiol, 2017. **2**: p. 17075.
402. Bindels, L.B., et al., *Towards a more comprehensive concept for prebiotics*. Nat Rev Gastroenterol Hepatol, 2015. **12**(5): p. 303-10.
403. Shepherd, E.S., et al., *An exclusive metabolic niche enables strain engraftment in the gut microbiota*. Nature, 2018. **557**(7705): p. 434-438.
404. Kimura, I., et al., *Free Fatty Acid Receptors in Health and Disease*. Physiol Rev, 2020. **100**(1): p. 171-210.
405. Lagkouvardos, I., et al., *Sequence and cultivation study of Muribaculaceae reveals novel species, host preference, and functional potential of this yet undescribed family*. Microbiome, 2019. **7**(1): p. 28.
406. Chung, Y.W., et al., *Functional dynamics of bacterial species in the mouse gut microbiome revealed by metagenomic and metatranscriptomic analyses*. PLoS One, 2020. **15**(1): p. e0227886.
407. Wu, Q., et al., *Intestinal hypoxia-inducible factor 2alpha regulates lactate levels to shape the gut microbiome and alter thermogenesis*. Cell Metab, 2021. **33**(10): p. 1988-2003 e7.
408. Hoffman, J.B., M.D. Flythe, and B. Hennig, *Environmental pollutant-mediated disruption of gut microbial metabolism of the prebiotic inulin*. Anaerobe, 2019. **55**: p. 96-102.

## CURRICULUM VITAE

**TAYLOR R. VALENTINO PH.D**

### **EDUCATION**

---

**University of Kentucky**, Lexington, KY

Ph.D., Physiology, January 2022

**2022**

Dissertation- Gut microbial metabolites mediate skeletal muscle plasticity.

Mentor: John McCarthy PhD, Committee Members: Steve Estus PhD, Michale Flythe PhD, Lance Johnson PhD and Mariana Nikolova-Karakashian, PhD.

**2015**

**San Francisco State University**, San Francisco, CA

Masters, Exercise Physiology May 2015

Thesis- The Influence of hydration status on core temperature during a 161-km ultramarathon.

Committee Members: Marialice Kern PhD, C. Matt Lee PhD and Maria J. Veri PhD.

**2009**

**San Francisco State University**, San Francisco, CA

Undergraduate, Kinesiology December 2009

### **PUBLICATIONS**

---

*Peer-reviewed research articles (listed from newest to oldest)*

**Valentino T**, Figueiredo V, Mobley CM, McCarthy JJ, Vechetti I. Evidence of myomiR regulation of the pentose phosphate pathway during mechanical load induced hypertrophy. *Physiologic Reports* .

**Valentino T**, Vechetti I, Mobley CB, Dungan C, Golden L, Goh J, McCarthy JJ. Dysbiosis of the gut microbiome impairs mouse skeletal muscle adaptation to exercise. *Journal of Physiology*.

Wen Y, Dungan C, Mobley C, Brooks, **Valentino T**, von Walden F, Murach K. Nucleus type-specific DNA methylation reveals an epigenetic “memory” of prior adaptation in skeletal muscle. *Function*.

**Valentino T**, Rule B, Mobley C, Brooks, Nikolova-Karakashian M, Vechetti I. Skeletal muscle cell growth alters the lipid composition of extracellular vesicles. *MDPI Membranes*.

Vechetti I, Peck B, Wen Y, Walton G, **Valentino T**...McCarthy J. Mechanical overload-induced muscle-derived extracellular vesicles promote adipose tissue lipolysis. *Faseb* .

Figueiredo V, Wen Y, Alkner B, Fernandez-Gonzalo R, Norrborn J, Vechetti I, **Valentino T**,...von Walden F. Genetic and epigenetic regulation of skeletal muscle ribosome biogenesis with exercise. *Journal of Physiology*.

Deng P, **Valentino T**, Flythe M, Moseley H, Leachman J, Morris A, Hennig B. Untargeted stable-isotope probing of the gut microbiota metabolome using <sup>13</sup>C-labeled dietary fibers. *Journal of Proteome Research*.

Wen Y, Vechetti IJ, **Valentino T**, McCarthy JJ. High-yield skeletal muscle protein recovery from TRIzol after RNA and DNA extraction. *Biotechniques* (2020).

Dungan C, **Valentino T**, Vechetti IJ, Zdunek C, Murphy M, Lin AL, McCarthy JJ, Peterson CA. Exercise-mediated alteration of hippocampal Dicer and miRNAs is associated with lower BACE1 and detergent soluble A $\beta$ <sup>1-42</sup> in female 3xTg-AD mice. *Journal of Neurophysiology* (2020).

Grosicki GJ, Riemann BL, Flatt AA, **Valentino T**, Luscgarten MS. Self-reported sleep quality is associated with gut microbiome composition in young, healthy individuals: a pilot study. *Sleep Medicine* (2020);73:76-81.

Mobley CB, Vechetti I, **Valentino T**, McCarthy J. Cores of Reproducibility (CORP): Using transgenic mice to study skeletal muscle physiology. *Journal Applied Physiology* (2020); 128(5):1227-1239.

Vechetti I., **Valentino T.**, Mobley CB, McCarthy J. The Role of extracellular vesicles in skeletal muscle and systemic adaptation to Exercise. *Journal of Physiology* (2020).

Hoffman M, **Valentino T**, Stuempfle K, Hassid B. A Randomized controlled trial of riboflavin for enhancement of ultramarathon recovery. *Sports Medicine Open* (2017);3(1):14.

**Valentino T**, Stuempfle K, Kern M, Hoffman M. The influence of hydration state on thermoregulation during a 161-km ultramarathon. *Research in Sport Medicine* (2016); 3: 1-10.

Stuempfle K, **Valentino T**, Hew-Butler T, Hecht R, Hoffman M. Nausea is associated with endotoxemia during an ultramarathon. *Journal Sports Science*. (2015); 1-7.

Hoffman M, Stuempfle K, **Valentino T**. Sodium does not prevent muscle cramping, dehydration, hyponatremia or nausea during an ultramarathon. *Sports Medicine Open*. (2015); 1:39.

## **PROFESSIONAL SERVICE & AWARDS**

---

- 2021** 2020 Thomas Getchell Grant Writing Workshop Award Recipient, University of Kentucky, Department of Physiology.
- 2021** 2020, 13<sup>th</sup> Annual Hardin Award Recipient, University of Kentucky, Department of Physiology.
- 2020-2021** University of Kentucky Department of Physiology Student Representative.
- 2020-2021** Graduate Student Council/Mental Health and Wellbeing Committee.
- 2019&2020** Science Fair Judge, Morton Middle School, Lexington, KY.
- 2019** Research blitz winner. University of Kentucky, Department of Physiology, Research and Education Day.
- 2015** Distinguished graduate student award, San Francisco State University, Department of Kinesiology.
- 2015** Finalist in the graduate category of the 29<sup>th</sup> annual California State University Student Research Competition.
- 2014** Favorite poster award, graduate division, Southwest American College of Sports Medicine Annual Chapter meeting

#### **PROFESSIONAL PRESENTATIONS**

---

- 2021** *Poster Presentation:* 2021, 12<sup>th</sup> Annual College of Medicine Trainee Poster Session, University of Kentucky: *Dysbiosis of the gut microbiome impairs skeletal muscle adaptation to exercise.*
- 2020** *Invited Speaker:* 2020 Miami Winter Symposium: Molecular Mechanisms Linking the Microbiome and Human Health. January 26<sup>th</sup>-29<sup>th</sup>, Miami Fl. *The Gut Microbiome is Necessary for Skeletal Muscle Adaptation to Exercise.*
- 2019** *Poster Presentation:* 2019 University of Kentucky Department of Physiology Research and Education Day. *Training the Microbiome for Skeletal Muscle Health.*

- 2016** *Poster Presentation: South West Chapter of the American College of Sports Medicine, October 2016: A Randomized Controlled Trial of Riboflavin for Enhancement of Ultramarathon Recovery.*
- 2015** *Invited Speaker: 2<sup>nd</sup> Annual, Medicine and Science in Ultra-Endurance Sports. June 23<sup>rd</sup>-24<sup>th</sup> 2015, Squaw Valley California; The Influence of Hydration State on Thermoregulation during a 161-km Ultramarathon.*
- 2014** *Poster Presentation: South West Chapter of The American College of Sports Medicine October 2014: The Influence of Hydration State on Thermoregulation during a 161-km ultramarathon.*

## **GRANTS & FELLOWSHIPS**

---

### **Department of Physiology**

*University of Kentucky, Lexington, Kentucky*

- 2021**      **Funding Agency: University of Kentucky**  
**Grant Title:** University of Kentucky Association of Emeriti Faculty Endowed Fellowship  
**Duration of grant:** 1 time payment  
**Total Award:** \$2,500
- 2020**      **Funding Agency:** National Institutes of Health F31 NRSA Predoctoral Fellowship  
**Project Title:** The gut microbiome and skeletal muscle atrophy  
**Amount requested:** \$86,518  
**Role:** Principal Investigator  
**Comments:** Not scored
- 2020**      **Funding Agency:** University of Kentucky, Department of Physiology  
**Fellowship Title:** Teaching Assistantship

**Duration of Fellowship:** 1 academic semester

**Award:** Stipend and tuition covered for one academic semester

**2019-2020**

**Funding Agency:** University of Kentucky, College of Medicine

**Fellowship Title:** Fellowship for Excellence in Graduate Research

**Duration of Fellowship:** One academic year

**Award:** Full tuition and stipend covered

**2018-2019**

**Funding Agency:** National Institute of Health

**Fellowship Title:** T-32, Graduate Training in Integrative Physiology

**Duration of Fellowship:** One academic year

**Award:** Full tuition and stipend covered

#### **SPONSORED RESEARCH PROJECTS**

---

**Project Title:** The Role of the Gut Microbiome in Sarcopenia

**Principal Investigator(s):** John J. McCarthy Ph.D. & Charlotte A. Peterson, Ph.D.

**Role in Project:** Graduate Student

**Effort:** 100%

**Institution/University:** University of Kentucky

**Source of Funding:** National Institutes of Health Exploratory/Developmental Research Grant Program

**Duration of Project:** 01/2021-01/2023

**Total Award:** \$275,000

**Grant Number:** 1 R21 AG071888-01